EANM procedural guidelines for radionuclide myocardial perfusion imaging with SPECT and SPECT/CT

Chair of writing committee (responsible for the coordination of the overall process):

Hein J. Verberne and Birger Hesse

Authors:

Hein J. Verberne, Wanda Acampa, Constantinos Anagnostopoulos, Jim Ballinger, Frank Bengel, Pieter De Bondt, Ronny R. Buechel, Alberto Cuocolo, Berthe L.F. van Eck-Smit, Albert Flotats, Marcus Hacker, Cecilia Hindorf, Philip A. Kaufmann, Oliver Lindner, Michael Ljungberg, Markus Lonsdale, Alain Manrique, David Minarik, Arthur J.H.A. Scholte, Riemer H.J.A. Slart, Elin Trägårdh, Tim C. de Wit, Birger Hesse

Correspondence to:

H.J. Verberne, MD PhD
Department of Nuclear Medicine, F2-238
Academic Medical Center
University of Amsterdam
Meibergdreef 9
1105 AZ Amsterdam
The Netherlands
Tel: *31-20-5669111, pager 58 436
Fax: *31-20-5669092
E-mail: h.j.verberne@amc.uva.nl

Author affiliations:

H.J. Verberne — Department of Nuclear Medicine, Academic Medical Center, University of Amsterdam, Amsterdam, The Netherlands
Tel: +31 20 566 9111, pager 58 436
Fax: +31 20 566 9092
E-mail: h.j.verberne@amc.uva.nl

W. Acampa — Institute of Biostructures and Bioimaging, National Council of Research, Naples, Italy
Tel: +39 0812203409
Fax: +39 0815457081
E-mail: acampa@unina.it

C. Anagnostopoulos — Center for Experimental surgery, Clinical and Translational Research, Biomedical research foundation, Academy of Athens, Greece
Tel: +30 210 65 97 126 or +30 210 65 97 067
Fax: +30 210 65 97 502
E-mail: cdanagnostopoulos@bioacademy.gr

J. Ballinger — Department of Nuclear Medicine, Guy's Hospital - Guy's & St Thomas' Trust Foundation, London, United Kingdom
Tel: +44 207 188 5521
Fax: +44 207 188 4094
E-mail: james.ballinger@gstt.nhs.uk

F. Bengel — Department of Nuclear Medicine, Hannover Medical School, Hannover, Germany
Tel:
Fax:
E-mail: bengel.frank@mh-hannover.de

P. De Bondt — Department of Nuclear Medicine, OLV Hospital, Aalst, Belgium
Tel:
Fax:
E-mail: pieter.de.bondt@olvz-aalst.be

R.R. Buechel
Cardiac Imaging, University Hospital Zurich, Zurich, Switzerland
Tel: +41 44 255 1059
Fax: +41 44 255 4414
E-mail: ronny.buechel@usz.ch

A. Cuocolo
Department of Advanced Biomedical Sciences, University Federico II, Naples, Italy
Tel: +39 0812203187, int.209
Fax: +39 0815457081
E-mail: cuocolo@unina.it

B.L.F. van Eck-Smit
Department of Nuclear Medicine, Academic Medical Center, University of Amsterdam, Amsterdam, The Netherlands
Tel:
Fax: +31 20 566 9092
E-mail: b.l.vaneck-smit@amc.uva.nl

A. Flotats
Nuclear Medicine Department, Hospital de la Santa Creu i Sant Pau, Universitat Autònoma de Barcelona, Barcelona, Spain
Tel: +34 93 553 7797
Fax: +34 93 553 7798
E-mail: aflotats@santpau.cat

M. Hacker
Division of Nuclear Medicine, Department of Biomedical Imaging and Image-guided Therapy, Medical University of Vienna, Vienna, Austria
Tel: +43 1 40400 55300/310
Fax: +43 1 40400 55320
E-mail: marcus.hacker@meduniwien.ac.at

C. Hindorf
Department of Radiation Physics, Skåne University Hospital, Lund, Sweden
Tel: +46 46 176366
Fax:
E-mail: cecilia.hindorf@skane.se

P.A. Kaufmann
Cardiac Imaging, University Hospital Zurich, Zurich, Switzerland
Tel: +41 44 255 1111
Fax: +41 44 255 4414
E-mail: pak@usz.ch

O. Linder
Heart and Diabetes Center North Rhine-Westphalia, University Hospital of the Ruhr-University Bochum, Institute for Radiology, Nuclear Medicine and Molecular Imaging, Bad Oeynhausen, Germany
Tel: +49 57 31 97 35 02
Fax: +49 57 31 97 21 90
E-mail: olindner@hdz-nrw.de

M. Ljungberg
Department of Medical Radiation Physics, Lund University, Lund, Sweden
Tel: +46 46 17 35 65
Fax: +46 46 17 85 40
E-mail: michael.ljungberg@med.lu.se

M. Lonsdale
Department of Clinical Physiology and Nuclear Medicine, Bispebjerg Hospital, Copenhagen, Denmark
Tel: +45 2613 5165
Fax: +45 3531 3954
E-mail: markus.lonsdale@regionh.dk

A. Manrique
Department of Nuclear Medicine, Service Commun Investigations chez l'Homme, GIP Cyceron, Caen University Hospital, Caen, France
Tel: +33 2 31 47 02 87
Fax: +33 2 31 47 01 30
E-mail: manrique@cyceron.fr

D. Minarik
Radiation physics, Skåne University Hospital, Malmö, Sweden
Tel: +46 40 331083
Fax:
E-mail: david.minarik@med.lu.se

A.J.H.A. Scholte — Department of Cardiology, Leiden University Medical Center, Leiden, The Netherlands
Tel: +31 71 5262020
Fax: +31 71 5266809
E-mail: a.j.h.a.scholte@lumc.nl

R.H.J.A. Slart — Department of Nuclear Medicine and Molecular Imaging, University of Groningen, University Medical Center Groningen, Groningen, The Netherlands
Tel: +31 50 3611835
Fax: +31 50 3611687
E-mail: r.h.j.a.slart@umcg.nl

E. Trägårdh — Clinical Physiology and Nuclear Medicine, Skåne University Hospital and Lund University, Malmö, Sweden.
Tel: +46 40 33 87 24
Fax: +46 40 33 66 20
E-mail: elin.tragardh@med.lu.se

T.C. de Wit — Department of Nuclear Medicine, Academic Medical Center, University of Amsterdam, Amsterdam, The Netherlands
Tel: +31 20 566 4550
Fax: +31 20 566 9092
E-mail: t.c.dewit@amc.uva.nl

B. Hesse — Department of Clinical Physiology and Nuclear Medicine & PET, Rigshospitalet, University Hospital of Copenhagen, Copenhagen, Denmark
Tel: +45 3545 4011
Fax: +45 3545 4015
E-mail: birger.hesse@regionh.dk

Abbreviations:

AC:	Attenuation correction
ALS:	Advanced life support
CCTA	Coronary CT angiography
COPD:	Chronic obstructive pulmonary disease
COR:	Centre of rotation
DRL:	Diagnostic reference levels
EF:	Ejection fraction
FBP:	Filtered back projection
FDG:	^{18}F-Fluorodeoxyglucose
FOV:	Field of view
FWHM:	Full-width at half-maximum
i.v.:	Intravenous
LBBB	Left bundle branch block
LEAP:	Low-energy, all-purpose (collimator)
LEGP:	Low-energy general purpose (collimator)
LEHR:	Low-energy high-resolution (collimator)
LV:	Left ventricular
LVEF:	Left ventricular ejection fraction
ML-EM:	Maximum likelihood expectation maximization
MPI	Myocardial perfusion imaging
NEMA:	National Electrical Manufacturers Association
OS-EM:	Ordered subsets expectation maximization
PVC:	Premature ventricular contractions
QC:	Quality control
SA block:	Sinoatrial block
SDS:	Summed difference score
SRS:	Summed rest score
SSS:	Summed stress score

Preamble

The update of the European procedural guidelines for radionuclide myocardial perfusion imaging (MPI) with SPECT is developed on initiative of and approved by the cardiovascular committee of the European Association of Nuclear Medicine (EANM). The present guidelines are based on the guidelines from 2005 [1]. The 2015 update includes all aspects of SPECT imaging from gating to hybrid imaging, but does not include myocardial perfusion evaluated by PET, which will be updated in a separate guideline. This document also updates relevant sections of the 2008 guidelines on radionuclide imaging of cardiac function [2] and the 2011 position statement on hybrid cardiac imaging [3]. The present guidelines have been created according to the joint statement of the Society of Nuclear Medicine and Molecular Imaging (SNMMI) and the EANM on guideline development [4]. The EANM guidelines are intended to present information specifically adapted to European practice, based on evidence from original scientific studies or on previously published guidelines (i.e.: national or European guidelines for MPI, the European Society of Cardiology (ESC), and the American College of Cardiology (ACC) / American Heart Association (AHA) / American Society of Nuclear Cardiology (ASNC) guidelines). In case of lack of published evidence, opinions are based on expert consensus and are indicated as such. Where more than one solution seems to be practised, and none has been shown to be superior to the others, the committee has tried to express specifically this state of knowledge.

Introduction

In recent years radionuclide imaging technologies have evolved rapidly with the development of new instrumentation and new agents. This has increased both the number and the complexity of choices for the clinician. The purpose of this guideline is to document the state-of-the-art applications and protocols and to disseminate this information to the European nuclear cardiology community. The guidelines are designed to assist physicians and other healthcare professionals in performing, interpreting and reporting radionuclide tomographic imaging examinations of myocardial perfusion including hybrid imaging. The guidelines do not discuss overall clinical indications for these examinations or the benefits and drawbacks of radionuclide myocardial perfusion imaging compared with other techniques, nor do they cover cost-benefit or cost-effectiveness aspects in diagnosis or prognosis.

List of contents

Patient information and preparation

The previous EANM guidelines remain the basis of the present recommendations, but below some principles and details are emphasized and/or added. Patient information and preparation can be subdivided into 1) information and preparation relevant for the patient and 2) information about the patient essential for the performance and logistics of the examination.

Information and preparation relevant for the patient

Written information should be provided to patients (and/or their relatives) in relation to scheduling, and in addition, oral information should be provided on the day of the procedure. Variations will depend on local traditions and regulations.

General information to be conveyed to (or obtained from) the patient should be given in an easily understandable language, aiming to cover:

- The purpose of the test
- Preparations before the test: interruption of medication, caffeine abstinence, need for fasting etc.
- A brief description of the procedure (e.g. type of stress test, duration of imaging and the need for the patient to remain in one position under a rotating camera)
- Information about the time(s) and date(s) and the duration of the examination.
  Advice on giving notice in advance if the patient is unable to attend
- An informed consent form, to be signed and collected according to local regulations
- Insurance: patients with (private) insurance should bring all insurance details. In some countries contact with the insurance company before the examination may be mandatory
- Adverse reactions: some centres prefer to describe adverse reaction in detail, in particular possible adverse reactions of stress test(s); other centres do not
- Information about the results of the examination: when and to whom the report will be forwarded.

Food and medication before the test

In general heavy meals should be avoided before a stress test. Medications that may interfere with responses to a stress test (anti-anginal drugs, dipyridamole or dipyridamole containing medication) should be interrupted if possible, and the patient must abstain from caffeine containing drugs and beverages (cf. table 5 in section on “Stress tests”).

Radiation exposure

Risks for the patient and accompanying persons may be described in more or less detail according to national rules and regulations. Description of the radioactive exposure of the examination may be related to more well-known X-ray examinations such as a CT scan of the abdomen or to everyday life events like a transatlantic flight or to that from the background radiation (cf. Sect. “Injected activities, dosimetry and radiation exposure”).

Pregnancy, lactation

Before radioactivity is injected into a woman of child-bearing age, the person involved is responsible for getting specific information regarding possible pregnancy or lactation (cf. Sect. “Injected activities, dosimetry and radiation exposure”).

Travel information

In recent years, the threat of nuclear terrorism has led to the widespread use of radiation detectors for security screening at airports and other public facilities. Patients who have received radiopharmaceuticals for nuclear cardiology studies may retain sufficient activity to trigger these detectors. In particular, patients who have received thalium-201 may trigger these detectors for up to 2 months following the examination. This should be described in more or less detail according to national rules and regulations.

Information about the patient essential for the planning, performance and interpretation of the examination:

- Check at several stages during the patient’s visit his or her identity, ideally before the start of each part of the examination: i.e. patients arrival at the department, prior to administration of the radiopharmaceutical and prior to the start of imaging
- Previous examinations: clinical data and previous relevant cardiovascular examinations must be available before the study. In some institutions, it may be relevant to ask patients to bring previous medical records and previous test results.

Radiopharmaceuticals and CT contrast agents

For myocardial perfusion imaging with SPECT, two technetium-99m (^{99m}Tc) labelled radiopharmaceuticals (sestamibi and tetrofosmin) and thallium-201 (^{201}Tl) chloride are commercially available. Increasingly, coronary CT contrast agents are being used for hybrid imaging.

^{99m}Tc sestamibi and tetrofosmin

Two ^{99m}Tc-labelled perfusion tracers are available commercially: ^{99m}Tc-2-methoxyisobutylisonitrile (sestamibi) and ^{99m}Tc-1,2-bis[bis(2-ethoxyethyl) phosphino] ethane (tetrofosmin). ^{99m}Tc has a half-life of 6 h and emits gamma photons at 140 keV.

^{99m}Tc-sestamibi is a cationic complex that diffuses passively through the capillary and cell membrane, although less readily than ^{201}Tl (see below), resulting in relatively slower immediate extraction. Myocardial uptake of the ^{99m}Tc-labelled tracers increases almost proportionately with increase in perfusion. However, the ^{99m}Tc-labelled tracers reach a plateau in myocardial uptake at a myocardial perfusion around twice resting levels. Within the cell it is retained in intact mitochondria, reflecting viable myocytes. Elimination of the radiotracer occurs through the hepatobiliary system and to a lesser extent the kidneys. Tetrofosmin is also cleared rapidly from the blood and its myocardial uptake is similar to that of sestamibi, with approximately 1.2% of the administered dose being taken up by the myocardium, likely by a similar mechanism. Elimination of tetrofosmin occurs mostly through the kidneys and the hepatobiliary system, and clearance is slightly more rapid than in the case of sestamibi [5].

The ^{99m}Tc-labelled radiopharmaceuticals should be administered through a secure intravenous (i.v.) line in accordance with local radiation protection practice. If it is given through the side arm of a three-way tap through which adenosine or dobutamine is running, then it should be given over 15–30 s to avoid a bolus of the pharmacological stressor being pushed ahead of the tracer. Otherwise it can be given as a bolus injection. The syringe with the tracer can be flushed with either saline or glucose to ensure that the full dose is given. If extravasation is suspected, imaging may be attempted and if sufficient activity uptake in the myocardium has been obtained the examination can be performed; otherwise, the examination should be repeated. Resting injections should ideally be given after the administration of sublingual nitrate, in particular in patients with a suspicion of severe myocardial ischaemia or old infarction. This is important because without the administration of sublingual nitrate myocardial viability may be underestimated in areas with reduced resting perfusion [6].

^{201}Tl

^{201}Tl thallous chloride was the first radionuclide used widely for myocardial perfusion studies. It decays by electron capture with a half-life of 73 h, emitting gamma photons of 135 and 167 keV (12% abundance) and X-rays of energy 67–82 keV (88% abundance) [7]. Following i.v. injection, ~88% is cleared from the blood after the first circulation, with ~4% of the injected activity localising in the myocardium in proportion to regional perfusion and viability. ^{201}Tl is a potassium analogue and ~60% of the administered activity enters the myocytes via the sodium-potassium, ATPase-dependent exchange mechanism, with the remainder entering passively along an electropotential gradient. The extraction efficiency is generally maintained under conditions of acidosis and hypoxia, and only when myocytes are irreversibly damaged is extraction reduced. Myocardial uptake of ^{201}Tl increases proportionately with perfusion when perfusion increases up to 2–2.5 times above resting levels before reaching a plateau in myocardial uptake. After initial uptake, prolonged retention depends on the intactness of cell membrane and hence on viability. Moreover, because ^{201}Tl is not trapped in myocytes or in other tissues, redistribution of ^{201}Tl occurs over several hours after administration. This redistribution/re-availability leads to ^{201}Tl myocardial extraction in regions that were ischaemic when ^{201}Tl was injected at peak stress, thus allowing redistribution images to be acquired that are fairly independent of perfusion and mainly reflect viability. Sensitivity of detection of viability in ^{201}Tl rest imaging can be enhanced by injection of a top up dose of ^{201}Tl after stress imaging [8].

Although ^{201}Tl is a good tracer for myocardial perfusion imaging it does, however, have several limitations:

- Relatively long physical half-life: high radiation burden for the patient
- Relatively low injected activity: low signal-to-noise ratio; images can be suboptimal particularly in obese patients, and low count levels impair high-quality, ECG-gated SPECT studies
- Relatively low energy emission: low-resolution images and significant scatter and attenuation by soft tissue.

In general the i.v. administration of ^{201}Tl follows the same protocol as for ^{99m}Tc labelled radiopharmaceuticals.

A summary of the characteristics of the different SPECT myocardial perfusion tracers is shown in table 1.

^{201}Tl has some advantages compared with both ^{99m}Tc-labelled tracers:

- Splanchnic uptake and excretion are markedly higher than for ^{201}Tl, which may occasionally complicate interpretation of the inferior wall perfusion

- The uptake of both ^{99m}Tc-labelled tracers as a function of myocardial perfusion is less avid than in the case of ^{201}Tl, and so defects may be less pronounced
- The initial myocardial distribution of ^{99m}Tc-tracers remains largely intact; thus, for stress and rest images separate injections are needed.

The ^{99m}Tc-labelled tracers offer other and probably more important advantages over ^{201}Tl:

- The higher energy of ^{99m}Tc leads to better quality images because of less attenuation and scatter
- The shorter half-life of ^{99m}Tc permits much higher activities to be administered, giving better counting statistics and thus allowing performance of left ventricular (LV) ECG gating or first-pass imaging, which provides additional functional information.

Adverse events

Nuclear medicine has been characterized by the rare occurrence of acute and chronic adverse events. In the period 1980–2000 fewer than 50 reports were registered annually in Europe [9]. Furthermore, the majority of the reported events were mild and transient in nature, such as rashes, flushing, metallic taste and vasovagal reactions. Very few adverse events required treatment. For ^{201}Tl extravasation must be avoided due to risk of local tissue necrosis. For ^{99m}Tc-labelled tracers a few cases of anaphylaxis, angioedema and erythroderma/exanthema have been reported [10-13]. These cases emphasize the fact that, although rare, adverse effects do occur, and the risk must not be totally ignored [14].

Coronary CT contrast agents

The use of contrast media for cardiac imaging is increasing as hybrid cardiac SPECT/CT and PET/CT, as well as coronary CT angiography and cardiac MRI, become more widely used [3].

For coronary CT angiography (CCTA), an intravenously injected contrast agent is needed. In general these contrast agents are iodine-based and due to the relatively high attenuation coefficient of iodine therefore result in high contrast between organs with and those without contrast. Coronary CT in combination with ECG-gating and a contrast agent permits visualization of the coronary artery lumen and detection of coronary artery stenoses [15, 16]. At the moment, there are four classes of contrast media available for clinical use: high osmolar ionic monomers, low osmolar non-ionic monomers, low osmolar ionic dimers and iso-osmolar non-ionic dimers. The contrast media are provided at various iodine concentrations and have different biochemical properties (viscosity, osmolarity, hydrophilic behaviour, ionic content and pH).

In general, the injection protocol should follow vendor recommendations dependent on the specific contrast agent and CT used. For coronary imaging in general, a contrast agent with a high concentration of iodine is used (300-400 mg/ml) to ensure adequate opacification of the small coronary arteries [17]. In total, approximately 60-90 ml of contrast agent is injected at an injection speed of 4-6 ml/s. Often, the bolus is split between a first bolus of pure contrast and then a bolus with a mix of contrast and saline, to reduce streak artefacts from contrast enhancement of the vena cava and right side of the heart. Otherwise, the contrast bolus is followed by a saline flush of 40-70 ml. With newest generation of CT scanners, a smaller contrast bolus with lower iodine concentration is likely sufficient to obtain good contrast enhancement of the coronary arteries [18].

Two contrast timing techniques are available to start the CCTA acquisition, based on arrival of contrast in the aorta: the bolus tracking and the bolus timing technique. Bolus tracking involves a series of axial low-dose images at 2 s intervals to track the arrival of the bolus of contrast material in the aorta. The CCTA is initiated when the contrast enhancement of the aorta reaches a certain predefined level, e.g. 100 Hounsfield units (HU). The bolus timing technique involves an extra low-dose scan acquisition of a single slice prior to the CCTA acquisition. Here, a small contrast bolus and saline flush are injected to determine the contrast arrival interval. The time between the start of the contrast injection and the arrival of contrast bolus in the aorta is used as the scan delay for the actual CCTA [3, 15].

Contraindications

Contraindications for iodine contrast can be divided into absolute and relative contraindications [19, 20]. Absolute contraindications include myasthenia gravis, mastocytosis, and post-thyroid carcinoma when follow-up with ^{131}I imaging or ^{131}I therapy is planned within 6 months of the CCTA. Relative contraindications are known contrast allergy, planned thyroid scan, and multiple myeloma.

The clinical benefit of using estimated glomerular filtration rate (eGFR) or calculated creatinine clearance in assessing preprocedural contrast induced nephrotoxicity (CIN) risk in patients with stable renal function is uncertain because much of the knowledge comes from studies that used only serum creatinine measurements. The threshold values at which different clinical actions should be taken (e.g., active IV hydration, avoidance of contrast medium administration) are neither proven nor generally agreed upon for either serum creatinine measurement or calculated creatinine clearance. In addition, the accuracy of these formulae has only been validated in the patient population for whom they were developed. The following is a suggested list of risk factors that may warrant pre-administration serum creatinine screening in patients who are scheduled to receive intravascular iodinated contrast medium. This list should not be considered definitive [21]:

- Age > 60
- History of renal disease, including: Dialysis, kidney transplant, single kidney, renal cancer, renal surgery
- History of hypertension requiring medical therapy
- History of diabetes mellitus

Metformin does not confer an increased risk of CIN. However, metformin can very rarely lead to lactic acidosis in patients with renal failure. In case of reduced renal function (i.e. estimated glomerular filtration rate < 45 ml/min/1.73m^2, or <60 ml/min/1.73m^2 in presence of diabetes mellitus or at least 2 risk factors for contrast nephropathy) alternative (imaging) strategies should be considered. However, when no alternatives are available adequate (clinical) hydration is the major preventive action against CIN.

If intravenous contrast agent is going to be administered, metformin should be discontinued at the time of the procedure and withheld for 48 h after the procedure. If the risk of nephrotoxicity is high, metformin can be reinstituted only after renal function has been reevaluated and found to be normal. If the risk of nephrotoxicity is low, metformin can be reinstituted without the need for renal function assessment. An alternative glucose-controlling drug should be considered during this time [22].

Adverse events

Strategies to reduce the risk in non-acute settings of contrast medium induced adverse reactions include the prophylactic use of oral anti-histamines and corticosteroid tablets. A classification system, stratifying adverse events due to iodinated contrast media by severity and type, is presented below [21, 23, 24]:

- *Minor*
    - Signs and symptoms are self-limited without evidence of progression. Mild reactions include: Pruritus, nausea and mild vomiting, diaphoresis
- *Moderate:*
    - Signs and symptoms are more pronounced and commonly require medical management. Some of these reactions have the potential to become severe if not treated. Moderate reactions include: Facial oedema, faintness, severe vomiting, urticaria, bronchospasm
- *Severe:*
    - Signs and symptoms are often life-threatening and can result in permanent morbidity or death if not managed appropriately. Severe reactions include: Laryngeal oedema, pulmonary oedema, respiratory arrest, hypotensive shock, convulsions, cardiac arrest
- *Delayed:*
    - Skin rash, thyrotoxicosis, kidney dysfunction.

The frequency of allergic-like and physiologic adverse events related to the intravascular administration of iodinated contrast media is low and has decreased considerably with changes in usage from ionic high-osmolality contrast agents (HOCA) to nonionic low-osmolality contrast agents (LOCA). Historically, acute adverse events occurred in 5-15% of all patients who received HOCA. Many patients receiving intravascular HOCA experienced physiologic disturbances (e.g., generalized warmth, nausea, or emesis), and this was often documented as a contrast reaction. HOCA are now rarely or never used for intravascular purposes because of their greater adverse event profile compared to LOCA. The reported overall acute adverse reaction rate (allergic-like + physiologic) for nonionic LOCA (i.e. iohexol, iopromide, or iodixanol) ranges from 0.2%, 0.6% to 0.7% [25-27]. Serious acute reactions to i.v. LOCA are rare, with an historical rate of approximately four in 10,000 (0.04%) [28].

Table 1. Comparison of properties of SPECT agents for MPI

Property	*^{99m}Tc-sestamibi*	*^{99m}Tc-tetrofosmin*	*^{201}Tl thallous-chloride*
Availability	Kit preparation with heating	Kit preparation at room temperature	Long half-life makes supply convenient
Imaging protocol	Separate injections at stress and rest (if a rest study is deemed necessary)		Stress and rest data from single injection
Imaging flexibility	Stress and rest on same or different days		Stress imaging must begin immediately
Image quality	Optimal for gamma cameras		Low emission energy, low count rate

Injected activities, dosimetry and radiation exposure

In general, the principle of keeping radiation exposure "As Low As Reasonable Achievable" (ALARA) must be adhered to. In addition, the activity of a radiopharmaceutical to be administered must be determined in accordance with national legislation and the European Council Directive Euratom 2013/59 [29]. This directive describes the basic safety standards for protection against the dangers arising from exposure to ionising radiation. One of the criteria is the designation of diagnostic reference levels (DRL) for radiopharmaceuticals, defined as levels of activity for groups of standard-sized patients and for broadly defined types of equipment. It is expressed that the levels will not be exceeded for standard procedures. In a 2013 ICRP publication on nuclear cardiology, biological effects of radiation, DRL, as well as dosimetric issues in MPI and CCTA for patients and staff are further discussed [30]. In addition, the public awareness and public concern with regard to radiation exposure in relation to medical procedures has been raised the last decade and should be acknowledged.

Activity amounts to inject

It is not possible to make precise recommendations regarding injected activities, since hard evidence documenting superior results with certain activities is not available. The activity to administer is, in general terms, a compromise between image quality and radiation exposure to the patient and staff. The higher the activity administered, the better the image quality and the higher the radiation exposure to the patient and staff. The activity to administer is dependent on type of equipment (single-head or a multiple head scintillation camera, or a camera based on a CZT detector), patient characteristics (body weight), acquisition protocol (1-day or 2-day protocols, imaging time, pixel size, gated acquisition), and the radiopharmaceutical (^{99m}Tc-compounds or ^{201}Tl-chloride). The reconstruction method may also be of importance, i.e. filtered back-projection vs. iterative reconstruction. When a 1-day ^{99m}Tc protocol is used (i.e. two administrations of activity on one day), the activity for the second examination has to be three times higher than the first administered activity [31]. It should be noted that if the stress examination is performed first, irrespective of a 1- or 2-day protocol, and reported as normal, the rest examination can be omitted [32].

There is limited evidence in the literature demonstrating activity amounts to be injected for optimal images in the different settings of patients and instrumentation. Coming down to a classical SPECT acquisition the following activities to administer are recommended, according to the ALARA principle, for a normal weight adult patient (e.g. BMI <25) for a gated study on a multiple-head scintillation camera, using filtered back-projection, an acquisition duration of 15 min and a pixel size of around 6 mm:

^{99m}Tc-sestamibi or ^{99m}Tc-tetrofosmin:

- Two-day protocol: 350 – 700 MBq/study
- One-day protocol: 250 – 400 MBq for the first injection, three times more for the second injection.

^{201}Tl-chloride:

- Stress redistribution: 74 – 111 MBq
- Re-injection: 37 MBq.

The above activities for ^{99m}Tc-sestamibi, ^{99m}Tc-tetrofosmin and ^{201}Tl-chloride should be considered only as a general indication. Camera systems based on new technology (e.g. CZT-cameras) have improved count sensitivity. This improved sensitivity can be used to either reduce the amount of activity accordingly or decrease image acquisition duration [33-37]. It should also be noted that local legislation and local DRLs may exist and must be followed. The activities to be administered for paediatric patients should be modified according to the recommendations by the EANM [38].

Radiation dosimetry

SPECT

The absorbed doses to various organs in healthy subjects following administration of ^{99m}Tc-sestamibi, ^{99m}Tc-tetrofosmin and ^{201}Tl-chloride are given in Table 2 [39-41]. As can be seen there are some small variations between the equivalent doses per injected activity to normal organs during rest and stress studies. However, the effective dose per injected activity during a stress study is 10 to 15 % lower than that from a rest study. The effective doses in the last column are calculated according to the method described by the ICRP [42]. For paediatric patients, additional values for absorbed dose per unit activity administered (mGy/MBq) are given in the ICRP reports [39-41]. The values of effective doses in Table 2 are the latest published in an ICRP report. However, the ICRP has adopted new phantoms for absorbed dose calculations, new weighting factors, and new bio-kinetic models [43-45]. Using these new models the effective dose per administered unit of activity to adults are [46]:

- ^{99m}Tc-tetrofosmin (stress and rest): 0.0058 and 0.0063 mSv/MBq, respectively
- ^{99m}Tc-sestamibi (stress and rest): 0.0066 and 0.0070 mSv/MBq, respectively
- ^{201}Tl-chloride (redistribution): 0.102 mSv/MBq.

These values are approximately 20% lower than the values calculated using the previous methods. The organs with the highest absorbed dose per unit activity administered (mGy/MBq) are the gallbladder

and kidneys for ^{99m}Tc-sestamibi, the gallbladder and colon for ^{99m}Tc-tetrofosmin, and the bone surface and kidney for ^{201}Tl-chloride (Table 2).

Hybrid systems

If the MPI is combined with a CT-scan for attenuation, calcium scoring (CACS) or CCTA, an additional dose is given to the patient. For an attenuation correction CT an additional 0.5-1.0 mSv is given. Absorbed doses from CACS and CCTA depend on the system and imaging protocol used and for CACS can be estimated to be <1 mSv. The absorbed dose for CCTA can be estimated between 2-5 mSv using commonly available single-source 64-slice CT scanners with a prospectively ECG triggered step-and-shoot acquisition protocol [47, 48]. The latest generation dual-source or 256- and 320-slice single source CT scanners enable even absorbed doses <1 mSv [49, 50].

Radiation exposure to relatives of patient and to hospital staff

Patient relatives

In general, radiation exposure to accompanying persons and relatives is very limited, and no special precautions are needed for studies with either ^{99m}Tc-labelled tracers or ^{201}Tl-chloride. Only close contact with infants should be restricted, cf. below under "Lactation". One-day protocols for patients taking care of infants should be avoided.

Staff

It should be noted that for the injected patient the absorbed dose is lower with ^{99m}Tc-labelled tracers than with ^{201}Tl-chloride; but the radiation exposure to the surroundings is lower with ^{201}Tl-chloride than with ^{99m}Tc-labelled tracers (cf. Tables 2 and 3). These values were calculated using conservative assumptions and are based on assumed number of cases that can only be reached in large hospitals. The radiation exposure to staff working in nuclear medicine or nuclear cardiology departments varies widely depending on workload, local work procedures etc., but the effective dose to technologists/physicians are generally well below limits. For further reading see e.g. [51, 52].

The radiation exposure to the staff of a general hospital outside the nuclear medicine department has been assessed in a "worst case scenario" by the German Radiation Protection Board (SSK) [53]. In addition, the exposure of relatives was calculated (Table 3). These data do not represent the exposure of staff performing the actual myocardial studies in a nuclear medicine or cardiology department.

Pregnant patients

In general MPI should not be performed in pregnant women since a number of alternative methods are available for cardiac imaging giving less or no radiation exposure. This holds true not only when

pregnancy is confirmed, but also for women in whom pregnancy is not excluded (e.g. a missed period or the period is known to be irregular). If MPI is considered necessary for a pregnant woman, special attention must be paid to the absorbed dose to the unborn child by [53]:

- Use a ^{99m}Tc-labelled radiopharmaceutical, never ^{201}Tl
- Possible reduction of administered activity (compensated by optimal imaging equipment etc.)
- Planning a 2-day procedure with the stress test first and omission of the rest study if the stress study is considered normal
- Frequent emptying of the urinary bladder after administration of the activity
- In SPECT/CT: optimization of the CT protocol (scan range, tube current and voltage).

When an MPI is performed during pregnancy, accidentally or otherwise, the absorbed dose to the foetus comes from external radiation emanating from the mother and internal irradiation from radioactivity transferred through the placenta. The foetal absorbed dose differs depending on the stage of pregnancy, with higher absorbed doses in the early stages. For ^{201}Tl-chloride the absorbed dose can reach 0.097 mGy/MBq. For ^{99m}Tc compounds it can reach up to 0.015 mGy/MBq for embryos [54]. This level of exposure does not imply any deterministic effects on the foetus, only a minute increase in stochastic risk. To reduce the exposure it is important that the mother voids her bladder often.

Lactating patients

In general, elective diagnostic nuclear medicine procedures should be delayed until the patient is no longer breast-feeding. However, according to the ICRP 106, the interruption of breast-feeding is not essential for ^{99m}Tc-labeled compounds [40]. But according to the principle of keeping exposure "as low as reasonably achievable", it can be recommended to:

- Use ^{99m}Tc-labelled tracers rather than ^{201}Tl
- Nurse the infant just before administration of the radiopharmaceutical
- Interrupt breastfeeding for 3 to 6 hours after the administration of dose
- Express the milk completely once and discard it
- Close contact with infants should be restricted for 6-12 hours.

Table 2. Absorbed dose per unit activity administered [46].

	Absorbed dose per unit administered activity (mGy/MBq)					*Absorbed dose for a standard examination* (mGy)*				
	^{99m}Tc-tetrofosmin		*^{99m}Tc-sestamibi*		*^{201}Tl-chloride*	*^{99m}Tc-tetrofosmin*		*^{99m}Tc-sestamibi*		*^{201}Tl-chloride*
	Stress	*Rest*	*Stress*	*Rest*		*Stress*	*Rest*	*Stress*	*Rest*	
Adrenals	4,4E-03	4,2E-03	6,6E-03	7,5E-03	5,7E-02	2,2	2,1	3,3	3,8	4,6
Bladder	1,4E-02	1,7E-02	9,8E-03	1,1E-02	3,9E-02	7,0	8,5	4,9	5,5	3,1
Bone Surface	6,3E-03	5,8E-03	7,8E-03	8,2E-03	3,8E-01	3,2	2,9	3,9	4,1	30,4
Brain	2,7E-03	2,3E-03	4,4E-03	5,2E-03	2,2E-02	1,4	1,2	2,2	2,6	1,8
Breasts	2,3E-03	2,0E-03	3,4E-03	3,8E-03	2,4E-02	1,2	1,0	1,7	1,9	1,9
Gallbladder	2,7E-02	3,6E-02	3,3E-02	3,9E-02	6,5E-02	13,5	18,0	16,5	19,5	5,2
GI tract										
Stomach	4,6E-03	4,5E-03	5,9E-03	6,5E-03	1,1E-01	2,3	2,3	3,0	3,3	8,8
SmallIntestine	1,1E-02	1,5E-02	1,2E-02	1,5E-02	1,4E-01	5,5	7,5	6,0	7,5	11,2
Colon	1,8E-02	2,4E-02	1,9E-02	2,4E-02	2,5E-01	9,0	12,0	9,5	12,0	20,0
Upper Large Intestine	2,0E-02	2,7E-02	2,2E-02	2,7E-02	1,8E-01	10,0	13,5	11,0	13,5	14,4
Lower Large Intestine	1,5E-02	2,0E-02	1,6E-02	1,9E-02	3,4E-01	7,5	10,0	8,0	9,5	27,2
Heart	5,2E-03	4,7E-03	7,2E-03	6,3E-03	1,9E-01	2,6	2,4	3,6	3,2	15,2
Kidneys	1,0E-02	1,3E-02	2,6E-02	3,6E-02	4,8E-01	5,0	6,5	13,0	18,0	38,4
Liver	3,3E-03	4,0E-03	9,2E-03	1,1E-02	1,5E-01	1,7	2,0	4,6	5,5	12,0
Lungs	3,2E-03	2,8E-03	4,4E-03	4,6E-03	1,1E-01	1,6	1,4	2,2	2,3	8,8
Muscles	3,5E-03	3,3E-03	3,2E-03	2,9E-03	5,2E-02	1,8	1,7	1,6	1,5	4,2
Oesophagus	3,3E-03	2,8E-03	4,0E-03	4,1E-03	3,6E-02	1,7	1,4	2,0	2,1	2,9
Ovaries	7,7E-03	8,8E-03	8,1E-03	9,1E-03	1,2E-01	3,9	4,4	4,1	4,6	9,6
Pancreas	5,0E-03	4,9E-03	6,9E-03	7,7E-03	5,7E-02	2,5	2,5	3,5	3,9	4,6
Red marrow	3,9E-03	3,8E-03	5,0E-03	5,5E-03	1,1E-01	2,0	1,9	2,5	2,8	8,8
Skin	1,4E-02	2,0E-03	2,9E-03	3,1E-03	2,1E-02	7,0	1,0	1,5	1,6	1,7
Spleen	4,1E-03	3,9E-03	5,8E-03	6,5E-03	1,2E-01	2,1	2,0	2,9	3,3	9,6
Testes	3,4E-03	3,1E-03	3,7E-03	3,8E-03	1,8E-01	1,7	1,6	1,9	1,9	14,4
Thymus	3,3E-03	2,8E-03	4,0E-03	4,1E-03	3,6E-02	1,7	1,4	2,0	2,1	2,9
Thyroid	4,7E-03	5,5E-03	4,4E-03	5,3E-03	2,2E-01	2,4	2,8	2,2	2,7	17,6
Uterus	7,0E-03	7,8E-03	7,2E-03	7,8E-03	5,0E-02	3,5	3,9	3,6	3,9	4,0
Remainder	3,8E-03	3,8E-03	3,3E-03	3,1E-03	5,4E-02	1,9	1,9	1,7	1,6	4,3
Effective dose	5,8E-03	6,3E-03	6,6E-03	7,0E-03	1,0E-01	2,9	3,2	3,3	3,5	8,2
	mSv/MBq	mSv/MBq	mSv/MBq	mSv/MBq	mSv/MBq	mSv	mSv	mSv	mSv	mSv

* The absorbed doses for a standard examination are calculated using an administered activity of 500 MBq for ^{99m}Tc-labelled tracers and 80 MBq for a single administration of ^{201}Tl.

Table 3. Exposure levels to staff outside nuclear medicine departments and to relatives after myocardial perfusion imaging (adopted from [53])

	^{201}*Tl-chloride*	^{99m}*Tc-sestamibi*/tetrofosmin
Personnel		
Nurses working at a general ward outside nuclear medicine	<0.5 mSv/year	<0.6 mSv/year
Doctors		
General ward	<0.05 mSv/year	0.1 mSv/year
Special functions	<0.1 mSv/year	1.1 mSv/year
Relatives or "helpers"		
In the hospital/at home	0.002 mSv/patient	<0.010 mSv/patient

Stress tests

In patients with suspected or known coronary artery disease (CAD) dynamic exercise is the first test of choice. However, patients must be able to exercise to a workload of at least 85% of age-adjusted maximal predicted heart rate (220-age) (Fig. 1; Table 4).

Dynamic exercise should not be performed in patients who cannot achieve an adequate haemodynamic response because of non-cardiac limitations including lung diseases, peripheral vascular disease, musculoskeletal diseases, neurological diseases or poor motivation. These patients should undergo pharmacological stress perfusion testing. There are two groups of medication that can be used for pharmacological stress: (1) the vasodilators adenosine, regadenoson, and dipyridamole and (2) the sympathomimetic agent dobutamine.

All stress procedures must be supervised by a qualified and appropriately trained health-care professional being either physician, nurse or technician [55]. Nonmedical staff (depending on national regulations) has to operate according to the locally approved procedure and may commonly work under the direct or indirect supervision of a physician. The staff must be experienced in the selection of the most appropriate form of stress for the clinical question being asked and must have the clinical skills to recognize patients with an increased risk of complications. Appropriate facilities for cardiopulmonary resuscitation must be available and the staff must have up-to-date knowledge of advanced life support (ALS) techniques or intermediate life support and immediate access to personnel with ALS expertise [55].

Preparations before a stress study:

- Clinical history should be obtained, including the indication for the test, symptoms, risk factors, medication and prior diagnostic or therapeutic procedures
- In diabetic patients, diet and insulin dosing should be optimized on the day of examination. In selected, insulin treated patients, it may be useful to check blood sugar concentration before an exercise stress test
- Patients should be haemodynamically and clinically stable for a minimum of 48 h prior to the test
- Cardiac medications, which may interfere with the stress test, should be interrupted, if possible (Table 5). In general, the decision on whether to interrupt drug administration should be left to the referring physician in agreement with the nuclear physician, and such interruption should ideally last for three to five half-lives of the drug
- Caffeine-containing beverages (coffee, tea, cola etc.), foods (chocolate etc.) and caffeine-containing medicaments (some pain relievers, stimulants and weight-control drugs) must be

discontinued for at least 12 h prior to stress testing as they antagonize the vasodilator effects; this should be a recommendation for every patient in order not to rule out any of the stress modalities. In exceptional cases, an increased adenosine dose, may overcome caffeine antagonism [56]. However, only a few high volume centres have experience with these dosages

- Methylxanthine containing medications must be withdrawn in vasodilator stress testing for at least five half-lives
- If pharmacological stress testing is planned, patients should be asked for prior adverse reactions to pharmacological stress agents.

Exercise stress testing procedure

Indications

This document will not review the indications, contraindications or diagnostic criteria for exercise stress testing, since these matters are covered by other specific guidelines [57-59]. Although exercise testing is generally a safe procedure, both myocardial infarction and death have been reported and can be expected to occur at a rate of about 1 per 10,000 tests, depending on the local case mix. Clinical judgment is needed in deciding which patients are appropriate for exercise testing.

The electrocardiogram, heart rate and blood pressure must be recorded during each stage of exercise. The patient should be continuously monitored for transient rhythm disturbances, ST segment changes, other electrocardiographic manifestations of heart diseases and symptoms. A single ECG lead during stress testing is not sufficient for the detection and recognition of arrhythmias or ischaemic patterns, but a twelve lead ECG is recommended.

Equipment and protocols

Both treadmill and bicycle ergometers are used for exercise testing. Several treadmill exercise protocols are available, differing in speed and inclination of the treadmill; the Bruce and modified Bruce protocols are the most widely used. The objective of exercise testing is to maximally increase myocardial oxygen consumption and by this means myocardial perfusion. The applied protocol to achieve this aim is secondary. Usually ≥ 85% of the age-predicted maximum heart rate is the surrogate of maximal myocardial hyperaemia. Beside heart rate there are other determinants of myocardial oxygen consumption and perfusion, such as systolic blood pressure. Thus, the rate pressure product (heart rate x systolic blood pressure) can be applied as another surrogate parameter of myocardial hyperaemia. Values >25,000 mmHg/min indicate good and values > 30,000 mmHg/min excellent hyperaemia [57, 60]. In general, exercise should be symptom limited, with the goal for patients to achieve ≥85% of their age-predicted maximum heart rate. Sometimes an exercise test has to be

terminated before ≥85% of maximal, age-predicted heart rate has been achieved. In this case it is recommended to switch/complement the stress testing modality and to perform a pharmacological stress test (Fig. 1). However, when the patient has the symptoms for which he or she was referred, administration of the radiopharmaceutical should be considered despite the suboptimal increase in heart rate.

Absolute contraindications to maximal, dynamic exercise are:

- Acute coronary syndrome, until the patient has been stable for at least 48 h and the risk is clinically assessed as acceptable
- Acute pulmonary embolism
- Severe pulmonary hypertension
- Acute aortic dissection
- Symptomatic severe aortic stenosis
- Hypertrophic, obstructive cardiomyopathy
- Uncontrolled cardiac arrhythmias causing symptoms or haemodynamic instability
- Acute myocarditis and pericarditis
- Active endocarditis.

Relative contraindications to maximal, dynamic exercise are:

- Patients with decompensated or inadequately controlled congestive heart failure
- Active deep vein thrombophlebitis or deep vein thrombosis
- Left bundle branch block, ventricular paced rhythm
- Hypertension with resting systolic or diastolic blood pressures > 200/110 mmHg
- Recent stroke or transient ischaemic attack
- Moderate to severe aortic stenosis.

A maximal exercise test should adhere to the following steps:

- Before exercise an i.v. cannula should be inserted for radiopharmaceutical injection
- The electrocardiogram must be monitored continuously during the exercise test and for at least 3–5 min of recovery. A 12-lead electrocardiogram print-out/record should be obtained at every stage of exercise, at peak exercise and during recovery (i.e., ideally every min and with the occurrence of special events such arrhythmias etc.)
- The blood pressure should be controlled at least every 2 to 3 min during exercise
- Exercise should be symptom limited, with the goal for the patient to achieve ≥85% of their age-predicted maximum heart rate (220-age)

- The radiopharmaceutical should be injected close to the peak exercise. The patients should be encouraged to continue the exercise for at least 1-2 min after the injection of the radiopharmaceutical.

Absolute indications for early termination of exercise are:

- Marked ST segment depression (≥3 mm)
- Ischaemic ST segment elevation of >1 mm in leads without pathological Q waves
- Appearance of sustained ventricular tachyarrhythmia
- Occurrence of supraventricular tachycardia or atrial fibrillation with a high heart rate response
- A decrease in systolic blood pressure of >20 mmHg, despite increasing work load
- Markedly abnormal increase of blood pressure (systolic blood pressure ≥250 mmHg or diastolic blood pressure ≥130 mmHg)
- Angina sufficient to cause distress to the patient
- Central nervous system symptoms (e.g. ataxia, dizziness or near-syncope)
- Peripheral hypoperfusion (cyanosis or pallor)
- Sustained ventricular tachycardia or fibrillation
- Inability of the patient to continue the test
- Technical difficulties in monitoring ECG or blood pressure.

Relative indications for early termination of exercise are:

- ST segment depression >2 mm horizontal or down-sloping
- Arrhythmias other than sustained ventricular tachycardia (including multifocal premature ventricular contractions (PVCs), triplets of PVCs, heart block or bradyarrhythmias), especially if symptomatic
- Fatigue, dyspnoea, cramp or claudication
- Development of bundle branch block or intraventricular conduction defect that cannot be distinguished from ventricular tachycardia.

Vasodilator stress testing with adenosine, regadenoson or dipyridamole

Mechanism of action

Vasodilators induce myocardial hyperaemia mediated by adenosine receptors independent of myocardial oxygen demand. Only A2A receptors induce coronary vasodilation and hereby a four to five-fold increase in myocardial blood flow in healthy coronary vessels. Beside the A2A receptor adenosine stimulates A1, A2B, and A3 adenosine receptors too, which provoke the adverse effects [61]. Regadenoson is a selective stimulator of the A2A receptor with minimal or no stimulation of the

other adenosine receptor subtypes [61]. Dipyridamole increases the tissue levels of adenosine by preventing the intracellular reuptake and deamination of adenosine [61]. Vasodilators result in a modest increase in heart rate and most often a modest decrease in both systolic and diastolic blood pressures.

Myocardium supplied by a diseased coronary artery has a reduced perfusion reserve and this leads to heterogeneity of perfusion during vasodilation or even to myocardial ischaemia caused by coronary steal. This results in heterogeneous uptake of the radiopharmaceutical.

Caffeine-containing beverages (coffee, tea, cola, etc.), foods (chocolate, etc.), some medicaments (e.g. pain relievers, stimulants and weight control drugs) and methylxanthine-containing medications that antagonise vasodilator action must be discontinued at least 12 h before vasodilator stress and at least five half-lives for long-acting methylxanthines. Dipyridamole or dipyridamole containing medication should be interrupted for at least 24 h (Table 5). Pentoxifylline and clopidogrel need not be discontinued. Ticagrelor, a direct-acting P2Y12-adenosine diphosphate receptor blocker, has been shown to significantly raise adenosine plasma levels so that more frequent and more severe adverse effects in adenosine and dipyridamole stress testing are likely [62, 63]. Interactions with regadenoson have not yet been studied. So far there are still no recommendations for dose adaption of vasodilators in stress testing for patients receiving ticagrelor.

Indications

The indications are the same as for exercise myocardial perfusion imaging but refer to patients not able or expected to be unable to achieve ≥85% of maximal age-predicted heart rate during exercise. Vasodilators (without exercise) should be preferred to exercise in cases of left bundle branch block (Fig. 1). Considering diagnostic performance of myocardial perfusion imaging there is no significant difference among the stress agents and modalities [64-66].

Absolute contraindications to vasodilator stress tests are:

- The same as for an exercise test. However, in acute coronary syndrome including unstable angina, vasodilator stress test may be considered when the patient has been stable for at least 48 h and the clinically assessed risk is deemed acceptable

In addition the following conditions contraindicate a vasodilator test:

- Severe chronic obstructive (in particular bronchospastic) pulmonary disease (COPD)
- Greater than first-degree heart block or sick sinus syndrome, without a pacemaker
- Symptomatic aortic stenosis and hypertrophic obstructive cardiomyopathy

- Systolic blood pressure <90 mmHg
- Cerebral ischaemia.

Relative contraindications to vasodilator stress tests are:

- For adenosine and dipyridamole: Mild to moderate asthma and COPD, cf. "Safety profile adenosine, regadenoson, dipyridamole"
- Severe sinus bradycardia (heart rate <40/min)
- Severe atherosclerotic lesions of extracranial artery
- Use of dipyridamole during the last 24 h (to avoid possible enhancement of the drug effect).

Procedure

An infusion or a syringe pump is necessary for adenosine administration at a constant infusion rate. Either two separate i.v. lines or one i.v. line with a dual-port Y-connector is required to allow injection of the radiopharmaceutical without interruption of the adenosine infusion. Dipyridamole and regadenoson can be administered intravenously by manual injection. A Y-connector is not needed. Electrocardiographic (ECG) and blood pressure monitoring should be carried out as with exercise stress testing.

Combination with low-level exercise

Low-level exercise can be performed routinely in conjunction with vasodilator tests. Low-level exercise significantly reduces the side effects (flushing, dizziness, nausea, headache, vasodilator-induced hypotension) and improves image quality due to lower bowel activity and higher target-background ratio. Accordingly, if possible low-level exercise is recommended in combination with vasodilator stress testing [67, 68]. Low-level exercise is not recommended for patients with left bundle branch block or ventricular paced rhythm (Fig. 1).

Adenosine dose

Adenosine should be given as a continuous infusion at 140 μg/kg/min over 4–6 min with injection of the radiopharmaceutical at 2–3 min (Fig. 2). The infusion should be continued for 2-3 min after the injection of the radiopharmaceutical. For patients at risk of complications (recent ischaemic event, borderline hypotension, inadequately controlled asthma), the infusion can be started at a lower dose (50 μg/kg/min). If this dose is tolerated for 1 min, the rate can be increased to 75, 100 and 140 μg/kg/min at 1-min intervals and then continued for 4 min. The radiopharmaceutical should be injected 1 min after starting the 140 μg/kg/min dose. A shorter duration of infusion may also be effective [69].

Regadenoson dose

Regadenoson is given as a slow bolus over 10 s followed by a 10 s flush of 5 to 10 ml NaCl 0.9%, 10 to 20 s later the radiopharmaceutical is injected (Fig. 3). Regadenoson is administered independent of patient weight in a dose of 0.4 mg in 5 ml.

Dipyridamole dose

Dipyridamole should be given as a continuous infusion at 140 μg/kg/min over 4 min. The radiopharmaceutical is injected 3–5 min after the completion of the infusion (Fig. 4). Dipyridamole is not licensed in all European countries (e.g. not in Germany) for myocardial perfusion stress testing.

Early termination of a vasodilator stress test

Vasodilators should be stopped early under the following circumstances:

- Severe hypotension (systolic blood pressure <80 mmHg)
- Persistent second-degree or sign of third-degree atrioventricular or sino-atrial block
- Wheezing
- Severe chest pain.

Safety profile

Adenosine

Minor side effects are common and occur in approximately 80% of patients. The common side effects are flushing (35–40%), chest pain (25–30%), dyspnea (20%), dizziness (7%), nausea (5%) and symptomatic hypotension (5%). Chest pain is non-specific and does not necessarily indicate myocardial ischaemia. High-degree atrioventricular (AV) and sino-atrial (SA) block occurs in approximately 7% of cases, ST segment depression ≥1 mm in 15–20% of cases. However, unlike chest pain, this is indicative of myocardial ischaemia. Fatal or nonfatal myocardial infarction is rare, the reported incidence being less than 1 in 1,000 cases. Because of the very short half-life of adenosine (<10 s), most side effects resolve rapidly on discontinuing the infusion. Theophylline or aminophylline are only rarely required [70].

Regadenoson

Compared to adenosine, regadenoson is associated with a lower incidence of chest pain, flushing, and throat, neck, or jaw pain, a higher incidence of headache and gastrointestinal discomfort and a lower combined symptom score in nearly all subgroups [71]. The safety of regadenoson was also studied in two randomized, double-blind, placebo-controlled crossover trials in patients with mild to moderate

asthma and moderate to severe COPD, respectively. Although dyspnoea was reported in respectively the regadenoson groups compared to none in the placebo groups there was no relation with a decline in forced expiratory volume in 1 s (FEV1) [72, 73]. Thus, regadenoson is also applicable in patients with mild asthma and COPD. In summary, despite their selectivity to the A2A receptor, side effects related to activation of the other adenosine receptors continue to occur albeit at a lower frequency and with less severity and duration compared to the selective adenosine agonists.

A less frequent but important side effect of regadenoson is the increased incidence of seizures. The exact incidence is unknown and the pathophysiological mechanism behind this increased incidence is not yet clear. Regadenoson may lower seizure threshold and aminophylline should not be used in cases of seizures associated with regadenoson. These seizures may be of new onset, or may be recurrences. In addition, some seizures are prolonged and may require urgent anticonvulsive management. It is recommended that during the initial triaging of patients, they should be asked about a history of seizures [74-76].

According to the available limited data, the absolute risk of transient ischaemic attack (TIA) and cerebrovascular accident (CVA) associated with regadenoson administration appears to be small and may not be different from other stress agents [77]. However, based on a recent advice of the European Medicines Agency a Direct Healthcare Professional Communication updated the regadenoson product information [78]:

- As aminophylline increases the risk of prolongation of a regadenoson induced seizure, and should therefore not be administered solely for the purpose of terminating a seizure induced by regadenoson
- Delay regadenoson administration in patients with elevated blood pressure until the latter is well controlled
- There is a rare but undesirable risk of a TIA and CVA associated with regadenoson administration.

Dipyridamole

More than 50% of patients develop side effects (flushing, chest pain, headache, dizziness or hypotension). The frequency of these side effects is less than that seen with adenosine, but they last longer (15–25 min) and theophylline or aminophylline (125–250 mg, i.v.) may be required, preferably not earlier than 3 min after the injection of the radiopharmaceutical. The incidence of high-degree AV and SA block with dipyridamole is less than that observed with adenosine (2%) [79].

Dobutamine stress testing

Mechanism of action

Dobutamine induces a dose-related increase in myocardial oxygen demand increasing heart rate, blood pressure and myocardial contractility (in severe ischaemic heart disease, contractility may be reduced with high doses of dobutamine). Due to these effects, it causes secondary coronary vasodilation similar to exercise stress. In areas supplied by significantly stenosed coronary arteries, the increase in flow is blunted, i.e. the flow reserve is reduced.

Dobutamine dose

Dobutamine is infused incrementally, starting at a dose of (5 to) 10 μg/kg/min and increasing at 3-5 min intervals to 20, 30 and 40 μg/kg/min. Atropine (0.25 mg i.v., one to three times with 1/2-min intervals) can be added if heart rate does not reach 85% of age-predicted maximal heart rate. β-blockers are dobutamine antagonists and should be discontinued for at least 3 to 4 half-lives before the test.

Indications

Dobutamine is a secondary pharmacological stressor that is used in patients who cannot undergo exercise stress and have contraindications to vasodilator stressors (Fig. 1).

Contraindications to dobutamine:

- The same as for dynamic exercise, cf. above
- In addition, β-blocker medication that has not been or could not be discontinued sufficiently long.

Contraindications to atropine administration under dobutamine stress:

- Narrow angle glaucoma
- Obstructive uropathy, including bladder neck obstruction from prostatic hypertrophy
- Atrial fibrillation with an uncontrolled heart rate
- Obstructive gastrointestinal disease or paralytic ileus.

Procedure

An infusion pump is necessary for dobutamine administration. Two separate i.v. lines or one i.v. line with a Y-connector is required for injection of radioisotope during dobutamine infusion. ECG monitoring and blood pressure monitoring should be performed as with other pharmacological stressors. Dobutamine infusion should start at a dose of (5–)10 μg/kg/min. The dobutamine dose should then be increased at 3-5 min intervals up to a maximum of 40 μg/kg/min. The

radiopharmaceutical should be injected when the heart rate is ≥85% of the age-predicted maximum heart rate (220-age). Dobutamine infusion should be continued for 2 min after the radiopharmaceutical injection. Atropine can be given in the presence of submaximal heart rate response (0.25 mg, i.v., one to three times with 1/2-min intervals) (Fig. 5) [80]. Patients should be informed of possible difficulties while driving in the 2 h following atropine administration due to reduced ocular accommodation.

Early termination of dobutamine

The indications for early termination of dobutamine are similar to those for exercise stress. Termination due to ventricular tachycardia or ST segment elevation is more likely with dobutamine than with other stressors.

Safety profile

Dobutamine has a relatively rapid onset and cessation of action (plasma half-life of 120 s), allowing control of its effects. Side effects occur in about 75% of patients. Most common are palpitation (29%), chest pain (31%), headache (14%), flushing (14%), dyspnoea (14%) and significant supraventricular or ventricular arrhythmias (8–10%). Ischaemic ST segment depression occurs in approximately one-third of patients undergoing dobutamine infusion. Severe side effects may require i.v. administration of a selective β-blocker such as esmolol (0.5 mg/kg over 1 min) or metoprolol (1 to 5 mg). Hypotension can also occur during dobutamine infusion and may indicate severe ischaemia.

Table 4. Types of stress tests used in myocardial perfusion imaging

Stress type		
Exercise		Bicycle stress
		Treadmill stress
Pharmacological	Vasodilation*	Adenosine
		Regadenoson
		Dipyridamole
	Sympathomimetic[$]	Dobutamine

* Consider to combine with low-level exercise. Except for patients with LBBB.

[$] Add atropine if necessary.

Table 5. Discontinuation of medication and food/beverage before stress testing

Medication	*Exercise*	*Vasodilator*	*Dobutamine (±atropine)*
Nitrates	interrupt (3-5 half-lives)	interrupt (3-5 half-lives)	interrupt (3-5 half-lives)
Beta blockers	interrupt (3-5 half-lives)	interruption recommended (3-5 half-lives)	interrupt (3-5 half-lives)
Calcium antagonists	interrupt (3-5 half-lives)	interruption recommended (3-5 half-lives)	interrupt (3-5 half-lives)
Drugs, food, beverages with caffeine	continue*	interrupt (> 12 h prior to stress)	continue*
Drugs, food, beverages with methylxanthines	continue*	interrupt (> 12 h prior to stress)	continue*
Dipyridamole	continue*	interrupt (> 24 h prior to stress)	continue*

* In order not to rule out any of the stress modalities it is recommended for every patient to interrupt caffeine-containing beverages (coffee, tea, cola etc.), foods (chocolate etc.) and caffeine-containing medication (some pain relievers, stimulants and weight-control drugs) as they antagonize the vasodilator effects.

Evidence for the significance of interruption of some of the drugs is still limited [81, 82].

Continue: no need to interrupt medication and food/beverage.

Figure 1. Selection of stress test modality

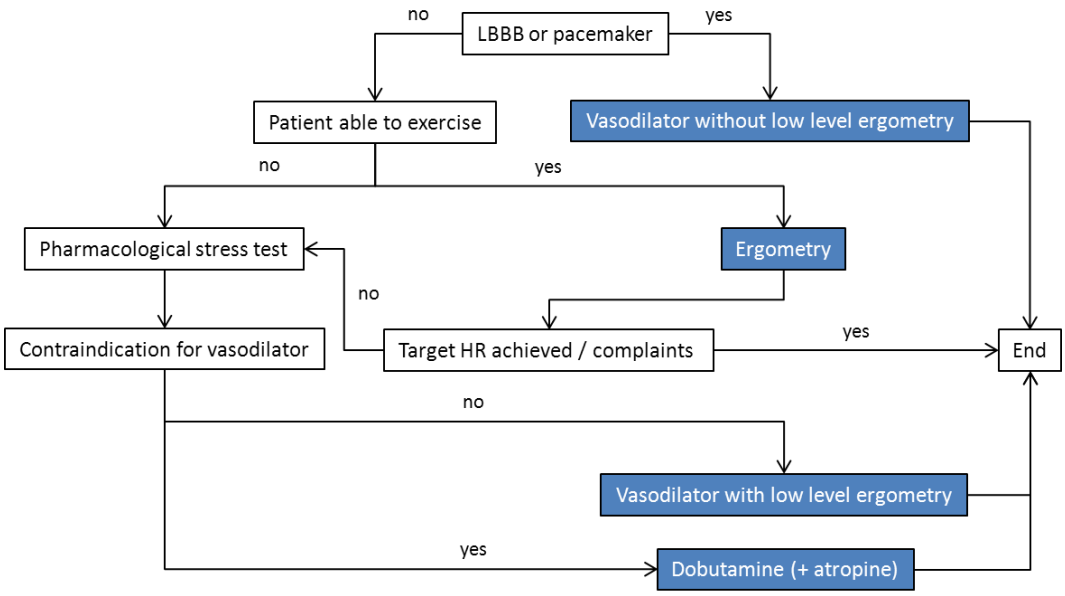

Except for patients with LBBB, consider to combine pharmacological vasodilatory stress with low-level exercise according to the ability of the patient to exercise. In case of pharmacological stress with dobutamine but without adequate heart rate response consider to add atropine.

Figure 2. Timeline of adenosine plus low-level exercise testing

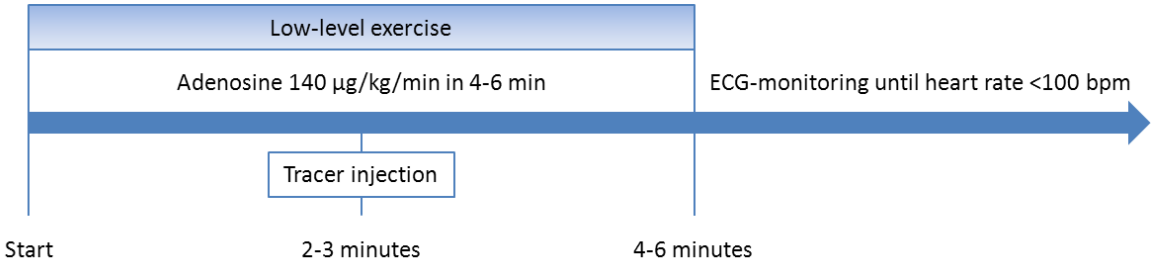

Figure 3. Timeline of regadenoson plus low-level exercise testing

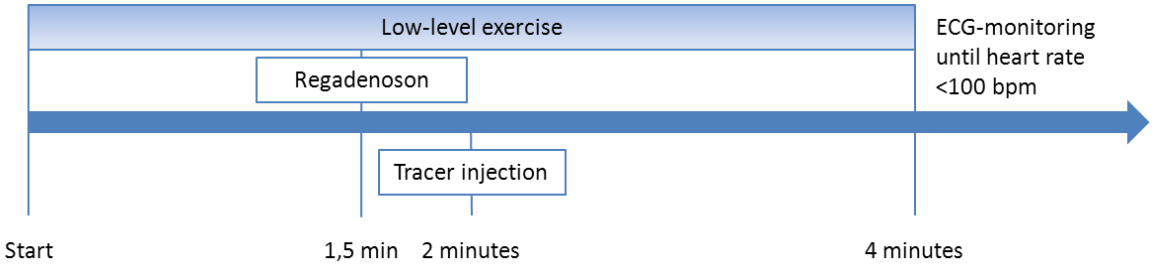

Figure 4. Timeline of dipyridamole plus low-level exercise testing

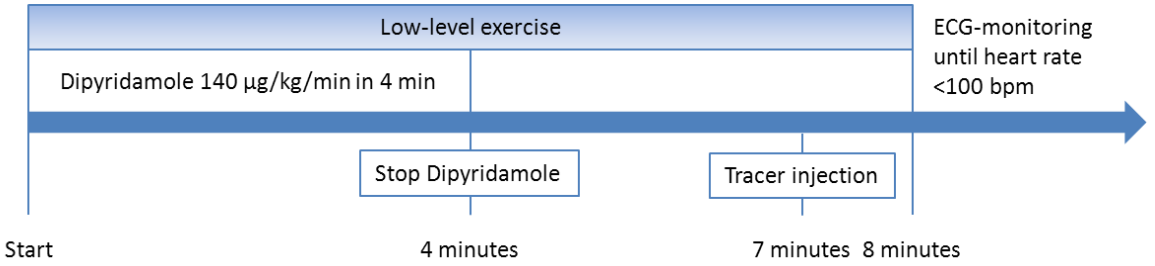

Figure 5. Timeline of dobutamine plus atropine stress testing

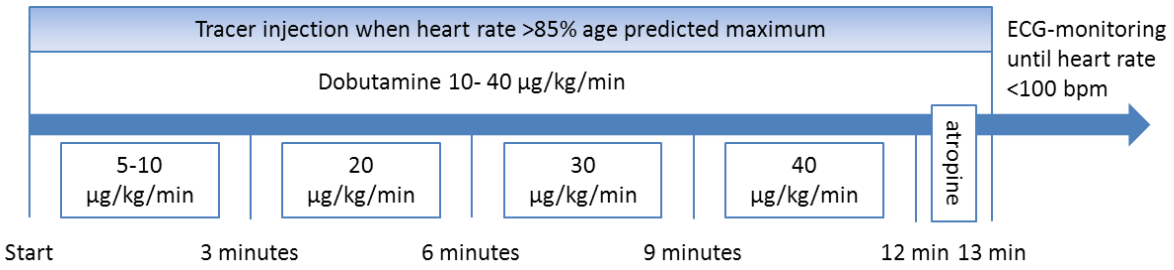

Instrumentation

MPI is usually performed on a traditional, multiple-head SPECT system with NaI (Tl)-crystals capable of ECG gating. Single-head systems are not considered state of the art anymore due to lower sensitivity and specificity, longer acquisition time and, thus an increased risk of patient motion. If available, attenuation correction is recommended.

SPECT

Detectors

MPI may be performed using a dual- or triple-head camera. Dual-detector systems should be in a 90° or "L" configuration if they are to be used for 180° scanning. In new-generation, dedicated cardiac, ultrafast-acquisition scanners, multiple detectors surrounding the patient simultaneously image the heart. Variations in these new design dedicated cardiac scanners comprise the number and type of scanning or stationary detectors and the use of NaI, CsI, or cadmium-zinc-telluride (CZT) solid-state detectors. They all have in common the potential for a 5- to 10-fold increase in count sensitivity at no loss of resolution, resulting in the potential for acquiring a scan in 2 min or less if the patient is injected with a standard dose. Some of this gain in sensitivity can be traded for a linear reduction in the injected dose to reduce the patients' exposure to radiation. With an ultrafast camera with a 10-fold increase in sensitivity using conventional radiopharmaceutical doses, the dose could be reduced by half and a 5-fold increase in sensitivity would still be maintained [83].

Crystals

Anger camera NaI-thallium (Tl) crystals are typically 1/4 to 3/8 inch thick, although they may be as thick as 5/8 in. The thicker the crystal, the greater the sensitivity of the Anger camera, because of the increased probability that a gamma ray passing through the crystal will interact. However, the thicker the crystal, the greater the spread of the emitted light photons produced from the scintillation, and the less precise the computation of gamma ray interaction location resulting in poorer intrinsic resolution of the camera [84]. An array of scintillation crystals is an alternative to the single-crystal Anger camera design. A large number of small crystals (e.g., 6 mm CsI (Tl) cubes) are coated with reflective material and packed into an array. An advantage of this pixelated design is that the scintillation light is much more focused than in an Anger camera.

Collimators

For Anger cameras, parallel-hole collimation is standard. The low-energy, high-resolution collimator is usually best for ^{99m}Tc, although some ''all-purpose'' collimators give excellent results. Imaging

with ^{201}Tl is usually best with the low-energy, medium-resolution (all-purpose) collimators instead of high-resolution collimators because the later limit count statistics.

Energy windows

For most modern Anger cameras, energy resolution is expected to be 9-10% for the 140-keV photons from ^{99m}Tc, and 15-17% for the 72-keV photons from ^{201}Tl. For CZT detectors, an energy resolution of 5 to 6% has been reported for ^{99m}Tc [84].

New developments

General-purpose SPECT systems with large detectors and parallel-hole collimator "waste" a large amount of physical detector area and due to their bulky detector heads, the distance from the heart to the detector is often larger than necessary. Therefore, the development of dedicated cardiac systems has always been an area of interest. Potential benefits include increased patient comfort, shorter acquisition times and/or reduced administered activity.

Since the publication of the first version of this guideline, some significant advances in technology for cardiac imaging have been made [83, 85, 86]. Besides, dedicated systems have emerged based on traditional scintillation detector technology, equipped with smaller crystals and thus having more compact design, as well as truly innovative cameras with a completely novel detector technology. Pixelated, solid-state detectors made of CdZnTe (an alloy of cadmium telluride and zinc telluride, CZT) offer better energy resolution and a virtually linear count rate response. As CZT replaces both the scintillation crystal and the attached photomultiplier tubes, the detectors are very compact. This has so far been exploited in two different, commercially available cameras. The D-SPECT® (Spectrum Dynamics) utilises 9 small rectangular detectors placed along a 90º arc. Each detector rotates around its own axis. All detectors together register photons from an area comparable to a traditional 180º acquisition. The other CZT system (the Discovery NM530c by GE Healthcare) uses a stationary, multiple-pinhole design with 19 holes, each with its own CZT detector. The collimators are arranged such that the area of the chest including the heart can be imaged. Clinical evaluations of both systems have demonstrated similar performance as traditional systems, but with shorter imaging times or lower administered activities [83]. In a recent study the D-SPECT® system was compared to a conventional SPECT camera showing improved image quality, comparable incidence of extracardiac activity, and achieving a reduction in absorbed dose to 1 mSv for a single injection [87].

Another variation from traditional design is the upright patient position offered in a number of dedicated systems. While more comfortable for the patient, the effect of posture on organ position must be considered when interpreting the images [88, 89]. Some cameras systems (e.g. Digirad Cardius) go one step further and employ a rotating patient chair instead of a rotating gantry.

Additionally, CsI(Tl) detectors allow for an optional X-ray based attenuation correction method. Another variation of the upright design (the CardiArc system) is based on three stationary arc-shaped crystals combined with a moving aperture, providing a similar function as a collimator. A problem with many different, dedicated cardiac systems is the scarcity of publications about their clinical validity [83].

An upgraded technology (IQ-SPECT, Siemens Healthcare) uses a conventional multi-purpose SPECT system with a radially symmetric, cardio-focal collimator that is characterised by a radially increasing focal spot distance. The proprietary reconstruction algorithm matches the collimators' spatially varying sensitivity profile. Reductions in acquisition time with no loss in image quality are claimed, but the clinical evidence is limited.

Camera vendors and various third party companies provide reconstruction software that implements iterative reconstruction based on Ordered Subset Expectation Maximisation (OS-EM). The advantage of these algorithms over traditional Filtered back projection (FBP, cf. also the section on "Reconstruction") is that information about the camera, patient and radiopharmaceutical can be exploited to reconstruct better images. CT images can be incorporated for estimation of attenuation and scatter; the collimator-detector-response can be modelled and used for resolution recovery; noise can be compensated by modelling the underlying characteristics of the decay process.

These reconstruction methods can achieve enhanced image quality that may be traded against shorter acquisition times or reduced administered activity. Fundamental to all these algorithms is that the correct choice of user-selectable parameters (typically number of iterations and subsets, regularisation, and filter parameters) is crucial for their potential benefit. Inadequate parameters most likely lead to insufficient image quality and artefacts. As implementations vary considerably across vendors, it is not possible to transfer settings between camera systems without prior validation.

Imaging protocols

^{99m}Tc-tracer protocols are described first, followed by ^{201}Tl protocols, dual-isotope, SPECT/CT and finally gated MPI. A summary of the drawbacks of different SPECT imaging protocols is given in Table 6.

^{99m}Tc-sestamibi and ^{99m}Tc-tetrofosmin

The ^{99m}Tc-labelled myocardial perfusion tracers exhibit minimal redistribution over time (particularly tetrofosmin), i.e., once these tracers are taken up by the myocytes they retain within these cells. Therefore separate injections are given in order to assess stress and resting perfusion. The 6-h half-life of ^{99m}Tc means that the two studies should ideally be performed on separate days to allow for the decay of activity from the first injection. However, different imaging protocols can be followed: 2-day, same-day (i.e. 1-day) stress–rest or same-day rest–stress protocols.

Two-day protocol

A 2-day protocol is preferable because it facilitates comparison between the rest and the stress studies and in addition, keeping the total radiation burden to the patient (and the staff) at a lower level compared with same-day protocols. The stress study should usually be performed first, since the rest study can be omitted if the stress study is interpreted as normal.

Same-day (1-day) protocol

The order of studies in a single-day protocol depends to some extent on the indication for the investigation. If the problem is to detect viable myocardium and reversibility of a defect, in a patient with previous infarction, it may be theoretically preferable to perform the rest study first. Conversely, when the study is performed for the diagnosis of myocardial ischaemia, the stress study should be performed first. Because this both avoids reduction of the contrast of a stress-induced defect by a previous normal rest study [90] and also obviates the need for an unnecessary rest study, if the rest scan is normal.

Semiconductor detectors can allow for a 1-day MPI protocol with low dose both during stress and at rest by subtraction of background activity of the preceding stress scan [33, 35].

Timing of imaging

Imaging should begin 15–60 min after injection to allow for hepatobiliary clearance; longer delays or repeated imaging are occasionally required for rest images and for stress images after vasodilators alone because of the risk of higher sub-diaphragmatic ^{99m}Tc activity.

Nitrates

To improve myocardial perfusion at rest, it is advocated to give the injections for the rest examination under nitrate cover. This is especially important when assessing myocardial viability because viability can be underestimated in areas with reduced resting perfusion [6, 91]. Sublingual nitroglycerine, usually at a dose of 400–800 μg, can be administered at least 5 min beforehand in order to improve rest perfusion and to increase the correspondence of the rest images with myocardial viability. Other nitrates such as buccal isosorbide dinitrate may also be used and these are ideally given (as with nitroglycerine) with the patient in a sitting or supine position to avoid symptomatic hypotension. If a resting study is planned to be performed under nitrate cover, phosphodiesterase use should be discontinued for 24-48 h prior to the myocardial perfusion imaging study.

Fluid intake

Fluid intake has been recommended to remove intestinal activity from the subdiaphragmatic region. Moreover, in some centres a fatty meal, water or coffee is offered between injection and imaging to aid clearance of tracer from the liver and gallbladder. The value of these interventions, however, are uncertain, and it may be counterproductive if there is retrograde passage of tracer from duodenum to stomach or if the tracer reaches the transverse colon [92, 93].

^{201}Tl

After an i.v. injection of ^{201}Tl at stress, the radiotracer is distributed in the myocardium according to myocardial perfusion and viability. ^{201}Tl subsequently redistributes from its initial distribution over several hours, thus allowing redistribution images, which reflect baseline perfusion and viability. Images can usually be acquired 3–4 h later. In some cases redistribution may be incomplete at 4 h. A second injection of ^{201}Tl can then be given and reinjection images acquired for a more accurate assessment of myocardial viability [8].

Different imaging protocols can be followed, depending on clinical indication(s) and local practices: stress redistribution, stress re-injection, stress redistribution–re-injection or stress re-injection–delayed 24-h imaging as briefly mentioned below.

Stress imaging

This should begin within 5–10 min of tracer injection and should be completed within 30 min of injection.

Redistribution imaging

Should be performed after 3–4 h of rest.

Re-injection

In patients with severe perfusion defects in the stress images and in patients where redistribution is thought to be incomplete at the time of redistribution imaging, a rest injection can be given (ideally after sublingual nitrates) with re-injection imaging after a further 60 min of redistribution [94]. This protocol is normally sufficient for the assessment of myocardial viability.

Delayed imaging

Imaging can also be performed 24 h after injection using a longer acquisition time for the assessment of myocardial viability.

Nitrates

As with the ^{99m}Tc labelled tracers, if a resting injection is given, for instance in a patient referred for viability evaluation or in a patient with a severe perfusion defect on the stress images, sublingual nitrates help to increase the resting myocardial perfusion and thereby helps to more accurately assess myocardial viability.

Dual-isotope imaging

This protocol is sometimes used to shorten the duration of a full stress-rest or stress-redistribution protocol, and also to take advantage of the superior ability of ^{201}Tl to assess myocardial viability (relative to the ^{99m}Tc labelled tracers), at the same time using ^{99m}Tc to provide, compared to ^{201}Tl, better functional information from ECG-gated imaging [95]. ^{201}Tl is injected at rest with imaging at 30–120 min, and sestamibi or tetrofosmin is then used for stress imaging. The disadvantages are the added expense and radiation burden of the two tracers, and the fact that changes between stress and rest mean that images of different tracers with different technical characteristics are compared. The advent of technological advances in gamma camera technology, including solid state technology, new collimator designs and incorporation of resolution recovery software, facilitates sequential or even simultaneous acquisition of stress and rest dual-isotope studies. These developments can result in a reduction of total radiation burden to the patient and staff compared to conventional dual-isotope studies, however, as technology is continuously evolving, no recommendations can be made at this stage for dual-isotope imaging protocols.

SPECT/CT

There are different types of integrated CT subsystems commercially available for SPECT/CT hybrid devices, which allow for application of different CT protocols.

- CT for attenuation correction (no contrast media, no ECG-gating, free tidal breathing) Including slowly-rotating, low-current, "non-diagnostic" CT-subsystems like those built into the GE Hawkeye or Philips BrightView XCT
- CT for coronary artery calcium scoring (no contrast media, with ECG-gating, breath-hold) [3]
- Coronary CT angiography (infusion of contrast media, with ECG gating, breath-hold) [3].

In general, it has to be considered that CT imaging is much faster than SPECT, where the heart position is averaged over the complete acquisition time (10-20 min), so that mis-registration artefacts can occur. As a consequence, free-breathing and end-expiratory breath-hold protocols during CT scanning are preferred over inspiration breath-hold protocols when the CT scan is performed for attenuation correction only [96]. General guidelines for CT-based transmission imaging for SPECT are listed in Table 7 [97].

For attenuation correction of perfusion SPECT studies, separate CT scans should be performed for the rest and stress MPI studies, even if recent studies demonstrate that the CT transmission scans are interchangeable in specific clinical settings [98]. Other recent studies have demonstrated that the CT scan can be used to approximate the extent of coronary calcification [99]. This approach, however, is less accurate as compared to dedicated calcium scans due to missing correction of the coronary motion and a much lower photon density. Otherwise, the coronary artery calcium score CT scan can be used for attenuation correction, but with the limitation that this scan may not register adequately with SPECT due to different acquisition time points [100, 101]. These are topics of ongoing research and software developments.

For detailed acquisition protocols of the coronary artery calcium scan and CCTA we refer to the joint position statement by the EANM, the ESCR and the European Council of Nuclear Cardiology [3].

Gated myocardial perfusion imaging

Myocardial perfusion studies should be acquired in a gated mode using an ECG-trigger. This subject will be discussed in further detail in the sections "Image acquisition: SPECT, SPECT/CT and gated SPECT" and "Data Analysis of left ventricular function". In general, when perfusion SPECT studies are acquired in an ECG-triggered, "gated" mode, three important advantages include:

- Evaluation of LV ejection fraction (EF), volumes and evaluation of LV regional wall motion and thickening as well as diastolic function
- Improvement of the diagnostic accuracy of perfusion imaging in the event of attenuation problems (apparently irreversible perfusion defects due to attenuation artefacts may be recognized as wrongly interpreted scar tissue, when function is maintained) [102]
- Performance of phase analysis for assessment of LV dyssynchrony.

Table 6. Disadvantages associated with different imaging protocols

Protocol	*Disadvantages*
^{99m}Tc-labelled tracers	
General	Tracer uptake often (rest and pharmacological stress studies) high in subdiaphragmatic regions with extracardiac activity
2-day stress/rest protocol	Logistics: patient must come on two different days if stress study is not normal
1-day stress/rest protocol	Reversibility may be underestimated without nitrates, if stress study is not normal
	Two tracer injections necessary, also with normal stress study
1-day rest/stress protocol	Stress defects less clearly visualised (interference with remaining myocardial activity from the rest study
^{201}Tl stress	
4-h redistribution	Attenuation artefacts may complicate evaluation of tracer distribution
	Evaluation of LVEF and wall motion is inferior compared with ^{99m}Tc-labelled tracers
	Absorbed dose to patient higher than with ^{99m}Tc
4- and 24-h redistribution	Logistics: patient must come on two different days
Re-injection	Additional absorbed dose
Dual-isotope protocol	
	Comparison of ^{201}Tl and ^{99m}Tc tracer uptake may be influenced by differences in attenuation and spill-over from extracardiac activity
	Absorbed dose to patient higher than with single ^{99m}Tc protocols

Table 7. General guidelines for CT-based transmission imaging for SPECT [97]

CT parameter	*General principle*	*Effect on patient absorbed dose*
Slice collimation	Collimation should approximate slice thickness of SPECT (e.g., 4–5 mm)	Thinner collimation often less dose efficient
Gantry rotation speed	Slower rotation helps blurring cardiac motion (e.g. 1 s/revolution or slower)	Increased radiation with slower gantry rotation
Table feed per gantry rotation (pitch)	Pitch should be relatively high (e.g., 1:1)	Inversely related to pitch
ECG gating	ECG gating is not recommended	Decreased without ECG gating
Tube potential	80–140 kVp is used, depending on manufacturer specification	Increases with higher kVp
Tube current	Because scan is acquired only for attenuation correction, low tube current is preferred (10-20 mA)	Increases with higher mA
Breathing instructions	End-expiration breath-hold or shallow free breathing is preferred	No effect
Reconstructed slice thickness	Thickness should approximate slice thickness of SPECT (e.g. 4–7 mm)	No effect

Image acquisition: SPECT, SPECT/CT and gated SPECT

As already stated in the section "Instrumentation" myocardial perfusion imaging is most commonly performed on a dual-head SPECT system with rotating detectors and NaI(Tl)-crystals. In this section the different patient related factors and SPECT related parameters influencing image acquisition are discussed.

SPECT

Patient positioning

Factors influencing patient position include camera/gantry design, minimization of artefacts, and patient comfort. The supine position with the arms raised above the head is routinely used for SPECT imaging with most currently available systems and protocols [103]. Prone imaging has been reported to reduce patient motion and attenuation of the inferior wall compared to supine imaging [104]. When no ECG-gating is performed, the combination of supine and prone images may be helpful. With this approach, attenuation artefacts due to breast and/or excessive lateral chest-wall fat can be identified due to the shift in position of the attenuating structures that occur in the prone position. Prone imaging does not eliminate attenuation artefacts, but simply changes the location. By comparing supine and prone images, artefactual defects will change their location whereas true perfusion defects will remain fixed [105]. When being used in this fashion, the acquisition time for a secondary (prone) image set is reduced by 20-40% [84]. It is important that comparison of the rest and stress studies is done with the patient in the same position. It has been demonstrated that prone imaging may be associated with artefactual, anteroseptal defects due to the more pronounced sternal attenuation in this position [106]. With this approach, supine and prone images need to be compared to their respective normal databases and only regions found concordantly abnormal by both positions are considered abnormal.

Camera orbit

For rotating detector systems, the main orbit options for cardiac SPECT imaging are circular, elliptical or body-contoured orbits. While conventional SPECT acquisition has been performed by rotating the detector(s) along circular orbits, recent trends in instrumentation (dual-detector cameras with 90° detectors), protocols (combined emission/transmission), and algorithms (attenuation, scatter, and resolution correction) are increasingly requiring noncircular orbits, i.e. elliptical or patient-contoured [105]. Circular orbits maintain a fixed radius of rotation so that all projection images have approximately the same resolution, given their fairly constant distance from the imaged heart. In general there is reduced (but more uniform) spatial resolution since the detector-to-source distance is greater. Conversely, non-circular orbits have the advantage of minimizing the distance between the

patient and the camera throughout the scan but may suffer from reconstruction artefacts due to changes in spatial resolution [107]. Data in favour of the circular orbit do not take into account the recent software compensations for variations in resolution with distance from the patient.

Angular sampling range

Because of the anterior position of the heart in the left hemi-thorax, the preferred orbit or angular sample range is 180° from 45° right anterior oblique (RAO) to 45° left posterior oblique (LPO). The recommended orbit range is largely dependent on the camera configuration [84]. For a 180° acquisition dual detectors should be in 90° or "L" configuration. For triple-head systems, 360° rotation is used. 180° acquisitions generally give higher contrast resolution but more geometric distortions than the 360° orbit. This is especially true for the relatively low energy photons from ^{201}Tl.

Pixel and matrix size

For current SPECT imaging system, the imaging resolution is between 13 and 16 mm [84]. The standard matrix size is 64x64 or 128x128 pixel, depending on the field of view and zoom factor. For spatial sampling, it is recommended to have two or three pixels over the imaging resolution, which provides a usable pixel range of 4.5-7.0 mm per pixel. The pixel size of 6.4±0.4 mm for a 64x64 image matrix has been extensively used in the currently available systems.

Acquisition type

The most commonly used acquisition mode of tomographic system with rotating heads is the "step-and-shoot" method. In this approach, the camera acquires a projection, but interrupts data recording during rotation to the next angle. An alternative is the "continuous" mode where the camera moves continuously and acquires each projection over an angular increment. This increases image counts at the expense of a small amount of blurring due to the motion of the camera head during image acquisition. It seems likely that the increase in count statistics counterweights the small amount of blurring due to camera motion. A combined acquisition mode is called "continuous step-and-shoot" acquisition.

Number of projections

For ^{99m}Tc, 64 or 128 views over 180° or 128 views over 360° are recommended [108]. For ^{201}Tl 32 views over 180° is sufficient, but 64 views may be used. For non-rotating systems the number of projections is dependent on the imaging system and the choice should consider the manufacturer's recommendation.

Time per projection and length of acquisition

Total acquisition times should be no longer than 20-30 min as they increase the likelihood of patient motion. Using conventional cameras and ^{99m}Tc-labelled tracers 25 s per projection angle is recommended. This time can be reduced for systems with greater sensitivity (e.g. multidetector, half ring) and should be adjusted based on the manufacturer's recommendation and validation of its use. If attenuation correction is performed with transmission sources (e.g. ^{153}Gadolinium, ^{57}Cobalt), the acquisition time increases a little. However, attenuation correction with CT reduces this additional time to around one minute.

Gated SPECT

Patient preparation

For gated acquisition, a 1- or 3-lead ECG is sufficient. The electrodes should be positioned ventrally in supine position or dorsally in prone position. Before the acquisition it is important to verify that the ECG monitor and acquisition display show the same heart rate and stable triggering. Patients with a fairly regular heart rhythm can be easily studied with gated SPECT. Patients with arrhythmias (atrial fibrillation, sinus arrhythmia, frequent premature beats, intermittent and dual-chamber pacing etc.) can also be studied with ECG triggering, if the arrhythmia is not too irregular, but acquisition times will be significantly prolonged with loss of accuracy [2]. Regular brady- or tachycardia (e.g. a-v block, atrial flutter etc.) does not interfere with acquisition of gated SPECT, but may have profound influence on LVEF and volume values observed, mostly due to longer or shorter LV filling intervals.

ECG gating

The gating of a SPECT acquisition is easily implemented using the QRS complex of the ECG signal, since the R-wave corresponds to end-diastole [106]. The gating hardware interfaces with the acquisition computer that controls the gantry. Data corresponding to each frame is automatically sorted by the camera into the appropriate image matrix. The R-wave has to be positive in most triggering systems. Ideally, the R-wave should be at least threefold higher than other positive waves (P and T) and should have the steepest rising slope of the ECG cycle [2].

Number of frames

Using ECG gated SPECT the heartbeat is usually divided into 8 or 16 temporal frames or gates. The R-wave of the QRS complex serves as the signal and starting point (triggering point) of the cardiac cycle. The cardiac cycle is divided into frames representing different phases of the cardiac cycle. After a gated SPECT acquisition with 8 gates and 64 projections, 8 raw data files each with 64 projection images are recorded. While 8-frame gating is still prevalent in gated perfusion SPECT imaging, it is obvious that the cardiac cycle can be more accurately described with more frequent temporal

sampling. Sixteen-frame gating offers the opportunity to assess diastolic left ventricular function. Eight-frame gating seems to be a reasonable compromise between the count statistics that should provide accurate edge definitions of the ventricular walls and the temporal resolution that is required to record the short end-systolic period. Eight-frame gating has a smoothing effect on the time-volume curve compared to 16-frame gating, thus leading to slightly lower end-diastolic volume (EDV), higher end-systolic volume (ESV), and lower LVEF, mainly due to inaccurate definition of ESV [105]. The 8-frame gating rate results in an average LVEF underestimation of 3.7-4 LVEF units in comparison with 16-frame gating [105], but the relationship between the two is predictable and quite uniform over a wide EF range. For both 8- and 16-frame gating, the number of rejected beats should be limited, to below 25%.

The beat length acceptance window

The unavoidable variability of the cardiac beat length during gated acquisitions even in regular heart rhythm has led to the creation of tolerances in the gating process. The beat length acceptance window aims to eliminate data from beats that are "too short" or "too long" while still accepting enough beats. A beat length acceptance window of 20% will allow accumulation of data from cardiac beats having duration within ±10% of the expected average duration. When deciding on setting for the cardiac beat length acceptance window, it is important to remember that a gated SPECT acquisition produces both gated short-axis images (reconstruction and reorientation of projection data of individual gating intervals) and standard short-axis images (reconstruction and reorientation of the sum of projection sets across all intervals). While cardiac function is assessed from the former, myocardial perfusion is derived from the latter. If too many beats are rejected by a narrow window in the presence of arrhythmia or gating problems, it hampers not only the assessment of cardiac function but perfusion data may also be compromised. This may be solved by an "extra frame" (a 9^{th} frame in 8-frame or 17^{th} frame in 16-frame gated SPECT imaging), in which all counts rejected by the acceptance window are stored. Thereby the extra frame can provide a convenient additional tool to assess how many counts were rejected, both globally and on a projection-by-projection basis. With an extra frame available a 20-30% beat acceptance window is recommended [106]. If no extra frame exists, it is advisable to open the acceptance window to 100% (allowing accumulation of data from beats of duration within ±50% of expected beats) or infinity so as to maximize the quality of the perfusion images [106]. As a final note, the premature ventricular contraction (PVC) rejection factor specifies the number of cardiac beats that the camera acquisition software must ignore immediately after a "bad beat". The PVC rejection factor is generally set to 1, meaning that the first beat after a bad beat is also rejected, regardless of its own length.

Time per projection and length of acquisition

Ideally, the length of acquisition (expressed in seconds per projection) for a gated ^{99m}Tc based SPECT study need not exceed that traditionally employed for a non-gated SPECT study [1, 106]. Time per projection must be adjusted to obtain an adequate myocardial count rate per interval, but the total acquisition time should not exceed 30 min due to risk of patient movement.

SPECT/CT

Detectors

The SPECT detectors in most SPECT/CT systems do not differ in any significant way from those of stand-alone SPECT systems. The SPECT sub-systems are typically large field of view (FOV), variable-angle, dual detector system. For hybrid imaging systems, the CT configuration can be a low-resolution CT (non-diagnostic CT) or a multi-detector-row CT with slices ranging from 2 up to 64. Any of these systems can be used for attenuation correction of MPI. For CACS at least 4-slice CT is required (≥6-slice recommended). For CCTA, at least a 16-slice scanner is required (≥64-slice multidetector-row CT recommended), with imaging capability for slice width of 0.4–0.6 mm and temporal resolution of 500 ms or less (≤350 ms is preferred) [109, 110].

Patient preparation

Patient preparation for MPI using hybrid devices is the same as for dedicated nuclear scanners. For MPI and CACS, a small-gauge i.v. line is sufficient. For CCTA a large-gauge, peripheral iv. access line (at least 20-gauge, but ideally 18-gauge) is placed. Moreover, for coronary CCTA studies patients with a history of mild allergy to iodinated contrast material may be pretreated [110] (cf. CCTA contrast agents).

Patient positioning

For MPI, supine (standard) or prone (optional) positioning can be used depending on local preferences [84]. For cardiac CT, supine positioning is standard. Appropriate table centring within the gantry is important to allow for proper function of angular z-axis tube current modulation.

Acquisition

SPECT/CT frequently uses an acquisition protocol that has a 128 × 128 matrix with a zoom factor of 1.0 so that the SPECT images can be registered with the CT. In SPECT/CT the position of the diaphragm on the SPECT should match as closely as possible that on the CT transmission images. Although a diagnostic CT scan of the chest typically is acquired during end-inspiration breath holding, this technique is not optimal for SPECT/CT because it may result in substantial respiratory motion mis-alignment on SPECT and CT images [111]. Between various breathing techniques free tidal

breathing with averaging of respiratory movement appears to be the best technique for attenuation correction by CT.

CT-tube current and voltage

Commonly, the tube current is modified to adjust for patient size/weight and desired image noise. It has been outlined that tube current should only be increased to a level necessary for acquiring images of adequate quality [110]. For cardiac imaging, 100-120 kV tube voltage is sufficient in most patients. Increasing tube voltage to 140 kV leads to a higher energy x-ray beam with better tissue penetration, resulting in a reduction of image noise, but also in substantially higher radiation exposure. In fact, the dose change is approximately proportional to the square of the tube voltage change [110]. For some extremely large patients, an increase in tube voltage to 140 kV may be necessary to achieve acceptable noise levels, but this should be a rare exception. For patients with normal body mass index (BMI) a tube voltage of 80-120 kV maintains adequate contrast-to-noise ratio [112]. Reducing voltage from 120 kV to 100 kV should be considered when BMI is below 30 kg/m^2 [110]. For CT images used for SPECT attenuation correction, it must be assured that the attenuation correction algorithm in the SPECT reconstruction is validated to work with the chosen tube voltage. Available CT dose modulation should be applied if this is supported for attenuation correction. Differences in dose modulation methods between vendors must be considered when re-using protocols from other scanners.

CT data acquisition

CT data acquisition for coronary angiography has seen major improvements over the last decades: Helical acquisition of the entire RR cycle with retrospective ECG gating has widely been replaced by acquisition techniques using prospective ECG triggering, allowing confinement of x-ray tube activation to a pre-specified small end-diastolic window. Prospective triggering allows for a substantial reduction of absorbed dose while maintaining image quality. But it is not applicable when the patient's heart rate remains high (>63 bpm) despite the use of a beta-blocker or in patients with arrhythmias [113, 114]. Prospective ECG triggering with a small acquisition window should be used for CCTA and CACS, whenever possible.

Contrast injection for CT coronary angiography

A dual power injector for administration of iodinated contrast media is required for CCTA examinations [109]. Typical contrast injection rates range from 4 to 6 mL/s dependent on body habitus and cardiac output. For a timing bolus scan, 10-20 mL of iodinated contrast medium is injected followed by an approximately 40 mL isotonic saline flush during an inspiratory breath-hold. Scanning is started 10 s later as a single CT slice at 2 cm above the aortic root, 1 image/2 s. Once the time to

peak contrast opacification in the aorta is determined an additional interval of 3-4 s is added to allow for opacification of the coronary arteries.

Quality control of instrumentation and image acquisition

Quality control (QC) involves the complete patient workflow including preparation, stress test, administration of the radiopharmaceutical, image acquisition, data processing, data interpretation and reporting. In this section, the focus is on the QC of image acquisition hardware, software, and of acquired data.

Gamma camera performance in SPECT mode should be monitored with regular intervals, as outlined in the related EANM guideline [115]. National recommendations and guidelines may demand further procedures. As an absolute minimum, systems should undergo tests checking for uniformity of detector response, geometric accuracy and — if applicable — multi-modality registration (Table 8). For traditional, Anger-style gamma cameras (multiple head, large-field of view NaI crystal detector with photomultiplier tubes), this translates to procedures testing planar uniformity, centre-of-rotation and multi-modality registration. The results must be within the limits imposed by the European Commission [116]. The manufacturers' recommendations should always be followed. An extensive description of these and additional tests are given in the previous version of this guideline and in a description published by the IAEA [1, 117].

Special care must be taken when using ^{201}Tl. Often, standard QC protocols use ^{99m}Tc as activity source, but many corrections are energy-dependent, especially those for uniformity and attenuation correction [1].

The above mentioned tests are designed to measure "raw" hardware performance. Advanced data processing is not incorporated. Thus, a system with adequate hardware performance may still exhibit poor clinical image quality because of incorrectly chosen processing parameters e. g. for iterative reconstruction. A simple way to check for overall correctness of the complete dataflow, is to check the "overall system performance" with a suitable phantom [115]. This phantom should be imaged with the clinically used protocol and reconstructed like a patient dataset. Further data processing should be performed correspondingly. If LVEF is reported in clinical studies, the test should be performed on a phantom with a cardiac inset and include calculation of systolic and diastolic volumes. In that case, an artificial ECG signal has to be recorded during acquisition — unless a gating phantom is available. It is mandatory that the performance of the tests is monitored over time and compared to baseline, especially after updates or service of the system. Experience shows that software patches often are installed silently or without proper and exhaustive description of their functionality.

In daily clinical routine, energy window settings should be checked at the start of each study. After acquisition, patient data should be reviewed immediately – before the patient leaves the department. Cinematic views and sinograms should be checked for blank views, artefacts and motion. Likewise, the reconstructed and reoriented images must be inspected. A common problem is extracardiac "hot

spots" close to the left ventricle. Patients with unusual orientation of the heart may need special processing in order to reorient in short axis and long axis images.

Gated acquisitions require some extra checking: The heart rate histogram should only comprise one narrow peak, the positioning of the systole and diastole in the cardiac cycle should be checked and the ECG data should be reviewed with respect to adequate and constant number of accepted beats along the acquisition arc. Compensation mechanisms may be used during reconstruction. If automatic edge detection is used for calculation of LVEF and similar parameters, endo- and epicardial edge definitions must be reviewed.

For combined modality systems, a critical processing step is alignment between SPECT and CT images before attenuation correction. This step is necessary despite perfect registration of SPECT and CT on phantom data, as motion artefacts (lungs, heart) usually interfere noticeably. The non-attenuation corrected images should be reviewed for QC purposes. Ideally, the additional registration step should be documented on a per-study basis.

In SPECT/CT systems, the CT part is often part of a separate QC scheme. The CT should comply with national and local guidelines. There is, however, general agreement to recommend checking CT number accuracy of water, image noise and uniformity (standard deviation) and artefacts in a water phantom on a daily basis [118]. Other, more advanced but very important QC aspects like dosimetry are beyond the scope of this document.

Table 8. Quality control – on a regular and daily basis and at each study

Regularly (weekly/monthly etc.)	*For each study*
Uniformity of detector response, geometric accuracy, planar uniformity, centre-of-rotation	Before start of study: patient data and energy window settings
Overall system performance	Cinematic views and sinograms should be checked for blank views, artefacts and motion
Daily CT QC (in SPECT/CT): CT number accuracy of water, image noise and uniformity (standard deviation) and artefacts in a water phantom	Reconstructed and reoriented images, extracardiac “hot spots”
For gated studies	Heart rate histogram, positioning of systole and diastole, adequate number of accepted beats
For automatic processing of LVEF	Endo- and epicardial edge definitions
For SPECT/CT	Alignment between CT and SPECT images before attenuation correction

Reconstruction methods

Myocardial perfusion images appear relatively uncomplicated, but they are highly processed and their appearance is a complex interaction of the various processes. Although sophisticated reconstruction methods are available including correction for motion, attenuation and scatter correction, these software tools cannot produce "miracles". It is therefore important to achieve optimal quality of the raw data by selecting the proper matrix size, angular sampling, zoom factor, patient-to-camera distance, energy window settings, and to assure that the camera is properly tuned and maintained through regular QC procedures. In addition, the acquired projection data should be checked for motion and the presence of high extra-cardiac uptake. This should be done before the patient leaves the department and before reconstruction is commenced (Table 9).

Given the measured projection data, which is essentially a collection of line-integrals through the activity distribution inside the patient, perpendicular to the detector for a certain angular direction, the reconstruction task is to produce an image of the activity that as closely as possible reflects the distribution when the measured data was acquired. Today, two main categories of reconstruction methods are available – (a) the analytical back-projection method and (b) the iterative reconstruction methods.

Filtered back-projection

Historically, FBP has been the main method of reconstruction used in SPECT as this was adapted from techniques used previously in other fields such as radioastronomy and electron microscopy [119]. FBP has the advantages of being fast and computationally relatively non-intensive. However, it takes no account of the basic physical processes underpinning emission tomography, which can be incorporated into the alternative iterative algorithms. Assumptions made by FBP are for instance the presence of an infinite number of projection angles, no stochastic noise, no photon attenuation, no scatter, no collimator blurring. Correction for these effects needs to be made pre- or post-reconstruction or is simply not possible. Over the last several years FBP rapidly lost ground to the iterative techniques, which currently is the most frequently used method of SPECT reconstruction.

The filters most common in FBP are generally low-pass filters such as the *Hanning* and *Butterworth* filters combined with the required ramp-filter to eliminate the blurring. These low-pass filters reduce the high spatial frequency components of the image and thus reduce the pixel-to-pixel noise but also at the expense of the spatial resolution in the image. In general, it is recommended to follow the cut-off frequency and power factors (if necessary) in the recommendations of the vendors, if standard doses of radionuclide tracers and imaging techniques are applied, although ideally they should be determined empirically by each department. Such evaluation should be based on the count statistics of an average

study produced by the normal acquisition protocol of the department. Ideally, a *cardiac phantom* should be used to facilitate this optimisation. The phantom can be imaged with and without simulated defects and at a range of count levels around the expected average. Ideally the chosen cut-off frequency should be based on the average count level. The phantom data allow for an estimation of the effects the chosen filter has. The filter should produce images of similar quality over a reasonable range of count levels around the average value. Optimisation should be based on data presented and assessed in the prevailing format used for reporting of the studies.

Negative numbers: These numbers occur in the reconstructed image because of the incomplete ramp-filtering caused by the (for practical reasons) limited number of projection angles. The most common method is to truncate these values to zero. However, this truncation results in the loss of linearity between the counts in the reconstructed images compared to the counts measured in the projection. This loss of linearity is especially of concern when quantification of activity is needed. Related to this, it must be remembered that FBP does not eliminate streak artefacts completely due to the finite number of projection angles, which means that counts will appear outside the body region in the SPECT images (Fig. 6). It should also be noted that in the case of large extra-cardiac activity uptake in the liver or gall bladder artefacts can sometimes be generated, resulting in false defects. This is because relatively large streaks of negative numbers due to the ramp filter pass through the heart region and thus reduce the counts.

Iterative reconstruction methods

The principles: This family of reconstruction methods has only been clinically available in this millennium, due to their computationally intensive nature [120]. The difference between iterative methods and FBP methods is that, in addition to the back-projection step, there is also a forward projecting step ("reprojection"). This step is required to calculate projection data (or line-integrals) along a path from an image matrix defined in the computer, simulating the distribution for which the actual measured SPECT data was obtained. The main idea of iterative reconstruction is to find a source distribution (3D volume) so that corresponding calculated projections agree with the measured projections.

An iterative procedure starts with an initial first guess of the activity distribution. This can be a flat image or an image obtained by FBP. The key feature in an iterative method is then the comparison between the measured projection data and the projection data, calculated from the image matrix. This comparison is often based on calculating the difference or the quota between the measured and the calculated projection bins (ML-EM/OS-EM methods). The difference (or the quota) is then back-projected on the image space along the direction to form an error image. When all of the projection angles have been processed in this way, a correction matrix has been formed that is multiplied with the

initial guess after proper normalisation. An updated image is created and the process has made its first iteration. The new updated version of the activity distribution can then be used as input for the same procedure to form the second (and more accurate) update. This is achieved since the difference between the measured data and calculated projection data will be decreased. After a certain number of iterations have been reached, the difference between the calculated projection and the measured one is assumed to be only a function of image noise, therefore the process is interrupted and the last updated image is used as the final reconstructed image. The flow-chart in Figure 7 summarizes these steps.

The most commonly used iterative methods in commercially available systems are the *Maximum-Likelihood Expectation Maximization (ML-EM)* method and its accelerated version called *Ordered-Subsets Expectation-Maximization (OS-EM)*. The equation that describes the iteration process is given by:

$$I_i^{new} = \frac{I_i^{old}}{\sum_j h_{ji}} \sum_j h_{ji} \frac{P_j}{\sum_k h_{jk} I_k^{old}} \quad (1)$$

where I_i is the i-th iteration of the image to be created, P is the measured projection profile and h_{ij} is the probability (sometimes called the system - or transfer matrix) that the pixel i will contribute to the projection bin j. In its simplest form that assumes no photon attenuation, no scatter contribution nor collimator blur, h_{ij} is unity along the ray-of-view for the current projection angle. This reduces the formula to:

$$I_i^{new} = \frac{I_i^{old}}{\sum_j h_{ji}} \sum_j \frac{P_j}{\sum_k I_k^{old}} \quad (2)$$

The summation term under I_i^{old} is needed because the back-projection step is a summation step and therefore a normalization with the number of projection angles is essential to keep the number of counts in the reconstructed images on the same level as that which was acquired.

ML-EM or OS-EM: The main problem with the ML-EM method has been the long time required to obtain acceptable accuracy in the reconstructed image. A successful method to accelerate the

convergence rate is the OS-EM method [121]. This method is identical to the ML-EM algorithm in its principals but differs in the stage in the process where the image is updated. In the ML-EM algorithm, the image is updated only after all projection angles have been processed (the summations in equation 2 runs over all projection angles). In the OS-EM algorithm, the image is instead updated after a subset of projections has been processed; for each iteration the summation runs over a different subset of projection angles. For example, a common number of subsets are sixteen for a sixty-four projection angle acquisition. Hence, the image is updated after four angles have been processed. The angles inside each subset are usually equidistantly distributed over the projection range for an optimal reconstruction. The acceleration in this method is roughly proportional to the number of subsets. An iteration is defined when all subsets are processed. The process is then repeated for the desired number of iterations. Sometimes, when using OS-EM, the phrase "ML-EM equivalent iterations" is used, which equals the product of the number of subsets and the number of OS-EM iterations. Figure 8 shows an example using images obtained with different iteration numbers for ML-EM and OS-EM.

In contrast to FBP, iterative methods generally do not have a clear definition of the point at which the images can be regarded as final. The number of necessary iterations depends on the method of choice and/or on the image noise. An increasing number of iterations generally leads to an increase of the likelihood of the reconstructed image belonging to the measured projections; however the amount of noise also increases up to a point that post-filtering might be required.

The physics model behind: It must be noted that the accuracy of the image strongly depends on the accuracy of the physics model used in the projection and (to a lesser extent) on the back-projection step. This means that if physical degradation factors are present in the measured projections, but not accounted for in the calculated projections, then the final image will not be correct. The results may include artefacts due to this iterative process that subsequently may result in a false positive judgement. However, the iterative process is well suitable to include physical effects, such as photon attenuation and contributions from photons scattered in the patient. The effect of photon attenuation can be included in the h function by calculation of the exponential between the current pixel location and the surface before summation of pixel values along the ray-of-view. This can be done either by using a fixed attenuation coefficient or by including a matched attenuation map, obtained by e.g. transmission SPECT or from a registered CT study. Thus, a non-homogeneous attenuation correction can then be incorporated in the forward projector step. The accuracy of such an attenuation correction is then mostly dependent on the accuracy of the obtained attenuation values. The collimator response can be included in h_{ij} by calculating the contribution (the probability of detection) in other projection bins from voxel i.

Filtering

The filter cut-off should not be varied routinely, as this may lead to separate parts of the same study being reconstructed and compared using different parameters. If a study appears to be of low counts the acquisition time, if possible, should be adjusted, to collect approximately the average count level, rather than altering filter parameters. Different filter parameters should be used with each isotope. ^{201}Tl myocardial perfusion images will generally require a smoother filter than those used with ^{99m}Tc-labelled radiopharmaceuticals due to the lower count levels obtained with thallium.

Filter definition: Care must be exercised when filter parameters from one manufacturer's system are compared with those from another system. The mathematical definition of the filter window may vary between different systems, e.g. the definition of the cut-off value of the *Butterworth* filter. The correct definition of the cut-off for this filter is the point at which the amplitude drops to $1/\sqrt{2}$, or 0.707 [122]. However, some manufacturers use simplified definitions of this filter where the cut-off is the point at which the amplitude drops to 0.5, or rolls-off to zero.

The use of *adaptive resolution recovery filters* should also be treated with care. These filters are used as constraining operators on the inverse filter. The inverse filter is essentially the reciprocal of the point-spread response function of the camera system. In theory deconvolution with this filter should produce ideal images with the degrading effects of the imaging process removed. However, this is impractical due to the high levels of noise amplification produced with clinical data. The adaptive filters constrain the inverse filter at high spatial frequencies and allow its use as a clinical filter.

The *Metz*, and more commonly, the *Wiener* filters are the functions generally used for constraining the inverse filter. These have been shown to improve quantification with myocardial perfusion SPECT in certain cases [123]. However, the power factors for these filters are dependent upon the properties of the noise power spectrum of the data. Therefore, the choice of a single power factor that will be applicable over a clinically realistic range of count levels is problematic. The use of an incorrect power factor can lead to erroneous enhancement of sections of the image spectrum [124], and introduce apparent defects (Fig. 9). For these reasons these filters should only be used by persons with expertise within this field.

Iterative reconstruction methods do not require a filtering step like the ramp-filter in FBP. If the acquired data are noisy, one can apply a low-pass 2D filter on the projection data or a 3D post-filter on the tomographic images. The same guidelines, as given above, are also applicable to iterative reconstruction methods.

The process of *resolution recovery* implemented in many commercial systems today also result in smoothing of the data since the resolution is modelled as a distance-dependent Gaussian function (i.e. a type of low-pass filter). Therefore, one should always investigate from tests or experimental

phantom measurements, whether or not an additional post-filter is required. Also, a combination of a general purpose collimator with a well-functioning collimator resolution recovery method may give comparable images as when using a high resolution collimator, but with better noise characteristics because of the higher geometrical sensitivity for such a collimator.

The need for filtering is very closely connected to the selection of acquisition parameters and collimator. One must always bear in mind the trade-off between count statistics and spatial resolution when selecting a protocol for a SPECT study. For example, if the noise in the projection data is such that extensive low-pass filtering is required when using high-resolution collimators, then the final results may appear similar to an acquisition using a general purpose collimator with less filtering applied. Also, the volumetric count statistics is generally reduced by a factor of eight when going from a 64 to 128 projection matrix since the slice thickness of each tomographic image is also reduced by a half. The number of projections will affect the reconstructed image, especially the FBP image, since the ramp filtering is not perfect for a limited number of projections. The streaks appearing in the image can subsequently reduce the contrast in infarcts or ischemic regions or reduce the accuracy in the volume calculation of the left ventricle.

Finally, when considering the choice of low-pass filtering, it must be remembered that the filter reduces the contrast between a defect and the surrounding normal tissue, which for a smaller defect can affect the calculated value of the severity of the defect. The magnitude of the filtering should always be balanced against the level of noise that is acceptable by the reader of the images.

Motion Correction

As mentioned, a number of proprietary motion correction packages are available from manufacturers on modern gamma camera systems. A variety of methods is used to correct for translational motion of the heart during the acquisition. Some methods apply external point sources [125], whilst others use fitting to an idealised sinogram [126]. If an automated method of correction is to be used, the applied algorithm should be tested for its appropriate working mechanism prior to clinical implementation. For example, for some sinogram-based fitting techniques the heart must be positioned away from the centre of the field. If the heart does lie at the centre, then the sinogram will describe a straight line instead of a sine wave and the algorithm may fail.

It should also be noted that these methods will only correct for relatively simple forms of motion. With commercial software systems correction for motion is usually only possible in the longitudinal axis. More complex motion patterns involving rotational motion cannot be adequately corrected using current methods. This may include the relatively common phenomenon of ‘upward creep’ [127]. It is therefore important to minimise motion by ensuring that the patient is comfortable [128]. Previous

work has demonstrated that movement by 1 pixel does not produce significant artefacts in the reconstructed images [126]. Hence it is recommended that only motion by ≥ 2 pixels justifies correction.

Reorientation of image data

Reorientation of the reconstructed transaxial data into the three standard image planes should always be consistent. Errors in reorientation can introduce artefacts, which may be misinterpreted as perfusion defects [129]. Automated methods of reorientation are available and have been shown to be at least as accurate as trained operators [130, 131]. If manual reorientation is chosen, the operators should use reproducible landmarks for definition of the long axes. Common landmarks include the apex and points on the valve plane.

New developments

Over the past few years several new software and detector technologies have been introduced. Two commercial systems, based on CZT solid state detectors, are now clinically available. These systems are dedicated to myocardial perfusion imaging but with completely different detector characteristics as compared to the NaI(Tl) scintillation camera techniques. Currently all major vendors offer the possibility to include resolution recovery (also called count recovery) in the OS-EM/ML-EM algorithm. The increased reconstructed resolution and less noise allows for slightly lower count statistics (hence lower injected dose) or shorter scan times [85]. However, such techniques require careful testing against phantom studies performed with validated hard- and software.

Technical and clinical implementation

In myocardial perfusion SPECT, both FBP and iterative methods are useful and have advantages and disadvantages. Correction for scatter and attenuation when using FBP needs to be done before using geometric-mean calculations on opposite projections [132] or after reconstruction using e.g. the Chang method [133]. Correction of detector blur is also difficult because of its distance dependence. Iterative methods allow the physical processes to be modelled in the projector step and will therefore be superior in correction for non-homogeneous attenuation and detector response. Scatter can be included either by a pre-subtraction step or preferably (due to the decreased noise problems) directly as an additive term in the projection step.

The reconstructed noise in iterative methods is less disturbing than for FBP due to the incomplete ramp filtering. However, in iterative reconstruction noise tends to increase with higher iteration numbers. A regularisation procedure that controls the stopping based on the neighbourhood count difference can be a way of ensuring the reconstruction stops in time. For most cases, the rule-of-thumb

of about 15 iterations for an ML-EM procedure can be applied and is often recommended by commercial vendors [134]. Low-pass *Fourier* filtering can introduce ring artefacts (the Gibbs phenomena) if the filter is not properly selected.

Overall, it is probably now best to use iterative techniques on systems where they are available to take advantage of the more accurate modelling of physical processes and the lower noise. However, FBP should still be used where quantitative comparison with normal databases is used during image assessment and the databases were created using data reconstructed with FBP.

Figure 6. Illustration of the streak artefacts inherent with the filtered back-projection process.

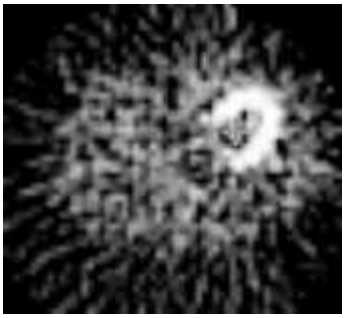

Figure 7. Flow-chart describing the step in an iterative procedure.

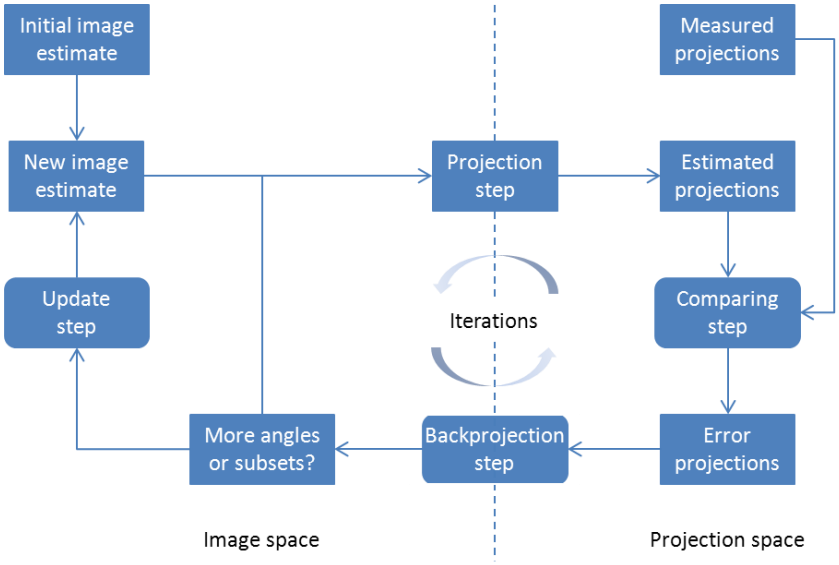

Figure 8. Different iteration numbers for the ML-EM and OS-EM reconstruction methods (64 angles and 16 subsets). Example of images obtained with different iteration numbers for ML-EM in the *upper row* and OS-EM in the *lower row*.

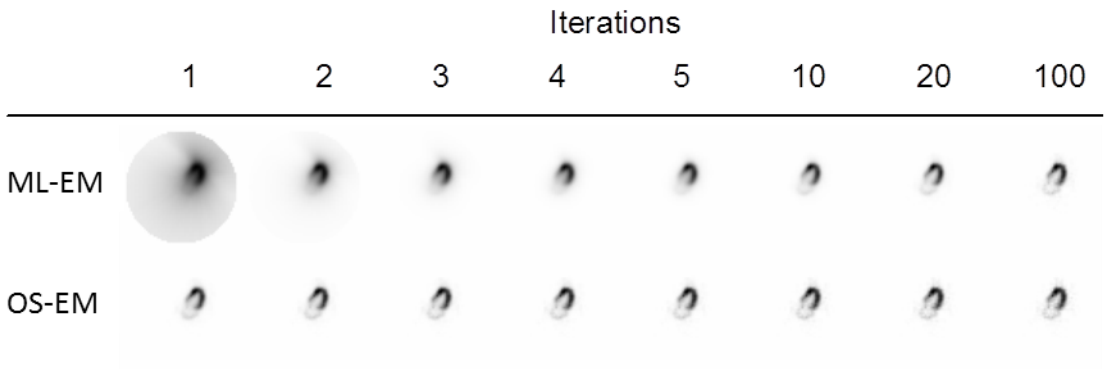

Figure 9. The same short-axis slices through a ventricle reconstructed with a conventional low-pass filter (the left two images) and with a resolution-recovery filter (the right two images).

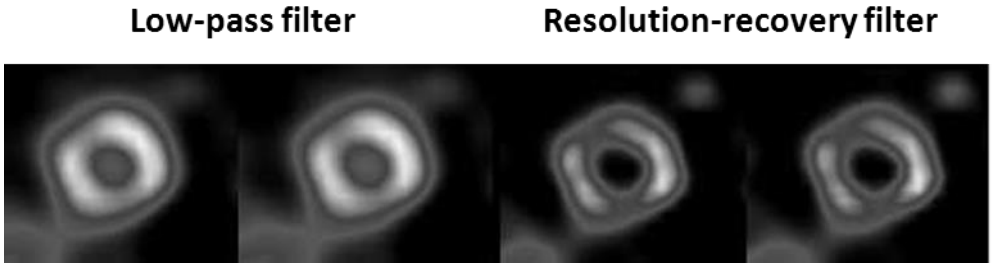

Attenuation and scatter correction

In addition to the pixel size, type of orbit etc., primary factors of concern for image quality are:

- *Attenuation* of photons in the body, which can lead to an apparently non-uniform distribution of activity in the myocardium and to the introduction of artefacts in the images
- Contribution of events in the image due to *scattering* of photons both within the body and in the detector, which degrades image contrast and potentially affects quantification of activity and relative distribution of perfusion
- Changes in *spatial resolution* with distance from the collimator face, which can alter the apparent distribution of activity in the myocardium.

The issue is quite complex:

- Attenuation is considered to have the most significant effect [129, 135-146], but failure to incorporate the effects of scatter into the AC technique may result in over-correction of the data and introduction of artefacts
- Most commercial camera systems now offer a combination of both software and hardware for non-uniform AC mainly based on CT data
- Most of the vendors now use the same type of quantification software (i.e. iterative reconstruction including modelling of non-uniform attenuation and triple-energy window scatter correction).

It is documented that correction with at least some systems does improve image quality and image interpretation. At present it is not possible to set exact guidelines for the best performance of AC because of technological developments and the significantly different requirements of the current, commercially available AC techniques. The only recommendation is to use some form of ML-EM/OS-EM method that includes the corrections [147]. Hence these guidelines attempt to define the key aspects of AC techniques that should be considered when using these techniques in clinical practice.

Attenuation correction

The amount of attenuation in a clinical study depends on several factors, including:

- The type and distribution of tissue (soft tissue, bone or lung)
- The energy of the radiation
- The distance between the source and the body outline for a particular projection angle.

Hence, a proper correction for soft tissue attenuation requires exact knowledge of the attenuation characteristics for each patient. While many schemes for the generation of the attenuation characteristics have been reported, nowadays the attenuation map of a patient is usually generated by a low-dose CT with a scaling from Hounsfield Unit (HU) numbers to attenuation values for the

appropriate photon energy. Older systems used transmission imaging with an external radiation source but because of known problems, regarding noise and down scatter, we recommend using low-dose CT if available.

Because of the variety of techniques used to generate attenuation maps of the body, it is important to be aware of the technical factors that influence the quality of the attenuation map. Specific guidelines for each vendor's system should be consulted with respect to a number of factors (Table 9).

Scatter correction

Unfortunately, emission data usually contain a significant percentage of scattered events. A wide range of algorithms is in use for scatter correction, and there are few data to support the use of any one specific algorithm [148]. Specific guidelines for each vendor's system should be consulted. Scatter correction on the emission data can be performed by:

- Use of one or more additional energy windows (to model the scatter component)
- A reduction of the primary energy window width to minimize scatter (e.g. 15% instead of 20%)
- Modelling of the scatter based on the emission data
- Empirical determination of an effective attenuation coefficient (does not remove scatter).

The use of additional energy windows or a reduction in the width of the energy window will increase statistical noise in the image data. However, it has been shown that if energy-window based scatter estimates are added in the forward projector of an iterative reconstruction method, the noise is considerably less than when subtracted from projection data prior to reconstruction. Modelling of the scatter is potentially the most attractive option as it does not incorporate additional noise into the data to the same degree as an energy window based method usually does, but the method is still not generally available on commercial systems [148].

Loss of resolution with depth

A number of other factors may influence the quality of myocardial perfusion studies. Acquisition parameters such as type of collimation, type of detector orbit, and acquisition arc all affect spatial resolution and result in changes in the resolution of the images with rotation. Some commercial systems employ algorithms of depth-dependent resolution recovery [149]. The purpose of depth-dependent resolution recovery algorithms is to improve the uniformity of resolution over the myocardium. The accuracy and validity of these algorithms has not been well studied. In some cases resolution recovery introduces the so-called Gibbs ringing artefacts, which are wave-formed variations of counts that often appear close to sharp edges. If resolution correction is used, phantom tests should be performed to investigate whether or not this is a problem for the current system. However,

compensating for changes in resolution should generally improve the overall detection of coronary disease [150].

Process of attenuation-scatter correction

It is also important to consider at what point the various corrections described above are applied to the data. An iterative algorithm that incorporates corrections for attenuation, scatter and loss of resolution with depth may perform better than programs that consider these corrections separately. For example, a scatter subtraction program may generate more noise than an ML-EM algorithm that includes a measured or modelled scatter estimate. Likewise, streak artefacts and negative pixel values with FBP may be poorly handled by a separate AC program.

Validation of attenuation-scatter correction devices

Any site contemplating the clinical use of AC in cardiac studies should perform some basic performance testing of the AC device, which should comprise at least two phantom imaging experiments [151] with a suitable myocardial phantom and an anthropomorphic phantom, respectively.

1. The myocardial phantom should be filled with the appropriate radioisotope (^{99m}Tc or ^{201}Tl). The LV cavity should be empty. The myocardium should be suspended in air and orientated as if in a patient. The gamma camera should perform a standard cardiac SPECT acquisition as would be performed in an AC study. No AC should be performed.
2. The left ventricle should then be filled with water and the myocardial phantom placed inside an anthropomorphic phantom. An AC study should be performed and the impact of AC, both with and without additional corrections for scatter and resolution recovery, should be assessed. Although there will be some minor self-attenuation within the walls of the myocardium, the uniformity of the myocardial phantom in air should serve as a good benchmark for comparison with the AC algorithm.

Because of large variations in body size and composition, phantom studies cannot show all the potential problems with an AC device. Hence, non-AC and AC data should be viewed side by side to enable the reviewer to determine changes in image quality resulting from the AC device (Fig. 10). In addition, the reviewer should evaluate the transmission data for soft tissue truncation and consistency in attenuation coefficient values. A simple check of the attenuation map can be done using region of interest analysis to determine the average attenuation coefficients for soft tissue, lung and bone. It is necessary to consult the manufacturer's documentation to determine how to convert a pixel value to an attenuation coefficient (usually a simple multiplication).

Prone SPECT

If AC methods are not available, scanning the patient in another position from the original acquisition (i.e. prone vs. supine and vice versa) may help to judge whether or not a regional reduction in counts on an area of the myocardium is due to attenuation. If the defect has changed in location or disappeared, then the suspected defect was caused by photon attenuation.

Application in clinical practice

Several large multicentre trials have demonstrated that the primary advantages of AC are increased specificity and normalcy rates [147]. While AC is of most value in resolving the true nature of fixed defects, variations in hepatic and bowel activity as well as variability in the position of the breast in women may also make it of value in patients with reversible defects [152]. A major factor to be considered when incorporating AC data into clinical practice is that many trained physicians mentally perform an internal AC based on their experience reviewing 'wrong' (uncorrected) images. Hence they may need to review both the non-AC and the AC images in order to re-learn the appearance of a normal myocardium, as well as understand any residual artefacts or limitations not compensated by the vendor's AC program (Table 10).

Table 9. Parameters of importance for the performance of an AC system

Parameters	*Check list*
Truncation of attenuation map in obese patients	Partial truncation of the patient in transmission beam, if the girth of the patient is greater than the field of view: how does the system handle that?
Matching CT resolution to SPECT resolution	Differences in resolution between CT and SPECT can result in artefacts close to the boundary between soft tissue and lungs. CT data should therefore be filtered to match the expected resolution of the SPECT images.
Fast CT acquisition artefacts	The difference in acquisition time between CT (fast) and SPECT (relatively slow) may lead to AC artefacts (mismatch between CT and SPECT). A 'tidal-breathing' CT protocol may help.
Beam-hardening	How does the system handle beam hardening for large patients and lateral views? Are the attenuation values depending on this effect?
QC of X-ray source	• Is there a QC procedure to ensure correct operation of the X-ray system? • Is there ability to check the accuracy of co-registration of X-ray and emission data? • Is there a check to verify proper scaling to emission photon energy?

Table 10. Summary of attenuation and scatter correction recommendations

Summary of attenuation and scatter correction recommendations	
Image quality and study interpretation	Will be improved by AC and scatter correction
The function of AC	Is highly dependent on hardware and the algorithms applied
Integration of AC	An iterative reconstruction method should be preferred to separate methods
Attenuation correction without scatter correction	Not recommended
Validation of AC	Must include phantom studies before clinical use
Patient studies display	Should always comprise both corrected and non-corrected data sets, viewed side-by-side
QC programs for the acquisition, analysis and review of AC studies	Must be established for the laboratory itself, though initially based on the recommendations from the equipment vendor
If AC methods are not available	An additional SPECT with a change of patient position (prone vs. supine) can provide information on possible attenuation effects, but cannot correct for it

Figure 10. Correct and incorrect attenuation and scatter correction of short axis slices from a normal myocardium in a cardiac phantom.

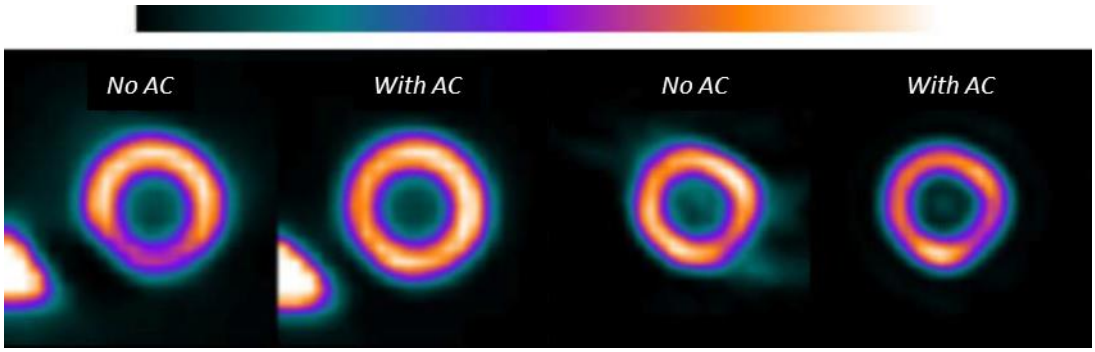

The 2 panels on the left shows that presence of an adjacent hot liver (×2 myocardial activity) results in artefacts in the FBP images, which are corrected after application of AC.

The 2 panels on the right illustrates that increased non-uniformity is shown in the attenuation-corrected images relative to those seen in the FBP images, owing to an error in the AC algorithm.

Data analysis of regional perfusion imaging

Adequate interpretation of MPI requires a systematic visual review of raw data and reconstructed images on a computer screen. The process includes:

- Simple analysis of raw data (QC)
- Stress parameters
- Processed image data (without and, if available, with attenuation-scatter correction and gated cine data)
- Quantitative data (incl. comparison with reference databases or computer aided diagnosis systems)
- Integration with clinical information.

Quantitative analysis is not only a valuable supplement to the visual interpretation of perfusion data, but several studies have also documented better reproducibility and less interobserver variations.

Visual interpretation

Review of original ("raw") data

Inspection and review of stress and rest raw data alongside each other, also in cine mode, are important for QC (cf. "Quality control of instrumentation and image acquisition"). It is also imperative to check the position of the heart within the zone of iso-sensitivity when using CZT cameras, and to visualise the heart by all the pinhole collimators when using multi-pinhole detectors systems (Table 11).

Results of gated studies

In addition to the QC, inspection of raw data may show:

- LV dilatation, either permanent or transient after stress
- Increased lung uptake of tracer, particularly ^{201}Tl
- Clearly visible RV tracer uptake: RV hypertrophy or (occasionally) generalised low LV uptake
- Extra-cardiac abnormalities: focal breast or lung accumulations, duodenal-gastric reflux, or bile obstruction.

Causes leading to inadequate stress-rest comparison:

- Inadequate stress, which may result in underestimation of the presence, severity and extent of stress induced perfusion abnormalities

- Lack of true rest in patients with critical coronary disease, which may lead to underestimation of the presence, severity and extent of the reversibility of perfusion defects.

Review of tomograms

Slices. All three image planes should be inspected: short-axis, horizontal long-axis and vertical long-axis. Stress and rest images should be aligned in a way that the tomograms are carefully displayed with anatomically corresponding stress and rest slices under each other. The short-axis tomograms should be displayed with the apical slices to the left and the base to the right. The vertical long-axis tomograms should be displayed with septal slices to the left and the lateral slices to the right. Similarly, the horizontal long-axis tomograms should be displayed with inferior slices to the left and anterior slices to the right.

Preferably, a format that allows simultaneous inspection of the three image planes is used. A continuous colour scale should be used. If AC has been applied, both images with and without correction should be evaluated (cf. section on "Attenuation and scatter correction").

Polar maps (bull's eye) display. This display represents LV perfusion in a single two-dimensional image and facilitates the assessment of the presence, location, extent and severity of perfusion abnormalities. Ventricular size, however, is not represented in the polar map. By digitally subtracting the rest polar map from the stress polar map, the presence, location, extent and severity of stress induced perfusion defects are easily reviewed. It is critical that the rest and stress polar maps are based on identical delineation and orientation of the LV and no marked differences between possible extracardiac activity accumulations adjacent to the LV. If corresponding parts of the polar maps do not represent identical parts of the LV myocardium, it can lead to serious, falsely positive differences in stress induced perfusion changes in the polar maps. It should be emphasised that the polar map does not disclose possible artefacts such as false perfusion defects caused by attenuation from by intervening tissue or a pacemaker, intra- or extracardiac hot spots.

Three-dimensional display. This display may also facilitate the assessment of the presence, extent and location of LV perfusion abnormalities. LV size and configuration can be displayed. In addition it may be helpful for correlation of perfusion data with other examinations such as echocardiography and coronary angiography (cf. section on "Data Analysis of hybrid imaging"), in particular in the communication with clinical cardiologists.

Visual analysis

Perfusion defects

An area of diminished uptake of the radiopharmaceutical has to be described with respect to localisation, severity and extent. If using a segmental model, the 17-segment model and the associated

nomenclature is recommended, as this model provides the best agreement with other imaging modalities such as MRI, echocardiography and anatomical data [153].

Regional tracer uptake. The distribution of the perfusion tracer may be assessed in relation to the activity distribution in healthy, gender-stratified, reference populations for the same LV region as [154, 155]:

- Normal: ≥70%
- Mildly reduced: 50-69%
- Moderately reduced: 30-49%
- Severely reduced: 10-29%
- Absent: <10%.

The percentages allow for the normal, regional variation of count rates, e.g. septal count rate to be lower than that in the lateral wall in healthy subjects.

Extent of a perfusion defect. The extent of a perfusion abnormality should not only be classified as small, intermediate or large. Quantitative data should be added (cf. below).

LV size and function

A visual assessment of the LV cavity should be performed. With gated studies, quantitative measurements of volumes can be acquired (cf. sections on "Data analysis of gated SPECT" and "Data analysis of hybrid imaging").

Quantitative analysis

Absolute quantification of regional myocardial perfusion is still only possible with PET, but a number of validated, quantitative programs for SPECT analysis of the relative perfusion distribution and cardiac function are commercially available. They can provide additional, clinically useful data, including prognostic information, and can increase both reliability and reproducibility of interpretations. However, quantitative analysis should be used in combination with the visual review of the images since technical problems and most artefacts will not be recognised if only quantitative analysis is performed.

Some programs include manual steps such as identification of apex and base in the short axis slices of the rest and stress studies, resulting in inter-operator variability. Completely automated programs have the advantage of low inter-operator variability, but considerable differences among different automated programs quantifying perfusion defects, ventricular volumes or EF should be taken into account, especially if more than one program is used at the same site.

Perfusion defects

Several programs can highlight regions with "significantly" reduced tracer uptake and quantify the extent and severity of perfusion defects. Most of this type of analysis is based on a database comprising a reference population, often a combination of subjects with low likelihood of CAD or normal coronary angiography and patients with known CAD. Computer aided diagnosis systems have recently been shown to perform at least as well as programs based on comparison with a "reference" data base including healthy subjects [156]. There are many parameters that potentially may influence MPI, e.g. gender, tracer, acquisition and processing protocols, patient position and AC. Both a suitably large database and similarity with the aforementioned parameters for the locally examined patient population are important for a reliable analysis. These conditions, however, are not always met, and the physician should be aware of this limitation, as well as the fact that small activity defects are often also found in healthy subjects.

Segmental models. One approach to quantify MPI is to first divide the myocardium into 17 segments. Each segment is scored separately using a 5-point model ranging from 0 (normal uptake) to 4 (uptake absent). The total scores of the LV are referred to as the summed stress score (SSS), summed rest score (SRS) and summed difference score (SDS: stress minus rest score). All scores have been shown to be of prognostic value (cf. section on "Data analysis of hybrid imaging"). In addition, the scores should be expressed as normalized to percent of the total LV involved with stress, rest, and ischaemic defects by dividing the summed scores by 68, the maximum potential score in the 17-segment model (4x17), and multiplying by 100, respectively [157, 158]:

$$score\ normalized\ to\ \%LV = \frac{\text{score (i.e., SSS, SDS or SDS)}}{68} * 100$$

Coronary artery supply and SPECT images. Some quantitative analysis programs may offer the option of assigning myocardial segments to a specific vascular territory. One has to bear in mind, however, that there is a large inter-individual variability in the territories subtended by the three main coronary arteries and their branches, and caution should be taken when assigning myocardial segments to specific vascular territories. Programs that allow matching of the angiographic data and perfusion data within one person are commercially available (cf. section on "Data analysis of hybrid imaging").

Pixel- and voxel-based models. A quantitative analysis can be performed of the polar maps and/or three-dimensional displays, where respective pixels and/or voxels with relative count values below reference limits are highlighted as black-outs. The number of pixels and/or voxels in the different vascular territories is calculated to give a quantification of the severity and extent of a perfusion defect.

Integration of perfusion and function

Mild reduction of regional tracer uptake may represent a mild perfusion reduction or an attenuation artefact. Information on wall motion and wall thickening in such regions may help to differentiate between these possibilities [159]. However, presence of regional wall motion and/or thickening does not exclude a stress-induced perfusion defect shown by ^{99m}Tc tracers, since the imaging is a reflection of post-stress (i.e. usually = resting) myocardial function. Moreover, LV function has been found to be an independent prognostic marker for cardiac events. The combined assessment of perfusion and function has major prognostic implications [160] (cf. sections on "Data analysis of left ventricular function" and "Data analysis of hybrid imaging").

Viability assessment

Myocardial viability is unlikely if regional tracer uptake is absent, and very likely if tracer uptake is similar to that in segments with normal function. Segments with uptake ≥55% of peak activity and with detectable wall thickening have been found to have a high likelihood of functional recovery after revascularisation [161], but may vary with the tracer used and the region of the LV. Lack of true baseline conditions at the time of ^{99m}Tc-tracer injection or incomplete redistribution of ^{201}Tl may lead to underestimation of myocardial viability. In order to increase the correspondence of the resting images with myocardial viability, nitroglycerin administration before injection of tracer at rest correctly increases the region assessed as viable [162, 163].

Table 11. Quality control of acquired SPECT data to prevent possible artefacts.

Artefacts	*Diagnosis and correction of artefacts*
Patient motion	If possible, make re-acquisition of the study. If not possible use motion correction (cf. section on "Reconstruction methods") In CZT detectors, check the panogram
Upward creep	In particular with ^{201}Tl, review cine. Use motion correction (cf. section on "Reconstruction methods")
Soft tissue attenuation	Inferior wall, particular in men Breast attenuation in women Pectoral muscles in athletic subjects. Use attenuation-scatter correction (cf. section on "Attenuation and scatter correction")
Scatter	Adjacent activity in bowel, liver, gall-bladder (cf. section "Attenuation and scatter correction")
Arrhythmias	Gated images should not be used if significant rejection (>1/3) of cardiac cycles has occurred (cf. section on "Gated SPECT")

Data analysis of left ventricular function

Analysis of gated SPECT images includes the determination of global parameters such as LV volumes and EF, and the visual assessment of regional wall motion, wall thickening and synchrony. Visual assessment is aided by commercially available software products employing algorithms for automated detection of LV endocardial and epicardial contours throughout the cardiac cycle.

Image display

The preferred method of display for gated SPECT is a continuous movie of all phases of the cardiac cycle, for short- and long-axis slices analogous to the common display of non-gated tomographic datasets. As a minimum, a static display should include apical, mid-ventricular and basal short axis, and mid-ventricular horizontal and vertical long axis slices in end-diastole and end-systole (Figure 11). A linear grey scale without computer-derived edges has been suggested to be the best display for evaluation [164]. However, it seems that a continuous colour scale may be an equal alternative for evaluation of regional wall thickening.

In addition to regular slice displays, commercial software tools allow for display of three-dimensional volumes and polar maps of wall thickening, wall motion and synchrony, which are based on automated contour detection algorithms and designed to calculate global parameters and to assist in regional wall motion analysis.

Global left ventricular size and function

A visual assessment of the LV cavity on post-stress and rest images (if available) should be performed first, in order to obtain an overall gross impression of LV size, global function and differences between post-stress and rest studies.

Transient LV cavity dilatation post-stress has been shown to be a marker of CAD severity and an independent predictor of cardiac events [165, 166]. It should be noted that the transient ischaemic dilatation (TID) ratio is calculated from non-gated images and included in most software packages used for functional gated SPECT analysis. It can be used as an adjunct to qualitative assessment of the cavity size, but it should not be interpreted as a stand-alone parameter outside of the context of other perfusion and function data. The presence of dilatation alone in the absence of other abnormalities is not predictive of more severe atherosclerosis or inferior outcome [167].

Quantitative global LV parameters, including end-diastolic volume, end-systolic volume, stroke volume and EF, are calculated automatically with the use of well-validated, commercially available, automated programs. The results are commonly based on computer-derived endocardial and epicardial contours. Prior to acceptance of global quantitative parameters, the contours should be reviewed for

edge detection errors and adjusted if necessary. Common sources of detection errors include large myocardial perfusion defects, extra-cardiac activity, small LV, LV hypertrophy and images with low counts. Using various techniques, the accuracy of volume calculations has been well validated against MRI, radionuclide angiography, and contrast ventriculography as reference standards [168-170]. Some caution should be exercised for interpretation and reporting. Firstly, values from different software packages should not be used interchangeably as the respective algorithms and their normal ranges may differ [171]. Normal limits of LVEF and volumes measured with gated SPECT are influenced by the number of frames, the tracer and the algorithm used. Also, differences in values between centres, according to their respective protocols, have been reported [172]. Finally, in small ventricles, more often observed in women, calculated volumes may be underestimated, resulting in overestimation of EF.

Regional wall motion and wall thickening

Regional LV function can be determined by analysis of wall motion or wall thickening. Visual analysis should be performed first. This can be assisted by software-based algorithms, which require QC of contours first.

Wall motion is defined as the movement of the endocardial border. Computer-generated contours can be helpful, for example with a fixed end-diastolic or end-systolic contour displayed on the cine images. *Wall thickening* is based on the increase in counts per pixel between diastole and systole. It is commonly accepted that wall motion and wall thickening are incorporated into a single qualification while noting the discordance between motion and thickening when it occurs. For instance, such discordance is commonly observed in the septal wall after coronary bypass surgery and in right ventricular overload: wall motion is decreased, whereas wall thickening is preserved. Regional assessment should be made according to the following classification of regional function:

- Normal: wall thickening and motion are both normal
- Hypokinesia: wall thickening and/or motion is decreased
- Akinesia: absence of both wall thickening and motion
- Dyskinesia: absence of wall thickening and paradoxical wall motion.

However, physiological and pathophysiological variations should be noted [173]:

- Wall motion at the base may be reduced compared with the apex in healthy subjects
- Greater excursions of the basal, lateral wall compared to the basal septum may be observed in healthy subjects
- Paradoxical septal motion may be observed in patients with a LBBB, a ventricular pacemaker, or a history of cardiac surgery.

Analysis of LV dyssynchrony

Measurement of LV dyssychrony by gated SPECT appears to be a robust and reproducible method [174, 175]. Bandwidth and standard deviation (SD) of the phase are used to describe LV dyssynchrony, and normal values for men (bandwidth 39±12°; SD 14±5°) and women (bandwidth 31 ±10°; SD 12±5°) have been published [175]. Phase analysis measured by gated SPECT was compared with tissue Doppler imaging and showed good correlation [176, 177]. Dyssynchrony by gated SPECT showed independent prognostic values in patients with normal and abnormal ventricular function, respectively [178-180]. Moreover, in combination with scar burden and assessment of site of late activation, it can be useful for predicting response to cardiac resynchronization therapy (CRT) [181].

Most of the commercially available packages provide data on dyssynchrony, but more validation is needed in large prospective trials to establish the accuracy and clinical value of these data. Furthermore the influence of variables like scar tissue [182], RV function and very low LVEF values on measurements of LV phase are not yet fully understood and need further clarification.

Integration of LV perfusion and functional data

The results of non-gated perfusion and gated LV function from the SPECT examination should be integrated to reach a final interpretation:

- Regional wall motion/wall thickening in apparently fixed perfusion defects may help in the discrimination of infarction (reduced wall motion/thickening) from attenuation artefacts (preserved wall motion/thickening). The number of equivocal interpretations is reduced [159]
- Presence of regional wall motion and/or thickening does not exclude a stress induced perfusion defect, because SPECT images reflect post-stress myocardial function
- Post-stress regional LV dysfunction, not present in rest images (myocardial stunning) improves sensitivity for detection of severe coronary artery disease [183]
- An end-systolic volume of >70ml and an LVEF of <45% in post-stress gated SPECT have an incremental prognostic value over pre-scan and perfusion results, predicting an adverse outcome [184].

Data analysis of hybrid imaging

Hybrid imaging is defined as the combination and fusion of two datasets by which both modalities significantly contribute to image information [185]. Typically, hybrid imaging is synergistic, i.e. more powerful than the sum of its parts as it provides information beyond that achievable with either data set alone, leading to improved sensitivity and specificity.

The term hybrid imaging is not valid for the combination of nuclear cardiac imaging with X-ray based AC where the (low-dose) CT images do not provide independent information, but only contributes to image quality improvement of the other modality (PET or SPECT) [3].

The following section provides recommendations for interpretation and analysis of cardiac SPECT/CCTA hybrid imaging. Specifics on acquisition of CCTA and calcium scoring have been briefly described in the section on "Image acquisition: SPECT, gated SPECT and SPECT/CT".

Hardware and software requirements

Dedicated workstations capable of two- and three-dimensional display of CCTA and SPECT data are a basic requirement for hybrid data analysis. Aside from projection of standard views of SPECT data as described in the sections "Reconstruction methods" and "Data analysis of regional perfusion imaging", the combination of hardware and software has to offer capabilities for volume rendering of stress and rest SPECT data sets (uncorrected and attenuation corrected), common reconstruction and reformatting techniques for CCTA data (including transaxial stacks, multiplanar (curved) reformations, maximum intensity projections and volume-rendering) [186], and automatic or manual image co-registration and fusion. If non-contrast enhanced CT data is acquired for AC of SPECT, the software should offer computation of coronary artery calcium scores.

Integration of myocardial perfusion SPECT with CCTA

The incremental value of hybrid cardiac imaging arises from spatial co-localization of a myocardial perfusion defect with a subtending coronary artery. Traditionally, this process is performed by mental integration of a standard myocardial segmentation model that allocates each segment to one of the three main coronary arteries (Figure 11) [153].

Notably, however, there is a substantial inter-individual anatomical variability of coronary arteries. Therefore, the so-called standard distribution of myocardial perfusion territories does not correspond with the patients' individual anatomy in more than half of the patients [187]. Most frequently, left circumflex artery segments are erroneously assigned to the right coronary artery territory, and standard left anterior descending artery segments are erroneously assigned to the left circumflex territory [188].

True hybrid cardiac imaging and data analysis using volume rendered, co-registered, and fused SPECT and CCTA datasets should be preferred over sole side-by-side analysis because of accurate segmental assignment to coronary artery territories and documented incremental value [189-191].

Fused images of myocardial perfusion SPECT and CCTA can be obtained using data sets acquired on a hybrid scanner (SPECT/CT) or via co-registration of images obtained from separate stand-alone scanners. Software-based automated registration is accurate and fast [191]. However, automated co-registration of data from cardiac imaging is more challenging than that from other body areas. Errors may arise from cardiac motion, breathing motion, and cardiac contraction [192]. Additionally, different anatomic features are depicted by the two modalities rendering automatic object recognition and image registration difficult, particularly if large perfusion defects are present in SPECT images. Accurate registration, however, is of utmost importance to accurately allocate subtending coronary arteries to areas with radiotracer uptake. Therefore, review of the registration is mandatory and manual correction must be performed if needed.

Data analysis

The combined diagnostic information from myocardial perfusion SPECT imaging and CCTA is complementary: The negative predictive value of CCTA to exclude CAD is close to perfect (Figure 12) [15, 193, 194]. However, specificity and positive predictive value of CCTA for identification of haemodynamically significant luminal narrowing have been documented to be less robust. CCTA is associated with a general overestimation of the severity of CAD stenosis and difficulties to differentiate between slight differences in stenosis severity. SPECT offers complementary diagnostic information as to the true hemodynamic significance of coronary artery lesions detected by CCTA. Also, uninterpretable segments on CCTA due to strong calcifications or artefacts can be well studied with SPECT. By contrast, CCTA adds to the diagnostic value of SPECT through documentation of multivessel disease (with possible balanced ischaemia not detectable by semi-quantitative SPECT analysis) or diagnosis of subclinical atherosclerosis.

Interpretation of CCTA studies is beyond the scope of this document and is covered in detail in the respective guidelines of the Society of Cardiovascular Computed Tomography [186]. In brief, CCTA should be first reviewed in transaxial images, complemented by multiplanar reformations to better visualize suspected lesions. Diagnostic conclusions are not based on three-dimensional volume rendered CCTA representations.

By contrast, in hybrid imaging a panoramic three-dimensional view is offered by integrating volume rendered CT data with the perfusion information from SPECT. This comprehensive information

improves both the identification of the culprit vessel and the diagnostic confidence for categorizing intermediate lesions and equivocal perfusion defects, thus optimizing management decisions.

Incidental cardiac and extracardiac CT findings are not uncommon [195]. Although most such findings are negligible, some may be of clinical relevance. Thus, it is recommended that images are additionally screened by a physician fully trained in CT readings, including non-contrast enhanced CT scans for attenuation correction and scouts.

At a practical level this concept requires careful coordination of the readout between nuclear physicians and radiologists, and the final discussion with the cardiologist. The benefit of such an interdisciplinary approach is that those fully trained in the specific modalities would interpret the images jointly, thus providing a high-quality result covering all aspects of hybrid SPECT/CCTA image acquisition.

The integration of coronary anatomy by CCTA and (quantitative) documentation of the true ischaemic burden through SPECT allows effective identification of 1) patients with CAD benefiting from optimal medical therapy versus those who should undergo coronary revascularization, 2) the culprit stenosis in patients with multiple coronary artery lesions thereby guiding clinicians on the appropriate method of revascularization, 3) patients with subclinical coronary atherosclerosis where more aggressive prevention may be indicated, and 4) patients with normal coronary arteries who can safely be deferred from any further cardiac testing.

In summary, the complimentary anatomic and functional information provided by hybrid SPECT/CCTA imaging has been demonstrated to confer added diagnostic value in CAD detection [188, 190, 191, 196, 197] and to effectively stratify risk and predict outcomes [198, 199], guide patient management [200], and to contribute to optimal downstream resource utilization [201].

Figure 11. Coronary artery territories in a 17-segment model.

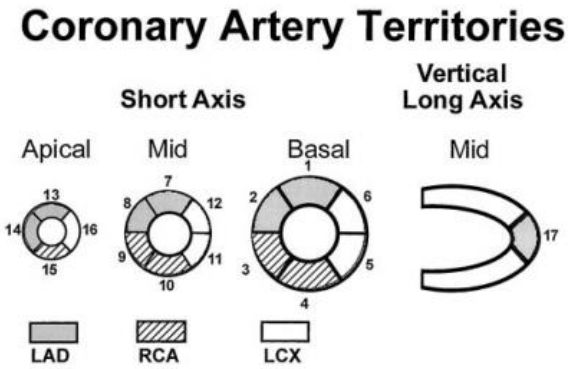

Standard myocardial segmentation, assigning all 17 myocardial segments to the territories of the left anterior descending (LAD), right coronary artery (RCA), and left circumflex (LCX) [153].

Figure 12. Coronary artery territories in a 17-segment model Myocardial perfusion SPECT, coronary computed tomography angiography (CCTA), and fused hybrid SPECT/CCTA of a 43 year old male patient presenting with typical angina.

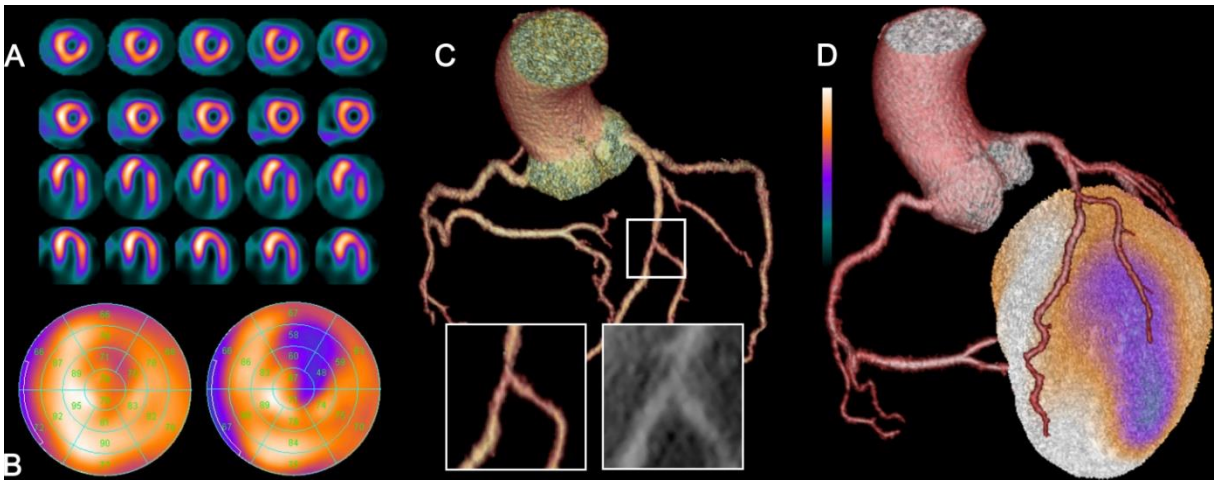

Myocardial perfusion SPECT documents a reversible perfusion defect in short axis and horizontal long axis slices (A) at rest (bottom rows) and stress (top rows). The corresponding polar plots (B) at rest (left plot) and stress (right plot) clearly depict the extent of the ischemic area in the anterolateral wall. CCTA (C) shows an intermediate stenosis (i.e. 50-70% luminal narrowing) due to non-calcified plaques in the middle/distal left anterior descending artery at the level of the second diagonal branch bifurcation. Fused hybrid SPECT/CCTA (D) reveals that the anterolateral ischemia corresponds with the vascular territory of the second diagonal branch, while the stenosis in the LAD does not cause any ischemia.

Reports, image display

Reports should be uniform with the ultimate goal of translating the images into clinical relevant information. The previous EANM guidelines and the joint position paper by the EANM and the European Association of Cardiovascular Imaging (EACVI) on reporting nuclear cardiology present more detailed recommendations, but below some principles are emphasized and/or added [1, 2, 84, 202].

It is crucial that the referring or treating physician directly understands the report as intended by the interpreter of the images. This implies careful attention to the general language and professional terminology used in the report. This means that:

- The report should be written in a simple way and, if possible, without use of technical terms
- Abbreviations and technical information should be avoided if not important for understanding of the report
- Quantitative data should replace or should be added to qualitative descriptions (e.g. do not use terms like small or medium-sized etc.)
- Protective expressions (e.g. is likely, cannot be excluded) should be used as little as possible. However, relevant doubt about the interpretation must be communicated.

The structured report

Since a well-structured report is more easily accessible for the referring physician, a structured report with adequate headings, in contrast to free text, should be used in current nuclear cardiology [203]. Headings may differ between different institutions and different countries, due to local tradition and legislation.

In general the following information should be included in the report:

- Administrative data for the patient, the referring physician, and the laboratory/department
- Indication for the study: presenting the purpose and appropriateness
- Stress test protocol and pathological findings during stress (whether exercise or pharmacological stress)
- Radiopharmaceutical and quantity (i.e. amount in MBq) administered
- Image acquisition (optional if following routine)
- Description of the findings: Normal or significant defects (reversibility, location, extent, severity); LV function (if the study is gated)

- Conclusion(s): Brief summary of findings leading to a clinically useful interpretation (ischaemia, scar tissue, suspicion of hibernating tissue etc.), prognostic information and recommendations regarding further diagnostic imaging may be given [204]
- Signature of the interpreting physician.

Images in the report

It is crucial that images accompanying the report are rather few, and they must illustrate and support the conclusion of the report.

Selection and presentation of images

Slices in all three image planes should be shown (short-axis, horizontal long-axis, and vertical long-axis), and stress and rest images (if both have been acquired) must be carefully aligned. The short-axis tomograms should be displayed with the apical slices to the left and the base to the right. The vertical long-axis tomograms should be displayed with septal slices to the left and the lateral slices to the right. Similarly, the horizontal long-axis tomograms should be displayed with inferior slices to the left and anterior slices to the right.

Polar plots of stress and rest should be shown, and black-out defects for reversible and irreversible defects may be presented. If gated, end-diastolic and –systolic images with or without edge contours should also be presented. 3-D images may be shown. Technical images and screen captures should generally not be used.

Several colour scales are available in current reporting environments. It is important to use the same, standardized scale for each type of study. Some centres prefer grey scales to colour scales for specific images.

References R

1. Hesse B, Tagil K, Cuocolo A, Anagnostopoulos C, Bardies M, Bax J et al. EANM/ESC procedural guidelines for myocardial perfusion imaging in nuclear cardiology. Eur J Nucl Med Mol Imaging 2005;32(7):855-97.

2. Hesse B, Lindhardt TB, Acampa W, Anagnostopoulos C, Ballinger J, Bax JJ et al. EANM/ESC guidelines for radionuclide imaging of cardiac function. Eur J Nucl Med Mol Imaging 2008;35(4):851-85.

3. Flotats A, Knuuti J, Gutberlet M, Marcassa C, Bengel FM, Kaufmann PA et al. Hybrid cardiac imaging: SPECT/CT and PET/CT. A joint position statement by the European Association of Nuclear Medicine (EANM), the European Society of Cardiac Radiology (ESCR) and the European Council of Nuclear Cardiology (ECNC). Eur J Nucl Med Mol Imaging. 2011;38(1):201-12.

4. Delbeke D, Chiti A, Christian P, Darcourt J, Donohoe K, Flotats A et al. SNMMI/EANM guideline for guideline development 6.0. J Nucl Med Technol 2012;40(4):283-9.

5. Munch G, Neverve J, Matsunari I, Schroter G, Schwaiger M. Myocardial technetium-99m-tetrofosmin and technetium-99m-sestamibi kinetics in normal subjects and patients with coronary artery disease. J Nucl Med. 1997;38(3):428-32.

6. Maurea S, Cuocolo A, Soricelli A, Castelli L, Nappi A, Squame F et al. Enhanced detection of viable myocardium by technetium-99m-MIBI imaging after nitrate administration in chronic coronary artery disease. J Nucl Med. 1995;36(11):1945-52.

7. Grunwald AM, Watson DD, Holzgrefe HH, Jr., Irving JF, Beller GA. Myocardial thallium-201 kinetics in normal and ischemic myocardium. Circulation. 1981;64(3):610-8.

8. Dilsizian V, Rocco TP, Freedman NM, Leon MB, Bonow RO. Enhanced detection of ischemic but viable myocardium by the reinjection of thallium after stress-redistribution imaging. N Engl J Med. 1990;323(3):141-6. doi:10.1056/nejm199007193230301.

9. Hesslewood SE. European system for reporting adverse reactions to and defects in radiopharmaceuticals: annual report 2000. Eur J Nucl Med Mol Imaging. 2002;29(5):Bp13-9.

10. Doukaki S, Arico M, Bongiorno MR. Erythroderma related to the administration of 99mTc-sestamibi: the first report. J Nucl Cardiol. 2010;17(3):520-2.

11. Hesse B, Vinberg N, Mosbech H. Exanthema after a stress Tc-99m sestamibi study: continue with a rest sestamibi study? Clinical physiology and functional imaging. 2011;31(3):246-8.

12. Makaryus JN, Makaryus AN, Azer V, Diamond JA. Angioedema after injection of Tc-99m sestamibi tracer during adenosine nuclear stress testing. J Nucl Cardiol. 2008;15(4):e26-7.

13. Mujtaba B, Adenaike M, Yaganti V, Mujtaba N, Jain D. Anaphylactic reaction to Tc-99m sestamibi (Cardiolite) during pharmacologic myocardial perfusion imaging. J Nucl Cardiol. 2007;14(2):256-8.

14. Hesse B, Vinberg N, Berthelsen AK, Ballinger JR. Adverse events in nuclear medicine - cause for concern? Eur J Nucl Med Mol Imaging. 2012;39(5):782-5.

15. Miller JM, Rochitte CE, Dewey M, Arbab-Zadeh A, Niinuma H, Gottlieb I et al. Diagnostic performance of coronary angiography by 64-row CT. N Engl J Med. 2008;359(22):2324-36.

16. Vavere AL, Arbab-Zadeh A, Rochitte CE, Dewey M, Niinuma H, Gottlieb I et al. Coronary artery stenoses: accuracy of 64-detector row CT angiography in segments with mild, moderate, or severe calcification--a subanalysis of the CORE-64 trial. Radiology. 2011;261(1):100-8.

17. ACR–NASCI–SPR Practice guideline for the performance and interpretation of cardiac computed tomography. http://www.acr.org/~/media/f4720a18f03b4a26a0c9c3cc18637d87.pdf. 2011. Accessed 21 May 2015.

18. Lembcke A, Schwenke C, Hein PA, Knobloch G, Durmus T, Hamm B et al. High-pitch dual-source CT coronary angiography with low volumes of contrast medium. Eur Radiol. 2014;24(1):120-7.

19. Hoffmann U, Ferencik M, Cury RC, Pena AJ. Coronary CT angiography. J Nucl Med. 2006;47(5):797-806.

20. Schroeder S, Achenbach S, Bengel F, Burgstahler C, Cademartiri F, de Feyter P et al. Cardiac computed tomography: indications, applications, limitations, and training requirements: report of a Writing Group deployed by the Working Group Nuclear Cardiology and Cardiac CT of the European Society of Cardiology and the European Council of Nuclear Cardiology. Eur Heart J. 2008;29(4):531-56.

21. ACR Committee on Drugs and Contrast Media. ACR Manual on Contrast Media, Version 9, 2013., http://www.acr.org/quality-safety/resources/~/media/37D84428BF1D4E1B9A3A2918DA9E27A3.pdf/. 2013. Accessed 21 May 2015.

22. Boellaard R, Delgado-Bolton R, Oyen WJ, Giammarile F, Tatsch K, Eschner W et al. FDG PET/CT: EANM procedure guidelines for tumour imaging: version 2.0. Eur J Nucl Med Mol Imaging. 2015;42(2):328-54.

23. Schopp JG, Iyer RS, Wang CL, Petscavage JM, Paladin AM, Bush WH et al. Allergic reactions to iodinated contrast media: premedication considerations for patients at risk. Emerg Radiol. 2013;20(4):299-306.

24. Thomsen HS. Contrast media safety-an update. Eur J Radiol. 2011;80(1):77-82.

25. Cochran ST, Bomyea K, Sayre JW. Trends in adverse events after IV administration of contrast media. AJR Am J Roentgenol. 2001;176(6):1385-8. doi:10.2214/ajr.176.6.1761385.

26. Mortele KJ, Oliva MR, Ondategui S, Ros PR, Silverman SG. Universal use of nonionic iodinated contrast medium for CT: evaluation of safety in a large urban teaching hospital. AJR Am J Roentgenol. 2005;184(1):31-4. doi:10.2214/ajr.184.1.01840031.

27. Wang CL, Cohan RH, Ellis JH, Caoili EM, Wang G, Francis IR. Frequency, outcome, and appropriateness of treatment of nonionic iodinated contrast media reactions. AJR Am J Roentgenol. 2008;191(2):409-15.

28. Katayama H, Yamaguchi K, Kozuka T, Takashima T, Seez P, Matsuura K. Adverse reactions to ionic and nonionic contrast media. A report from the Japanese Committee on the Safety of Contrast Media. Radiology. 1990;175(3):621-8.

29. Council Directive 2013/59/Euratom of 5 December 2013 laying down basic safety standards for protection against the dangers arising from exposure to ionising radiation, and repealing Directives 89/618/Euratom, 90/641/Euratom, 96/29/Euratom, 97/43/Euratom and

2003/122/Euratom. http://eur-lex.europa.eu/legal-content/EN/TXT/?uri=OJ:L:2014:013:TOC. 2014. Accessed 21 May 2015.

30. Cousins C, Miller DL, Bernardi G, Rehani MM, Schofield P, Vano E et al. ICRP PUBLICATION 120: Radiological protection in cardiology. Ann ICRP. 2013;42(1):1-125.

31. Heo J, Powers J, Iskandrian AE. Exercise-rest same-day SPECT sestamibi imaging to detect coronary artery disease. J Nucl Med. 1997;38(2):200-3.

32. Tragardh E, Valind S, Edenbrandt L. Adding attenuation corrected images in myocardial perfusion imaging reduces the need for a rest study. BMC Med Imaging. 2013;13:14.

33. Duvall WL, Croft LB, Ginsberg ES, Einstein AJ, Guma KA, George T et al. Reduced isotope dose and imaging time with a high-efficiency CZT SPECT camera. J Nucl Cardiol. 2011;18(5):847-57.

34. Herzog BA, Buechel RR, Katz R, Brueckner M, Husmann L, Burger IA et al. Nuclear myocardial perfusion imaging with a cadmium-zinc-telluride detector technique: optimized protocol for scan time reduction. J Nucl Med. 2010;51(1):46-51.

35. Nkoulou R, Pazhenkottil AP, Kuest SM, Ghadri JR, Wolfrum M, Husmann L et al. Semiconductor detectors allow low-dose-low-dose 1-day SPECT myocardial perfusion imaging. J Nucl Med. 2011;52(8):1204-9.

36. Oddstig J, Hedeer F, Jogi J, Carlsson M, Hindorf C, Engblom H. Reduced administered activity, reduced acquisition time, and preserved image quality for the new CZT camera. J Nucl Cardiol. 2013;20(1):38-44.

37. Sharir T, Ben-Haim S, Merzon K, Prochorov V, Dickman D, Ben-Haim S et al. High-speed myocardial perfusion imaging initial clinical comparison with conventional dual detector anger camera imaging. JACC Cardiovasc Imaging. 2008;1(2):156-63.

38. Lassmann M. The new EANM paediatric dosage card. Eur J Nucl Med Mol Imaging. 2008;35(9):1748.

39. ICRP, 1998. Radiation dose to patients from radiopharmaceuticals (addendum 2 to ICRP publication 53). Ann ICRP. 1998;28(3):1-126.

40. ICRP, 2008. Radiation dose to patients from radiopharmaceuticals. Addendum 3 to ICRP Publication 53. ICRP Publication 106. Approved by the Commission in October 2007. Ann ICRP. 2008;38(1-2):1-197.

41. Mattsson S, Johansson L, Leide Svegborn S, Liniecki J, Noßke D, Stabin M et al. Radiation Dose to Patients from Radiopharmaceuticals A fourth addendum to ICRP Publication 53. In: Ann ICRP. http://www.icrp.org/docs/Radiation%20Dose%20to%20Patients%20from%20Radiopharmaceuticals%20-%20A%20fourth%20addendum%20to%20ICRP%20Publication%2053.pdf. 2013. Accessed 21 May 2015.

42. ICRP, 1991. 1990 Recommendations of the International Commission on Radiological Protection. ICRP Publication 60. Ann ICRP 1991;21:3.

43. ICRP, 2006. Human alimentary tract model for radiological protection. ICRP Publication 100. A report of The International Commission on Radiological Protection. Ann ICRP. 2006;36(1-2):25-327, iii.

44. ICRP, 2007. The 2007 Recommendations of the International Commission on Radiological Protection. ICRP publication 103. Ann ICRP. 2007;37(2-4):1-332.

45. ICRP, 2009. Adult Reference Computational Phantoms. ICRP Publication 110. Ann ICRP. 2009;39(2).

46. Andersson M, Johansson L, Minarik D, Leide-Svegborn S, Mattsson S. Effective dose to adult patients from 338 radiopharmaceuticals estimated using ICRP biokinetic data, ICRP/ICRU computational reference phantoms and ICRP 2007 tissue weighting factors. EJNMMI Physics. 2014;1(1):9.

47. Buechel RR, Husmann L, Herzog BA, Pazhenkottil AP, Nkoulou R, Ghadri JR et al. Low-dose computed tomography coronary angiography with prospective electrocardiogram triggering: feasibility in a large population. J Am Coll Cardiol. 2011;57(3):332-6.

48. Maruyama T, Takada M, Hasuike T, Yoshikawa A, Namimatsu E, Yoshizumi T. Radiation dose reduction and coronary assessability of prospective electrocardiogram-gated computed tomography coronary angiography: comparison with retrospective electrocardiogram-gated helical scan. J Am Coll Cardiol. 2008;52(18):1450-5.

49. Achenbach S, Marwan M, Ropers D, Schepis T, Pflederer T, Anders K et al. Coronary computed tomography angiography with a consistent dose below 1 mSv using prospectively electrocardiogram-triggered high-pitch spiral acquisition. Eur Heart J. 2010;31(3):340-6.

50. Fuchs TA, Stehli J, Bull S, Dougoud S, Clerc OF, Herzog BA et al. Coronary computed tomography angiography with model-based iterative reconstruction using a radiation exposure similar to chest X-ray examination. Eur Heart J. 2014;35(17):1131-6.

51. ORAMED. http://www.oramed-fp7.eu/en. 2008. Accessed 21 May 2015.

52. Vanhavere F, Ginjaume M, Carinou E, Gualdrini G, Clairand I, Sans-Merce M. International Workshop on Optimization of Radiation Protection of Medical Staff, ORAMED 2011. Rad Meas. 2011;46(11):1195-6. doi:http://dx.doi.org/10.1016/j.radmeas.2011.09.005.

53. Strahleneschutzkommission. Strahlenexposition von Personen durch nuklearmedizinisch untersuchte Patienten. http://www.ssk.de/SharedDocs/Beratungsergebnisse_PDF/1998/Strahlenexposition_durch_Patienten.html?nn=2041716. 1998. Accessed 21 May 2015.

54. Russell JR, Stabin MG, Sparks RB, Watson E. Radiation absorbed dose to the embryo/fetus from radiopharmaceuticals. Health Physics. 1997;73(5):756-69.

55. Myers J, Arena R, Franklin B, Pina I, Kraus WE, McInnis K et al. Recommendations for clinical exercise laboratories: a scientific statement from the American Heart Association. Circulation. 2009;119(24):3144-61.

56. Reyes E, Loong CY, Harbinson M, Donovan J, Anagnostopoulos C, Underwood SR. High-dose adenosine overcomes the attenuation of myocardial perfusion reserve caused by caffeine. J Am Coll Cardiol. 2008;52(24):2008-16.

57. Fletcher GF, Ades PA, Kligfield P, Arena R, Balady GJ, Bittner VA et al. Exercise standards for testing and training: a scientific statement from the American Heart Association. Circulation. 2013;128(8):873-934.

58. Fox K, Garcia MA, Ardissino D, Buszman P, Camici PG, Crea F et al. Guidelines on the management of stable angina pectoris: executive summary: The Task Force on the

Management of Stable Angina Pectoris of the European Society of Cardiology. Eur Heart J. 2006;27(11):1341-81.

59. Montalescot G, Sechtem U, Achenbach S, Andreotti F, Arden C, Budaj A et al. 2013 ESC guidelines on the management of stable coronary artery disease: the Task Force on the management of stable coronary artery disease of the European Society of Cardiology. Eur Heart J. 2013;34(38):2949-3003.

60. Krivokapich J, Huang SC, Schelbert HR. Assessment of the effects of dobutamine on myocardial blood flow and oxidative metabolism in normal human subjects using nitrogen-13 ammonia and carbon-11 acetate. Am J Cardiol. 1993;71(15):1351-6.

61. Zoghbi GJ, Iskandrian AE. Selective adenosine agonists and myocardial perfusion imaging. J Nucl Cardiol. 2012;19(1):126-41.

62. Bonello L, Laine M, Kipson N, Mancini J, Helal O, Fromonot J et al. Ticagrelor increases adenosine plasma concentration in patients with an acute coronary syndrome. J Am Coll Cardiol. 2014;63(9):872-7.

63. Voci P, Pizzuto F. Coronary flow reserve with a turbo: a warning for the use of adenosine as a provocative test in patients receiving ticagrelor? J Am Coll Cardiol. 2014;63(9):878-9.

64. Iskandrian AE, Bateman TM, Belardinelli L, Blackburn B, Cerqueira MD, Hendel RC et al. Adenosine versus regadenoson comparative evaluation in myocardial perfusion imaging: results of the ADVANCE phase 3 multicenter international trial. J Nucl Cardiol. 2007;14(5):645-58.

65. Mahmarian JJ, Cerqueira MD, Iskandrian AE, Bateman TM, Thomas GS, Hendel RC et al. Regadenoson induces comparable left ventricular perfusion defects as adenosine: a quantitative analysis from the ADVANCE MPI 2 trial. JACC Cardiovasc Imaging. 2009;2(8):959-68.

66. Navare SM, Mather JF, Shaw LJ, Fowler MS, Heller GV. Comparison of risk stratification with pharmacologic and exercise stress myocardial perfusion imaging: a meta-analysis. J Nucl Cardiol. 2004;11(5):551-61.

67. Brinkert M, Reyes E, Walker S, Latus K, Maenhout A, Mizumoto R et al. Regadenoson in Europe: first-year experience of regadenoson stress combined with submaximal exercise in patients undergoing myocardial perfusion scintigraphy. Eur J Nucl Med Mol Imaging. 2014;41(3):511-21.

68. Thomas GS, Prill NV, Majmundar H, Fabrizi RR, Thomas JJ, Hayashida C et al. Treadmill exercise during adenosine infusion is safe, results in fewer adverse reactions, and improves myocardial perfusion image quality. J Nucl Cardiol. 2000;7(5):439-46.

69. Treuth MG, Reyes GA, He ZX, Cwajg E, Mahmarian JJ, Verani MS. Tolerance and diagnostic accuracy of an abbreviated adenosine infusion for myocardial scintigraphy: a randomized, prospective study. J Nucl Cardiol. 2001;8(5):548-54.

70. Cerqueira MD, Verani MS, Schwaiger M, Heo J, Iskandrian AS. Safety profile of adenosine stress perfusion imaging: results from the Adenoscan Multicenter Trial Registry. J Am Coll Cardiol. 1994;23(2):384-9.

71. Cerqueira MD, Nguyen P, Staehr P, Underwood SR, Iskandrian AE. Effects of age, gender, obesity, and diabetes on the efficacy and safety of the selective A2A agonist regadenoson

versus adenosine in myocardial perfusion imaging integrated ADVANCE-MPI trial results. JACC Cardiovasc Imaging. 2008;1(3):307-16.

72. Leaker BR, O'Connor B, Hansel TT, Barnes PJ, Meng L, Mathur VS et al. Safety of regadenoson, an adenosine A2A receptor agonist for myocardial perfusion imaging, in mild asthma and moderate asthma patients: a randomized, double-blind, placebo-controlled trial. J Nucl Cardiol. 2008;15(3):329-36.

73. Thomas GS, Tammelin BR, Schiffman GL, Marquez R, Rice DL, Milikien D et al. Safety of regadenoson, a selective adenosine A2A agonist, in patients with chronic obstructive pulmonary disease: A randomized, double-blind, placebo-controlled trial (RegCOPD trial). J Nucl Cardiol. 2008;15(3):319-28.

74. Agarwal V, DePuey EG. Regadenoson and seizures: A real clinical concern. J Nucl Cardiol. 2014;21(5):869-70.

75. Fukuda M, Suzuki Y, Hino H, Morimoto T, Ishii E. Activation of central adenosine A(2A) receptors lowers the seizure threshold of hyperthermia-induced seizure in childhood rats. Seizure. 2011;20(2):156-9.

76. Page RL, 2nd, Spurck P, Bainbridge JL, Michalek J, Quaife RA. Seizures associated with regadenoson: a case series. J Nucl Cardiol. 2012;19(2):389-91.

77. Hage FG. Regadenoson for myocardial perfusion imaging: Is it safe? J Nucl Cardiol. 2014;21(5):871-6.

78. Pharmacovigilance Risk Assessment Committee (PRAC), Minutes of the meeting on 5-8 May 2014. 2014. http://www.ema.europa.eu/docs/en_GB/document_library/Minutes/2014/06/WC500169468.pdf. 2014. Accessed 21 May 2015.

79. Lette J, Tatum JL, Fraser S, Miller DD, Waters DD, Heller G et al. Safety of dipyridamole testing in 73,806 patients: the Multicenter Dipyridamole Safety Study. J Nucl Cardiol. 1995;2(1):3-17.

80. McNeill AJ, Fioretti PM, el-Said SM, Salustri A, Forster T, Roelandt JR. Enhanced sensitivity for detection of coronary artery disease by addition of atropine to dobutamine stress echocardiography. Am J Cardiol. 1992;70(1):41-6.

81. Reyes E, Stirrup J, Roughton M, D'Souza S, Underwood SR, Anagnostopoulos C. Attenuation of adenosine-induced myocardial perfusion heterogeneity by atenolol and other cardioselective beta-adrenoceptor blockers: a crossover myocardial perfusion imaging study. JJ Nucl Med. 2010;51(7):1036-43.

82. Yoon AJ, Melduni RM, Duncan SA, Ostfeld RJ, Travin MI. The effect of beta-blockers on the diagnostic accuracy of vasodilator pharmacologic SPECT myocardial perfusion imaging. J Nucl Cardiol. 2009;16(3):358-67.

83. Garcia EV, Faber TL, Esteves FP. Cardiac dedicated ultrafast SPECT cameras: new designs and clinical implications. JJ Nucl Med. 2011;52(2):210-7.

84. Holly TA, Abbott BG, Al-Mallah M, Calnon DA, Cohen MC, DiFilippo FP et al. Single photon-emission computed tomography. J Nucl Cardiol. 2010;17(5):941-73.

85. DePuey EG. Advances in SPECT camera software and hardware: currently available and new on the horizon. J Nucl Cardiol. 2012;19(3):551-81; quiz 85.

86. Hutton BF. Developments in cardiac-specific SPECT imaging. Q J Nucl Med Mol Imaging. 2012;56(3):221-9.

87. Einstein AJ, Blankstein R, Andrews H, Fish M, Padgett R, Hayes SW et al. Comparison of Image Quality, Myocardial Perfusion, and Left Ventricular Function Between Standard Imaging and Single-Injection Ultra-Low-Dose Imaging Using a High-Efficiency SPECT Camera: The MILLISIEVERT Study. JJ Nucl Med. 2014;55(9):1430-7.

88. Ben-Haim S, Almukhailed O, Neill J, Slomka P, Allie R, Shiti D et al. Clinical value of supine and upright myocardial perfusion imaging in obese patients using the D-SPECT camera. J Nucl Cardiol. 2014;21(3):8.

89. Chawla D, Rahaby M, Amin AP, Vashistha R, Alyousef T, Martinez HX et al. Soft tissue attenuation patterns in stress myocardial perfusion SPECT images: a comparison between supine and upright acquisition systems. J Nucl Cardiol. 2011;18(2):281-90.

90. Heo J, Kegel J, Iskandrian AS, Cave V, Iskandrian BB. Comparison of same-day protocols using technetium-99m-sestamibi myocardial imaging. J Nucl Med. 1992;33(2):186-91.

91. Thorley PJ, Bloomer TN, Sheard KL, Sivananthan UM. The use of GTN to improve the detection of ischaemic myocardium using 99Tcm-tetrofosmin. Nucl Med Commun. 1996;17(8):669-74.

92. Hurwitz GA, Clark EM, Slomka PJ, Siddiq SK. Investigation of measures to reduce interfering abdominal activity on rest myocardial images with Tc-99m sestamibi. Clin Nucl Med. 1993;18(9):735-41.

93. van Dongen AJ, van Rijk PP. Minimizing liver, bowel, and gastric activity in myocardial perfusion SPECT. J Nucl Med. 2000;41(8):1315-7.

94. Rocco TP, Dilsizian V, McKusick KA, Fischman AJ, Boucher CA, Strauss HW. Comparison of thallium redistribution with rest "reinjection" imaging for the detection of viable myocardium. Am J Cardiol. 1990;66(2):158-63.

95. Berman DS, Kiat HS, Van Train KF, Germano G, Maddahi J, Friedman JD. Myocardial perfusion imaging with technetium-99m-sestamibi: comparative analysis of available imaging protocols. J Nucl Med. 1994;35(4):681-8.

96. Utsunomiya D, Nakaura T, Honda T, Shiraishi S, Tomiguchi S, Kawanaka K et al. Object-specific attenuation correction at SPECT/CT in thorax: optimization of respiratory protocol for image registration. Radiology. 2005;237(2):662-9.

97. Dilsizian V, Bacharach SL, Beanlands RS, Bergmann SR, Delbeke D, Grople RJ et al. PET myocardial perfusion and metabolism clinical imaging. . http://www.asnc.org/imageuploads/ImagingGuidelinesPET. 2008. Accessed 21 May 2015.

98. Lehner S, Sussebach C, Todica A, Uebleis C, Brunner S, Bartenstein P et al. Influence of SPECT attenuation correction on the quantification of hibernating myocardium as derived from combined myocardial perfusion SPECT and (18)F-FDG PET. J Nucl Cardiol. 2014;21(3):578-87.

99. Einstein AJ, Johnson LL, Bokhari S, Son J, Thompson RC, Bateman TM et al. Agreement of visual estimation of coronary artery calcium from low-dose CT attenuation correction scans in hybrid PET/CT and SPECT/CT with standard Agatston score. J Am Coll Cardiol. 2010;56(23):1914-21.

100. Burkhard N, Herzog BA, Husmann L, Pazhenkottil AP, Burger IA, Buechel RR et al. Coronary calcium score scans for attenuation correction of quantitative PET/CT 13N-ammonia myocardial perfusion imaging. Eur J Nucl Med Mol Imaging. 2010;37(3):517-21.

101. Schepis T, Gaemperli O, Koepfli P, Ruegg C, Burger C, Leschka S et al. Use of coronary calcium score scans from stand-alone multislice computed tomography for attenuation correction of myocardial perfusion SPECT. Eur J Nucl Med Mol Imaging. 2007;34(1):11-9.

102. Choi JY, Lee KH, Kim SJ, Kim SE, Kim BT, Lee SH et al. Gating provides improved accuracy for differentiating artifacts from true lesions in equivocal fixed defects on technetium 99m tetrofosmin perfusion SPECT. J Nucl Cardiol. 1998;5(4):395-401.

103. Segall GM, Davis MJ. Prone versus supine thallium myocardial SPECT: a method to decrease artifactual inferior wall defects. J Nucl Med. 1989;30(4):548-55.

104. Strauss HW, Miller DD, Wittry MD, Cerqueira MD, Garcia EV, Iskandrian AS et al. Procedure guideline for myocardial perfusion imaging. Society of Nuclear Medicine. J Nucl Med. 1998;39(5):918-23.

105. Slomka PJ, Nishina H, Abidov A, Hayes SW, Friedman JD, Berman DS et al. Combined quantitative supine-prone myocardial perfusion SPECT improves detection of coronary artery disease and normalcy rates in women. J Nucl Cardiol. 2007;14(1):44-52.

106. Hayes SW, Berman DS, Germano G. Stress testing and imaging protocols. . In: Germano G, Berman DS, editors. Clinical Gated Cardiac SPECT. Second Edition: Blackwell Publishing Company, Inc., New York 2006.

107. Eisner RL, Nowak DJ, Pettigrew R, Fajman W. Fundamentals of 180 degree acquisition and reconstruction in SPECT imaging. J Nucl Med. 1986;27(11):1717-28.

108. Updated imaging guidelines for nuclear cardiology procedures, part 1. J Nucl Cardiol. 2001;8(1):G5-g58.

109. Abbara S, Arbab-Zadeh A, Callister TQ, Desai MY, Mamuya W, Thomson L et al. SCCT guidelines for performance of coronary computed tomographic angiography: a report of the Society of Cardiovascular Computed Tomography Guidelines Committee. J Cardiovasc Comput Tomogr. 2009;3(3):190-204.

110. Delbeke D, Coleman RE, Guiberteau MJ, Brown ML, Royal HD, Siegel BA et al. Procedure Guideline for SPECT/CT Imaging 1.0. J Nucl Med. 2006;47(7):1227-34.

111. Mark DB, Berman DS, Budoff MJ, Carr JJ, Gerber TC, Hecht HS et al. ACCF/ACR/AHA/NASCI/SAIP/SCAI/SCCT 2010 expert consensus document on coronary computed tomographic angiography: a report of the American College of Cardiology Foundation Task Force on Expert Consensus Documents. Catheter Cardiovasc Interv. 2010;76(2):E1-42.

112. Hermann F, Martinoff S, Meyer T, Hadamitzky M, Jiang C, Hendrich E et al. Reduction of radiation dose estimates in cardiac 64-slice CT angiography in patients after coronary artery bypass graft surgery. Inves Radiol. 2008;43(4):253-60.

113. Herzog BA, Husmann L, Landmesser U, Kaufmann PA. Low-dose computed tomography coronary angiography and myocardial perfusion imaging: cardiac hybrid imaging below 3mSv. Eur Heart J. 2009;30(6):644.

114. Husmann L, Herzog BA, Gaemperli O, Tatsugami F, Burkhard N, Valenta I et al. Diagnostic accuracy of computed tomography coronary angiography and evaluation of stress-only single-photon emission computed tomography/computed tomography hybrid imaging: comparison of prospective electrocardiogram-triggering vs. retrospective gating. Eur Heart J. 2009;30(5):600-7.

115. Busemann Sokole E, Plachcinska A, Britten A, Lyra Georgosopoulou M, Tindale W, Klett R. Routine quality control recommendations for nuclear medicine instrumentation. Eur J Nucl Med Mol Imaging. 2010;37(3):662-71.

116. RADIATION PROTECTION N° 162: Criteria for acceptability of medical radiological equipment used in diagnostic radiology, nuclear medicine and radiotherapy. http://ec.europa.eu/energy/nuclear/radiation_protection/doc/publication/162.pdf. 2012. Accessed 21 May 2015.

117. IAEA. Quality Assurance for SPECT Systems. IAEA Human Health Series, vol 6. Vienna: 2009.

118. Shepard SJ, Paul Lin PJ, Boone JM, Cody DD, Fisher JR, Frey GD et al. AAPM report no. 74: Quality Control in Diagnostic Radialogy. Medical Physics Publishing, http://www.aapm.org/pubs/reports/rpt_74.pdf. 2002. Accessed 21 May 2015.

119. Bracewell RN, Riddle AC. Inversion of fan-beam scans in radioastronomy. Astrophysics Journal. 1967;150.

120. Hutton BF, Hudson HM, Beekman FJ. A clinical perspective of accelerated statistical reconstruction. Eur J Nucl Med. 1997;24(7):797-808.

121. Hudson HM, Larkin RS. Accelerated image reconstruction using ordered subsets of projection data. IEEE Trans Med Imaging. 1994;13(4):601-9.

122. Butterworth S. On the theory of filter amplifiers. Exp Wireless and Wireless Eng. 1930;7:536-41.

123. Links JM, Jeremy RW, Dyer SM, Frank TL, Becker LC. Wiener filtering improves quantification of regional myocardial perfusion with thallium-201 SPECT. J Nucl Med. 1990;31(7):1230-6.

124. Miller TR, Sampathkumaran KS. Design and application of finite impulse response digital filters. Eur J Nucl Med. 1982;7(1):22-7.

125. Germano G, Chua T, Kavanagh PB, Kiat H, Berman DS. Detection and correction of patient motion in dynamic and static myocardial SPECT using a multi-detector camera. J Nucl Med. 1993;34(8):1349-55.

126. Matsumoto N, Berman DS, Kavanagh PB, Gerlach J, Hayes SW, Lewin HC et al. Quantitative assessment of motion artifacts and validation of a new motion-correction program for myocardial perfusion SPECT. J Nucl Med. 2001;42(5):687-94.

127. Friedman J, Van Train K, Maddahi J, Rozanski A, Prigent F, Bietendorf J et al. "Upward creep" of the heart: a frequent source of false-positive reversible defects during thallium-201 stress-redistribution SPECT. J Nucl Med. 1989;30(10):1718-22.

128. Cooper JA, McCandless BK. Preventing patient motion during tomographic myocardial perfusion imaging. J Nucl Med. 1995;36(11):2001-5.

129. DePuey EG, Garcia EV. Optimal specificity of thallium-201 SPECT through recognition of imaging artifacts. J Nucl Med. 1989;30(4):441-9.

130. Germano G, Kavanagh PB, Chen J, Waechter P, Su HT, Kiat H et al. Operator-less processing of myocardial perfusion SPECT studies. J Nucl Med. 1995;36(11):2127-32.

131. Slomka PJ, Hurwitz GA, Stephenson J, Cradduck T. Automated alignment and sizing of myocardial stress and rest scans to three-dimensional normal templates using an image registration algorithm. J Nucl Med. 1995;36(6):1115-22.

132. Sorenson JA. Methods for quantitating radioactivity in vivo by external counting measurements Madison, WI: University of Wisconsin; 1971.

133. Chang LT. A Method for Attenuation Correction in Radionuclide Computed Tomography. IEEE Trans Nucl Science 1978;25(1):6.

134. Llacer J, Veklerov E. Feasible images and practical stopping rules for iterative algorithms in emission tomography. IEEE Trans Med Imaging. 1989;8(2):186-93.

135. Chouraqui P, Livschitz S, Sharir T, Wainer N, Wilk M, Moalem I et al. Evaluation of an attenuation correction method for thallium-201 myocardial perfusion tomographic imaging of patients with low likelihood of coronary artery disease. J Nucl Cardiol. 1998;5(4):369-77.

136. Corbett JR, Ficaro EP. Clinical review of attenuation-corrected cardiac SPECT. J Nucl Cardiol. 1999;6(1 Pt 1):54-68.

137. Ficaro EP. Should SPET attenuation correction be more widely employed in routine clinical practice? For. Eur J Nucl Med Mol Imaging. 2002;29(3):409-12.

138. Ficaro EP, Fessler JA, Shreve PD, Kritzman JN, Rose PA, Corbett JR. Simultaneous transmission/emission myocardial perfusion tomography. Diagnostic accuracy of attenuation-corrected 99mTc-sestamibi single-photon emission computed tomography. Circulation. 1996;93(3):463-73.

139. Hendel RC, Berman DS, Cullom SJ, Follansbee W, Heller GV, Kiat H et al. Multicenter clinical trial to evaluate the efficacy of correction for photon attenuation and scatter in SPECT myocardial perfusion imaging. Circulation. 1999;99(21):2742-9.

140. Hendel RC, Corbett JR, Cullom SJ, DePuey EG, Garcia EV, Bateman TM. The value and practice of attenuation correction for myocardial perfusion SPECT imaging: a joint position statement from the American Society of Nuclear Cardiology and the Society of Nuclear Medicine. J Nucl Cardiol. 2002;9(1):135-43.

141. Kluge R, Sattler B, Seese A, Knapp WH. Attenuation correction by simultaneous emission-transmission myocardial single-photon emission tomography using a technetium-99m-labelled radiotracer: impact on diagnostic accuracy. Eur J Nucl Med. 1997;24(9):1107-14.

142. Matsunari I, Boning G, Ziegler SI, Nekolla SG, Stollfuss JC, Kosa I et al. Attenuation-corrected 99mTc-tetrofosmin single-photon emission computed tomography in the detection of viable myocardium: comparison with positron emission tomography using 18F-fluorodeoxyglucose. J Am Coll Cardiol. 1998;32(4):927-35.

143. Prvulovich EM, Lonn AH, Bomanji JB, Jarritt PH, Ell PJ. Effect of attenuation correction on myocardial thallium-201 distribution in patients with a low likelihood of coronary artery disease. Eur J Nucl Med. 1997;24(3):266-75.

144. Rigo P, Van Boxem P, Foulon J, Safi M, Engdahl J, Links J. Quantitative evaluation of a comprehensive motion, resolution, and attenuation correction program: initial experience. J Nucl Cardiol. 1998;5(5):458-68.

145. Vidal R, Buvat I, Darcourt J, Migneco O, Desvignes P, Baudouy M et al. Impact of attenuation correction by simultaneous emission/transmission tomography on visual assessment of 201Tl myocardial perfusion images. J Nucl Med. 1999;40(8):1301-9.

146. Wackers FJ. Should SPET attenuation correction be more widely employed in routine clinical practice? Against. Eur J Nucl Med Mol Imaging. 2002;29(3):412-5.

147. O'Connor M K, Kemp B, Anstett F, Christian P, Ficaro EP, Frey E et al. A multicenter evaluation of commercial attenuation compensation techniques in cardiac SPECT using phantom models. J Nucl Cardiol. 2002;9(4):361-76.

148. Zaidi H, Koral KF. Scatter modelling and compensation in emission tomography. Eur J Nucl Med Mol Imaging. 2004;31(5):761-82.

149. Links JM, Becker LC, Rigo P, Taillefer R, Hanelin L, Anstett F et al. Combined corrections for attenuation, depth-dependent blur, and motion in cardiac SPECT: a multicenter trial. J Nucl Cardiol. 2000;7(5):414-25.

150. Narayanan MV, King MA, Pretorius PH, Dahlberg ST, Spencer F, Simon E et al. Human-observer receiver-operating-characteristic evaluation of attenuation, scatter, and resolution compensation strategies for (99m)Tc myocardial perfusion imaging. J Nucl Med. 2003;44(11):1725-34.

151. Wackers FJ. Attenuation compensation of cardiac SPECT: a critical look at a confusing world. J Nucl Cardiol. 2002;9(4):438-40.

152. Gallowitsch HJ, Sykora J, Mikosch P, Kresnik E, Unterweger O, Molnar M et al. Attenuation-corrected thallium-201 single-photon emission tomography using a gadolinium-153 moving line source: clinical value and the impact of attenuation correction on the extent and severity of perfusion abnormalities. Eur J Nucl Med. 1998;25(3):220-8.

153. Cerqueira MD, Weissman NJ, Dilsizian V, Jacobs AK, Kaul S, Laskey WK et al. Standardized myocardial segmentation and nomenclature for tomographic imaging of the heart. A statement for healthcare professionals from the Cardiac Imaging Committee of the Council on Clinical Cardiology of the American Heart Association. Circulation. 2002;105(4):539-42.

154. Shehata AR, Ahlberg AW, White MP, Mann A, Fleming IA, Levine MG et al. Dipyridamole-dobutamine stress with Tc-99m sestamibi tomographic myocardial perfusion imaging. Am J Cardiol. 1998;82(4):520-3.

155. Van Train KF, Areeda J, Garcia EV, Cooke CD, Maddahi J, Kiat H et al. Quantitative same-day rest-stress technetium-99m-sestamibi SPECT: definition and validation of stress normal limits and criteria for abnormality. J Nucl Med. 1993;34(9):1494-502.

156. Johansson L, Edenbrandt L, Nakajima K, Lomsky M, Svensson SE, Tragardh E. Computer-aided diagnosis system outperforms scoring analysis in myocardial perfusion imaging. J Nucl Cardiol. 2014;21(3):416-23.

157. Berman DS, Abidov A, Kang X, Hayes SW, Friedman JD, Sciammarella MG et al. Prognostic validation of a 17-segment score derived from a 20-segment score for myocardial perfusion SPECT interpretation. J Nucl Cardiol. 2004;11(4):414-23.

158. Berman DS, Kang X, Van Train KF, Lewin HC, Cohen I, Areeda J et al. Comparative prognostic value of automatic quantitative analysis versus semiquantitative visual analysis of exercise myocardial perfusion single-photon emission computed tomography. J Am Coll Cardiol. 1998;32(7):1987-95.

159. Smanio PE, Watson DD, Segalla DL, Vinson EL, Smith WH, Beller GA. Value of gating of technetium-99m sestamibi single-photon emission computed tomographic imaging. J Am Coll Cardiol. 1997;30(7):1687-92.

160. Sharir T, Germano G, Kang X, Lewin HC, Miranda R, Cohen I et al. Prediction of myocardial infarction versus cardiac death by gated myocardial perfusion SPECT: risk stratification by the amount of stress-induced ischemia and the poststress ejection fraction. J Nucl Med. 2001;42(6):831-7.

161. Acampa W, Cuocolo A, Petretta M, Bruno A, Castellani M, Finzi A et al. Tetrofosmin imaging in the detection of myocardial viability in patients with previous myocardial infarction: comparison with sestamibi and Tl-201 scintigraphy. J Nucl Cardiol. 2002;9(1):33-40.

162. Greco C, Ciavolella M, Tanzilli G, Sinatra R, Macrina F, Schillaci O et al. Preoperative identification of viable myocardium: effectiveness of nitroglycerine-induced changes in myocardial Sestamibi uptake. Cardiovasc Surg (London, England). 1998;6(2):149-55.

163. Peix A, Lopez A, Ponce F, Morales J, de la Vega AR, Chesa CS et al. Enhanced detection of reversible myocardial hypoperfusion by technetium 99m-tetrofosmin imaging and first-pass radionuclide angiography after nitroglycerin administration. J Nucl Cardiol. 1998;5(5):469-76.

164. Germano G, Berman DS. Acquisition and processing for gated perfusion SPECT: technical aspects. . In: Germano G, Berman DS, editors. Clinical cardiac SPECT. Armonk, New York: Futura Publishing Company; 1999. p. 93-113.

165. Mazzanti M, Germano G, Kiat H, Kavanagh PB, Alexanderson E, Friedman JD et al. Identification of severe and extensive coronary artery disease by automatic measurement of transient ischemic dilation of the left ventricle in dual-isotope myocardial perfusion SPECT. J Am Coll Cardiol. 1996;27(7):1612-20.

166. McClellan JR, Travin MI, Herman SD, Baron JI, Golub RJ, Gallagher JJ et al. Prognostic importance of scintigraphic left ventricular cavity dilation during intravenous dipyridamole technetium-99m sestamibi myocardial tomographic imaging in predicting coronary events. Am J Cardiol. 1997;79(5):600-5.

167. Halligan WT, Morris PB, Schoepf UJ, Mischen BT, Spearman JV, Spears JR et al. Transient Ischemic Dilation of the Left Ventricle on SPECT: Correlation with Findings at Coronary CT Angiography. J Nucl Med. 2014;55(6):917-22.

168. Cochet H, Bullier E, Gerbaud E, Durieux M, Godbert Y, Lederlin M et al. Absolute quantification of left ventricular global and regional function at nuclear MPI using ultrafast CZT SPECT: initial validation versus cardiac MR. J Nucl Med. 2013;54(4):556-63.

169. Ioannidis JP, Trikalinos TA, Danias PG. Electrocardiogram-gated single-photon emission computed tomography versus cardiac magnetic resonance imaging for the assessment of left ventricular volumes and ejection fraction: a meta-analysis. J Am Coll Cardiol. 2002;39(12):2059-68.

170. Soneson H, Hedeer F, Arevalo C, Carlsson M, Engblom H, Ubachs JF et al. Development and validation of a new automatic algorithm for quantification of left ventricular volumes and

function in gated myocardial perfusion SPECT using cardiac magnetic resonance as reference standard. J Nucl Cardiol. 2011;18(5):874-85.

171. Schaefer WM, Lipke CS, Standke D, Kuhl HP, Nowak B, Kaiser HJ et al. Quantification of left ventricular volumes and ejection fraction from gated 99mTc-MIBI SPECT: MRI validation and comparison of the Emory Cardiac Tool Box with QGS and 4D-MSPECT. JJ Nucl Med. 2005;46(8):1256-63.

172. Verberne HJ, Dibbets-Schneider P, Spijkerboer A, Stokkel M, van Eck-Smit BL, Sokole EB. Multicenter intercomparison assessment of consistency of left ventricular function from a gated cardiac SPECT phantom. J Nucl Cardiol. 2006;13(6):801-10.

173. Sharir T, Berman DS, Waechter PB, Areeda J, Kavanagh PB, Gerlach J et al. Quantitative analysis of regional motion and thickening by gated myocardial perfusion SPECT: normal heterogeneity and criteria for abnormality. J Nucl Med. 2001;42(11):1630-8.

174. Chen J, Garcia EV, Bax JJ, Iskandrian AE, Borges-Neto S, Soman P. SPECT myocardial perfusion imaging for the assessment of left ventricular mechanical dyssynchrony. J Nucl Cardiol. 2011;18(4):685-94.

175. Chen J, Garcia EV, Folks RD, Cooke CD, Faber TL, Tauxe EL et al. Onset of left ventricular mechanical contraction as determined by phase analysis of ECG-gated myocardial perfusion SPECT imaging: development of a diagnostic tool for assessment of cardiac mechanical dyssynchrony. J Nucl Cardiol. 2005;12(6):687-95.

176. Boogers MJ, Chen J, Veltman CE, van Bommel RJ, Mooyaart EA, Al Younis I et al. Left ventricular diastolic dyssynchrony assessed with phase analysis of gated myocardial perfusion SPECT: a comparison with tissue Doppler imaging. Eur J Nucl Med Mol Imaging. 2011;38(11):2031-9.

177. Marsan NA, Henneman MM, Chen J, Ypenburg C, Dibbets P, Ghio S et al. Left ventricular dyssynchrony assessed by two three-dimensional imaging modalities: phase analysis of gated myocardial perfusion SPECT and tri-plane tissue Doppler imaging. Eur J Nucl Med Mol Imaging. 2008;35(1):166-73.

178. Pazhenkottil AP, Buechel RR, Nkoulou R, Ghadri JR, Herzog BA, Husmann L et al. Left ventricular dyssynchrony assessment by phase analysis from gated PET-FDG scans. J Nucl Cardiol. 2011;18(5):920-5.

179. Uebleis C, Hellweger S, Laubender RP, Becker A, Sohn HY, Lehner S et al. Left ventricular dyssynchrony assessed by gated SPECT phase analysis is an independent predictor of death in patients with advanced coronary artery disease and reduced left ventricular function not undergoing cardiac resynchronization therapy. Eur J Nucl Med Mol Imaging. 2012;39(10):1561-9.

180. Zafrir N, Nevzorov R, Bental T, Strasberg B, Gutstein A, Mats I et al. Prognostic value of left ventricular dyssynchrony by myocardial perfusion-gated SPECT in patients with normal and abnormal left ventricular functions. J Nucl Cardiol. 2014;21(3):532-40.

181. Boogers MM, Van Kriekinge SD, Henneman MM, Ypenburg C, Van Bommel RJ, Boersma E et al. Quantitative gated SPECT-derived phase analysis on gated myocardial perfusion SPECT detects left ventricular dyssynchrony and predicts response to cardiac resynchronization therapy. J Nucl Med. 2009;50(5):718-25.

182. Ludwig DR, Friehling M, Schelbert EB, Schwartzman D. Impact of scar on SPECT assay of left ventricular contraction dyssynchrony. Eur J Nucl Med Mol Imaging. 2014;41(3):529-35.

183. Lima RS, Watson DD, Goode AR, Siadaty MS, Ragosta M, Beller GA et al. Incremental value of combined perfusion and function over perfusion alone by gated SPECT myocardial perfusion imaging for detection of severe three-vessel coronary artery disease. J Am Coll Cardiol. 2003;42(1):64-70.

184. Sharir T, Germano G, Kavanagh PB, Lai S, Cohen I, Lewin HC et al. Incremental prognostic value of post-stress left ventricular ejection fraction and volume by gated myocardial perfusion single photon emission computed tomography. Circulation. 1999;100(10):1035-42.

185. Kaufmann PA. Cardiac hybrid imaging: state-of-the-art. Ann Nucl Med. 2009;23(4):325-31.

186. Raff GL, Abidov A, Achenbach S, Berman DS, Boxt LM, Budoff MJ et al. SCCT guidelines for the interpretation and reporting of coronary computed tomographic angiography. J Cardiovasc Comput Tomogr. 2009;3(2):122-36.

187. Javadi MS, Lautamaki R, Merrill J, Voicu C, Epley W, McBride G et al. Definition of vascular territories on myocardial perfusion images by integration with true coronary anatomy: a hybrid PET/CT analysis. J Nucl Med. 2010;51(2):198-203.

188. Gaemperli O, Bengel FM, Kaufmann PA. Cardiac hybrid imaging. Eur Heart J. 2011;32(17):2100-8.

189. Gaemperli O, Schepis T, Valenta I, Husmann L, Scheffel H, Duerst V et al. Cardiac image fusion from stand-alone SPECT and CT: clinical experience. J Nucl Med. 2007;48(5):696-703.

190. Santana CA, Garcia EV, Faber TL, Sirineni GK, Esteves FP, Sanyal R et al. Diagnostic performance of fusion of myocardial perfusion imaging (MPI) and computed tomography coronary angiography. J Nucl Cardiol. 2009;16(2):201-11.

191. Slomka PJ, Baum RP. Multimodality image registration with software: state-of-the-art. Eur J Nucl Med Mol Imaging. 2009;36 Suppl 1:S44-55.

192. Slomka PJ. Software approach to merging molecular with anatomic information. J Nucl Med. 2004;45 Suppl 1:36s-45s.

193. Budoff MJ, Dowe D, Jollis JG, Gitter M, Sutherland J, Halamert E et al. Diagnostic performance of 64-multidetector row coronary computed tomographic angiography for evaluation of coronary artery stenosis in individuals without known coronary artery disease: results from the prospective multicenter ACCURACY (Assessment by Coronary Computed Tomographic Angiography of Individuals Undergoing Invasive Coronary Angiography) trial. J Am Coll Cardiol. 2008;52(21):1724-32.

194. Meijboom WB, Meijs MF, Schuijf JD, Cramer MJ, Mollet NR, van Mieghem CA et al. Diagnostic accuracy of 64-slice computed tomography coronary angiography: a prospective, multicenter, multivendor study. J Am Coll Cardiol. 2008;52(25):2135-44.

195. Husmann L, Tatsugami F, Aepli U, Herzog BA, Valenta I, Veit-Haibach P et al. Prevalence of noncardiac findings on low dose 64-slice computed tomography used for attenuation correction in myocardial perfusion imaging with SPECT. Int J Cardiovasc Imaging. 2009;25(8):859-65.

196. Rispler S, Keidar Z, Ghersin E, Roguin A, Soil A, Dragu R et al. Integrated single-photon emission computed tomography and computed tomography coronary angiography for the assessment of hemodynamically significant coronary artery lesions. J Am Coll Cardiol. 2007;49(10):1059-67.

197. Sato A, Nozato T, Hikita H, Miyazaki S, Takahashi Y, Kuwahara T et al. Incremental value of combining 64-slice computed tomography angiography with stress nuclear myocardial perfusion imaging to improve noninvasive detection of coronary artery disease. J Nucl Cardiol. 2010;17(1):19-26.

198. Pazhenkottil AP, Nkoulou RN, Ghadri JR, Herzog BA, Buechel RR, Kuest SM et al. Prognostic value of cardiac hybrid imaging integrating single-photon emission computed tomography with coronary computed tomography angiography. Eur Heart J. 2011;32(12):1465-71.

199. van Werkhoven JM, Schuijf JD, Gaemperli O, Jukema JW, Boersma E, Wijns W et al. Prognostic value of multislice computed tomography and gated single-photon emission computed tomography in patients with suspected coronary artery disease. J Am Coll Cardiol. 2009;53(7):623-32.

200. Pazhenkottil AP, Nkoulou RN, Ghadri JR, Herzog BA, Kuest SM, Husmann L et al. Impact of cardiac hybrid single-photon emission computed tomography/computed tomography imaging on choice of treatment strategy in coronary artery disease. Eur Heart J. 2011;32(22):2824-9.

201. Fiechter M, Ghadri JR, Wolfrum M, Kuest SM, Pazhenkottil AP, Nkoulou RN et al. Downstream resource utilization following hybrid cardiac imaging with an integrated cadmium-zinc-telluride/64-slice CT device. Eur J Nucl Med Mol Imaging. 2012;39(3):430-6.

202. Tragardh E, Hesse B, Knuuti J, Flotats A, Kaufmann PA, Kitsiou A et al. Reporting nuclear cardiology: a joint position paper by the European Association of Nuclear Medicine (EANM) and the European Association of Cardiovascular Imaging (EACVI). Eur Heart J Cardiovasc Imaging. 2015;16(3):272-9.

203. Hendel RC, Wackers FJ, Berman DS, Ficaro E, Depuey EG, Klein L et al. American society of nuclear cardiology consensus statement: reporting of radionuclide myocardial perfusion imaging studies. J Nucl Cardiol. 2003;10(6):705-8.

204. Doukky R, Hayes K, Frogge N, Balakrishnan G, Dontaraju VS, Rangel MO et al. Impact of appropriate use on the prognostic value of single-photon emission computed tomography myocardial perfusion imaging. Circulation. 2013;128(15):1634-43.